nature water

Article https://doi.org/10.1038/s44221-023-00053-0

Exploring the water–food nexus reveals the interlinkages with urban human conflicts in Central America

In the format provided by the authors and unedited

Supplementary Information for the Manuscript

"Exploring the water-food nexus reveals novel interlinkages with urban human conflicts in Central America"

Supplementary Methods

S1. Data and Materials.

To study the societal impacts of droughts through the water-food nexus, we develop a theoretical framework using both agro-hydrological spatially distributed indicators and variables expressing societal conditions. We retrieved the main drought events from the Emergency Events Database (EM-DAT)[1] and we assigned to each event a level of impact obtained by the Principal Component Analysis (PCA) of the informative variables: number of deaths, affected and economic damage (Table S1, Fig. S1). Conflicts data, population maps and rural-urban catchment areas were collected, respectively, from the Social Conflict Analysis Database (SCAD)[2], WorldPop[3] and Cattaneo *et al.*[4]. The Sub-national Human Development Index were retrieved from Global Data Lab[5] and used in the analysis as an indicator of social development including the human health, education and standard of living dimensions[6]. Water and food indicators were developed as spatially explicit raster maps at 5 arc-min resolution per each year for the entire time period considered, using the WATNEEDS model[7] (Section S2). As water indicators, we selected the green water availability (GWA), calculated as the total amount of green water (m^3) needed for agricultural production, available per person (m^3/cap/year). The index of food security was computed considering the annual agricultural production in terms of the total kcal available per person.

Table S1. EM-DAT[1] drought events involved in the CD model. For each event the duration, the correspondent area mapped (km^2), the number of deaths, affected and the economic damage ('000 $) have been listed. The results of the PCA performed on the three components (deaths, affected, damage) are shown, as well as the resulting impact classes.

Event_ID	Duration [start-end]	Mapped Area (km^2)	Deaths (count)	Damage ('000 $)	Affected (count)	PCA	Impact class
HND-1997-9305	[1997-1997]	40000	-	-	-	-	-
SLV-1998-9216	[1998-1998]	4400	-	170000	-	-	3
HND-2000-9860	[2000-2000]	8800	-	-	1125	-	1
SLV-2001-9383	[2001-2001]	9200	-	22400	400000	0.1758	3
GTM-2001-9383	[2001-2001]	5200	41	14000	113596	-0.4423	3
HND-2001-9383	[2001-2004]	55600	-	-	195000	-	4
HND-2002-9838	[2002-2002]	20400	-	-	82000	-	4
HND-2004-9363	[2004-2004]	135600	-	-	137500	-	4
SLV-2009-9415	[2009-2009]	25600	-	27000	-	-	2
GTM-2009-9415	[2009-2009]	28000	-	-	2500000	-	4
HND-2009-9559	[2009-2011]	36400	-	-	45000	-	3
GTM-2012-9355	[2012-2012]	36800	-	-	266485	-	4
HND-2012-9379	[2012-2012]	80800	-	-	125000	-	4
SLV-2014-9580	[2014-2015]	15200	-	100000	700000	-0.1196	3
GTM-2014-9277	[2014-2016]	57200	-	100000	1300000	-2.438	4
HND-2014-9332	[2014-2015]	95200	-	-	571710	-	4

Figure S1: Graphical representation of the droughts event reported in EM-DAT database[1]. They have been classified basing on the impact and duration.

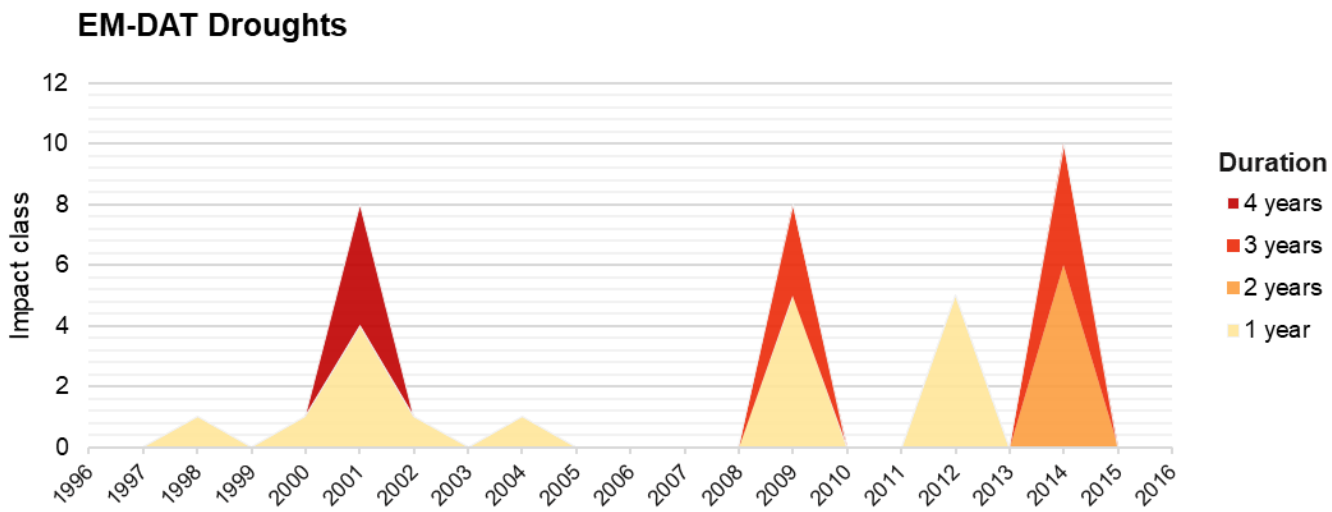

Table S2. Descriptive statistics per year of the variables included in the Bayesian econometric model CWFs. For each covariate, mean (top-left), standard deviation (top-right), the 1st (25%) and the 3rd (75%) quartiles (bottom) are reported. For the conflict also the total number per year is provided.

Variable	1996		1997		1998		1999		2000		2001	
Conflicts	2.49E-02	2.77E-01	1.44E-02	1.95E-01	0.0327654	2.99E-01	1.83E-02	2.23E-01	2.88E-02	2.03E-01	4.19E-02	4.30E-01
	(0.00E+00	0.00E+00)	(0.00E+00	0.00E+00)	(0.00E+00	0.00E+00)	(0.00E+00	0.00E+00)	(0.00E+00	0.00E+00)	(0.00E+00	0.00E+00)
HDI	4.93E-01	6.52E-02	5.01E-01	6.36E-02	13.60419397	6.28E-02	5.13E-01	6.19E-02	5.23E-01	6.05E-02	5.32E-01	5.93E-02
	(4.43E-01	5.47E-01)	(4.48E-01	5.52E-01)	(4.59E-01	5.58E-01)	(4.74E-01	5.62E-01)	(4.87E-01	5.68E-01)	(4.96E-01	5.73E-01)
Population	2.95E+04	7.37E+04	2.98E+04	7.45E+04	30028.35645	7.51E+04	3.03E+04	7.57E+04	3.05E+04	7.63E+04	3.09E+04	7.70E+04
	(3.70E+03	3.70E+03)	(3.74E+03	3.74E+03)	(3.77E+03	3.77E+03)	(3.80E+03	3.80E+03)	(3.83E+03	3.83E+03)	(3.94E+03	3.94E+03)
Water	1.34E+03	2.90E+03	1.54E+03	3.18E+03	1634.141767	3.53E+03	1.73E+03	3.84E+03	1.87E+03	3.84E+03	1.63E+03	3.75E+03
	(9.14E+00	9.14E+00)	(9.19E+00	9.19E+00)	(9.57E+00	9.57E+00)	(1.23E+01	1.23E+01)	(1.34E+01	1.34E+01)	(1.04E+01	1.04E+01)
Food	1.02E+03	1.83E+03	1.19E+03	1.62E+03	1267.440104	1.70E+03	1.60E+03	2.42E+03	1.96E+03	2.67E+03	1.24E+03	1.90E+03
	(7.86E+01	7.86E+01)	(1.19E+02	1.19E+02)	(1.43E+02	1.43E+02)	(1.52E+02	1.52E+02)	(2.43E+02	2.43E+02)	(1.23E+02	1.23E+02)
Water (Trade)	4.31E+02	2.99E+02	4.37E+02	3.04E+02	444.5621827	3.05E+02	4.50E+02	3.04E+02	4.51E+02	3.06E+02	4.34E+02	3.03E+02
	(2.87E+01	2.87E+01)	(9.19E+00	9.19E+00)	(2.70E+01	2.70E+01)	(3.44E+01	3.44E+01)	(1.34E+01	1.34E+01)	(1.04E+01	1.04E+01)
Food (Trade)	4.32E+05	3.73E+05	5.17E+05	4.03E+05	536705.0441	4.05E+05	5.89E+05	4.25E+05	6.46E+05	4.42E+05	5.03E+05	3.96E+05
	(1.22E+05	1.22E+05)	(1.38E+05	1.38E+05)	(1.52E+05	1.52E+05)	(1.60E+05	1.60E+05)	(1.97E+05	1.97E+05)	(1.47E+05	1.47E+05)
Access	4.99E+08	6.82E+08	6.53E+08	9.23E+08	0.51615933	1.00E+09	7.77E+08	1.06E+09	8.47E+08	1.21E+09	6.43E+08	8.00E+08
	(1.39E+08	6.06E+08)	(1.52E+08	7.59E+08)	(1.67E+08	8.65E+08)	(1.82E+08	9.46E+08)	(1.85E+08	1.02E+09)	(1.80E+08	8.42E+08)
Surplus-Demand gap	1.95E-02	1.00E-01	1.24E-02	5.70E-02	0.371713825	3.43E-02	2.14E-03	1.28E-02	1.11E-03	6.42E-03	6.52E-03	4.17E-02
	(0.00E+00	0.00E+00)	(0.00E+00	0.00E+00)	(0.00E+00	0.00E+00)	(0.00E+00	0.00E+00)	(0.00E+00	0.00E+00)	(0.00E+00	0.00E+00)
Drought Impact	0.00E+00	0.00E+00	3.28E-01	8.44E-01	0.043250328	3.58E-01	0.00E+00	0.00E+00	2.88E-02	1.67E-01	8.74E-01	1.61E+00
	(0.00E+00	0.00E+00)	(0.00E+00	0.00E+00)	(0.00E+00	0.00E+00)	(0.00E+00	0.00E+00)	(0.00E+00	0.00E+00)	(0.00E+00	0.00E+00)
Number of conflicts	**19**		**11**		**25**		**14**		**22**		**32**	

Variable	2002		2003		2004		2005		2006		2007	
Conflicts	4.59E-02	5.56E-01	4.98E-02	6.11E-01	3.93E-02	3.67E-01	3.80E-02	4.22E-01	2.75E-02	3.41E-01	3.01E-02	2.95E-01
	(0.00E+00	0.00E+00)	(0.00E+00	0.00E+00)	(0.00E+00	0.00E+00)	(0.00E+00	0.00E+00)	(0.00E+00	0.00E+00)	(0.00E+00	0.00E+00)
HDI	5.39E-01	5.88E-02	5.46E-01	5.85E-02	5.52E-01	5.85E-02	5.59E-01	5.90E-02	5.69E-01	5.23E-02	5.79E-01	4.75E-02
	(5.01E-01	5.78E-01)	(5.07E-01	5.82E-01)	(5.12E-01	5.88E-01)	(5.16E-01	5.95E-01)	(5.26E-01	5.84E-01)	(5.34E-01	5.98E-01)
Population	3.15E+04	7.79E+04	3.21E+04	7.86E+04	3.27E+04	7.95E+04	3.33E+04	8.05E+04	3.40E+04	8.17E+04	3.46E+04	8.28E+04
	(3.97E+03	3.97E+03)	(4.16E+03	4.16E+03)	(4.26E+03	4.26E+03)	(4.35E+03	4.35E+03)	(4.40E+03	4.40E+03)	(4.51E+03	4.51E+03)
Water	1.72E+03	3.84E+03	1.78E+03	3.75E+03	1.85E+03	4.04E+03	1.63E+03	3.53E+03	1.56E+03	3.28E+03	1.61E+03	3.28E+03
	(1.12E+01	1.12E+01)	(9.12E+00	9.12E+00)	(8.94E+00	8.94E+00)	(8.07E+00	8.07E+00)	(9.24E+00	9.24E+00)	(9.83E+00	9.83E+00)
Food	1.45E+03	2.06E+03	1.65E+03	2.42E+03	1.65E+03	2.31E+03	1.54E+03	2.10E+03	1.46E+03	2.12E+03	1.51E+03	2.15E+03
	(1.87E+02	1.87E+02)	(1.79E+02	1.79E+02)	(1.82E+02	1.82E+02)	(1.73E+02	1.73E+02)	(1.60E+02	1.60E+02)	(1.64E+02	1.64E+02)
Water (Trade)	4.45E+02	3.04E+02	4.52E+02	3.06E+02	4.44E+02	3.08E+02	4.45E+02	3.06E+02	4.45E+02	3.06E+02	4.43E+02	3.06E+02
	(1.12E+01	1.12E+01)	(3.43E+01	3.43E+01)	(8.94E+00	8.94E+00)	(2.88E+01	2.88E+01)	(3.46E+01	3.46E+01)	(3.03E+01	3.03E+01)
Food (Trade)	5.76E+05	4.15E+05	6.05E+05	4.29E+05	5.93E+05	4.24E+05	5.89E+05	4.30E+05	5.76E+05	4.21E+05	5.89E+05	4.31E+05
	(1.66E+05	1.66E+05)	(1.60E+05	1.60E+05)	(1.74E+05	1.74E+05)	(1.57E+05	1.57E+05)	(1.68E+05	1.68E+05)	(1.56E+05	1.56E+05)
Access	7.63E+08	1.03E+09	8.22E+08	1.11E+09	8.16E+08	1.11E+09	8.12E+08	1.13E+09	8.24E+08	1.15E+09	8.95E+08	1.21E+09
	(1.83E+08	9.30E+08)	(1.91E+08	9.86E+08)	(1.97E+08	9.85E+08)	(1.77E+08	1.00E+09)	(2.04E+08	1.02E+09)	(2.07E+08	1.10E+09)
Surplus-Demand gap	3.68E-03	2.03E-02	2.27E-03	1.21E-02	2.24E-03	1.34E-02	3.49E-03	1.97E-02	4.34E-03	2.28E-02	5.12E-03	2.25E-02
	(0.00E+00	0.00E+00)	(0.00E+00	0.00E+00)	(0.00E+00	0.00E+00)	(0.00E+00	0.00E+00)	(0.00E+00	0.00E+00)	(0.00E+00	0.00E+00)
Drought Impact	2.67E-01	1.00E+00	0.00E+00	0.00E+00	1.85E+00	2.00E+00	0.00E+00	0.00E+00	0.00E+00	0	0.00E+00	0
	(0.00E+00	0.00E+00)	(0.00E+00	0.00E+00)	(0.00E+00	0.00E+00)	(0.00E+00	0.00E+00)	(0.00E+00	0.00E+00)	(0.00E+00	0.00E+00)
Number of conflicts	**35**		**38**		**30**		**29**		**21**		**23**	

Variable	2008		2009		2010		2011		2012		2013	
Conflicts	1.05E-02	1.35E-01	3.93E-02	5.03E-01	2.10E-02	3.23E-01	1.70E-02	2.07E-01	3.41E-02	2.38E-01	2.23E-02	2.53E-01
	(0.00E+00	0.00E+00)	(0.00E+00	0.00E+00)	(0.00E+00	0.00E+00)	(0.00E+00	0.00E+00)	(0.00E+00	0.00E+00)	(0.00E+00	0.00E+00)
HDI	5.80E-01	4.23E-02	5.83E-01	3.88E-02	5.86E-01	3.66E-02	5.91E-01	3.48E-02	5.92E-01	3.48E-02	5.95E-01	3.57E-02
	(5.40E-01	5.99E-01)	(5.47E-01	6.00E-01)	(5.57E-01	5.99E-01)	(5.67E-01	6.01E-01)	(5.64E-01	6.02E-01)	(5.66E-01	6.04E-01)
Population	3.53E+04	8.38E+04	3.60E+04	8.50E+04	3.67E+04	8.61E+04	3.75E+04	8.77E+04	3.82E+04	8.92E+04	3.90E+04	9.07E+04
	(4.61E+03	4.61E+03)	(4.63E+03	4.63E+03)	(4.79E+03	4.79E+03)	(4.92E+03	4.92E+03)	(5.16E+03	5.16E+03)	(5.18E+03	5.18E+03)
Water	1.67E+03	3.56E+03	1.65E+03	3.60E+03	1.62E+03	3.32E+03	1.44E+03	3.01E+03	1.55E+03	3.18E+03	1.36E+03	2.67E+03
	(1.07E+01	1.07E+01)	(8.96E+00	8.96E+00)	(9.49E+00	9.49E+00)	(8.83E+00	8.83E+00)	(9.17E+00	9.17E+00)	(8.99E+00	8.99E+00)
Food	1.68E+03	2.38E+03	1.52E+03	2.11E+03	1.78E+03	2.47E+03	1.40E+03	1.98E+03	1.64E+03	2.30E+03	1.47E+03	2.08E+03
	(1.96E+02	1.96E+02)	(1.66E+02	1.66E+02)	(2.08E+02	2.08E+02)	(1.50E+02	1.50E+02)	(1.87E+02	1.87E+02)	(1.49E+02	1.49E+02)
Water (Trade)	4.43E+02	3.07E+02	4.27E+02	3.06E+02	4.39E+02	3.06E+02	4.26E+02	3.05E+02	4.21E+02	3.04E+02	4.26E+02	3.04E+02
	(3.04E+01	3.04E+01)	(8.96E+00	8.96E+00)	(2.67E+01	2.67E+01)	(2.64E+01	2.64E+01)	(9.17E+00	9.17E+00)	(2.85E+01	2.85E+01)
Food (Trade)	6.08E+05	4.35E+05	5.76E+05	4.29E+05	6.24E+05	4.44E+05	5.61E+05	4.32E+05	5.90E+05	4.37E+05	5.76E+05	4.36E+05
	(1.72E+05	1.72E+05)	(1.45E+05	1.45E+05)	(1.81E+05	1.81E+05)	(1.39E+05	1.39E+05)	(1.57E+05	1.57E+05)	(1.43E+05	1.43E+05)
Access	9.03E+08	1.23E+09	9.12E+08	1.26E+09	9.74E+08	1.29E+09	8.63E+08	1.17E+09	9.76E+08	1.35E+09	9.36E+08	1.28E+09
	(2.05E+08	1.09E+09)	(2.07E+08	1.13E+09)	(2.25E+08	1.21E+09)	(1.88E+08	1.04E+09)	(2.21E+08	1.18E+09)	(2.07E+08	1.13E+09)
Surplus-Demand gap	5.25E-03	2.25E-02	6.85E-03	2.93E-02	5.81E-03	2.41E-02	1.22E-02	4.41E-02	6.94E-03	2.88E-02	1.06E-02	3.89E-02
	(0.00E+00	0.00E+00)	(0.00E+00	0.00E+00)	(0.00E+00	0.00E+00)	(0.00E+00	0.00E+00)	(0.00E+00	0.00E+00)	(0.00E+00	0.00E+00)
Drought Impact	0.00E+00	0.00E+00	8.83E-01	1.43E+00	0.00E+00	0.00E+00	0.00E+00	0.00E+00	1.54E+00	1.95E+00	0.00E+00	0.00E+00
	(0.00E+00	0.00E+00)	(0.00E+00	0.00E+00)	(0.00E+00	0.00E+00)	(0.00E+00	0.00E+00)	(0.00E+00	0.00E+00)	(0.00E+00	0.00E+00)
Number of conflicts	**8**		**30**		**16**		**13**		**26**		**17**	

Variable	2014		2015		2016	
Conflicts	2.10E-02	2.28E-01	7.34E-02	7.87E-01	5.50E-02	4.28E-01
	(0.00E+00	0.00E+00)	(0.00E+00	0.00E+00)	(0.00E+00	0.00E+00)
HDI	6.10E-01	4.09E-02	6.13E-01	4.36E-02	6.16E-01	4.25E-02
	(5.80E-01	6.32E-01)	(5.76E-01	6.38E-01)	(5.77E-01	6.38E-01)
Population	3.98E+04	9.22E+04	4.07E+04	9.41E+04	4.15E+04	9.50E+04
	(5.28E+03	5.28E+03)	(5.42E+03	5.42E+03)	(5.46E+03	5.46E+03)
Water	1.42E+03	2.92E+03	1.42E+03	3.15E+03	1.45E+03	3.04E+03
	(8.06E+00	8.06E+00)	(8.21E+00	8.21E+00)	(8.93E+00	8.93E+00)
Food	1.19E+03	1.76E+03	1.17E+03	1.86E+03	1.28E+03	1.84E+03
	(1.28E+02	1.28E+02)	(1.24E+02	1.24E+02)	(1.41E+02	1.41E+02)
Water (Trade)	4.20E+02	3.04E+02	4.28E+02	3.04E+02	4.27E+02	3.06E+02
	(8.06E+00	8.06E+00)	(2.92E+01	2.92E+01)	(2.97E+01	2.97E+01)
Food (Trade)	4.97E+05	4.02E+05	4.85E+05	3.93E+05	5.20E+05	4.10E+05
	(1.31E+05	1.31E+05)	(1.33E+05	1.33E+05)	(1.30E+05	1.30E+05)
Access	8.75E+08	1.25E+09	8.20E+08	1.14E+09	7.85E+08	8.19E+08
	(2.19E+08	1.08E+09)	(2.16E+08	1.03E+09)	(2.15E+08	1.07E+09)
Surplus-Demand gap	9.36E-03	4.23E-02	1.07E-02	4.23E-02	1.56E-02	5.68E-02
	(0.00E+00	0.00E+00)	(0.00E+00	0.00E+00)	(0.00E+00	0.00E+00)
Drought Impact	2.15E+00	1.96E+00	0.00E+00	0.00E+00	0.00E+00	0.00E+00
	(0.00E+00	0.00E+00)	(0.00E+00	0.00E+00)	(0.00E+00	0.00E+00)
Number of conflicts	**16**		**56**		**42**	

Table S3. Moran's Index and p-values of the Moran's test for spatial autocorrelation. They are reported per year and per each variable.

Variable	1996		1997		1998		1999		2000		2001		2002	
	Moran's I	p-value	Moran's I	p-value	Moran's I	p-value	Moran's I	p-value	Moran's I	p-value	Moran's I	p-value	Moran's I	p-value
Conflicts	0.043	0.003	-0.005	0.612	0.032	0.028	-0.007	0.639	0.038	0.014	0.012	0.162	-0.004	0.590
HDI	0.421	0.000	0.399	0.000	0.386	0.000	0.371	0.000	0.367	0.000	0.361	0.000	0.365	0.000
Population	0.834	0.000	0.826	0.000	0.835	0.000	0.822	0.000	0.829	0.000	0.820	0.000	0.815	0.000
Water	0.328	0.000	0.328	0.000	0.328	0.000	0.328	0.000	0.328	0.000	0.331	0.000	0.334	0.000
Food	0.392	0.000	0.406	0.000	0.413	0.000	0.416	0.000	0.405	0.000	0.414	0.000	0.425	0.000
Water (Trade)	0.430	0.000	0.351	0.000	0.388	0.000	0.384	0.000	0.362	0.000	0.414	0.000	0.370	0.000
Food (Trade)	0.468	0.000	0.550	0.000	0.531	0.000	0.565	0.000	0.591	0.000	0.464	0.000	0.503	0.000
Access	0.303	0.000	0.377	0.000	0.381	0.000	0.358	0.000	0.364	0.000	0.341	0.000	0.390	0.000
Surplus-Demand gap	0.128	0.000	0.268	0.000	0.184	0.000	0.163	0.000	0.124	0.000	0.179	0.000	0.149	0.000
Drought Impact	0.466	0.000	0.543	0.000	0.529	0.000	0.554	0.000	0.569	0.000	0.462	0.000	0.493	0.000

Variable	2003		2004		2005		2006		2007		2008		2009	
	Moran's I	p-value	Moran's I	p-value	Moran's I	p-value	Moran's I	p-value	Moran's I	p-value	Moran's I	p-value	Moran's I	p-value
Conflicts	0.004	0.333	0.017	0.104	0.001	0.434	0.016	0.126	0.077	0.767	-0.006	0.630	0.007	0.283
HDI	0.372	0.000	0.377	0.000	0.387	0.000	0.388	0.000	0.386	0.000	0.376	0.000	0.362	0.000
Population	0.798	0.000	0.795	0.000	0.792	0.000	0.825	0.000	0.835	0.000	0.829	0.000	0.828	0.000
Water	0.340	0.000	0.342	0.000	0.345	0.000	0.346	0.000	0.348	0.000	0.353	0.000	0.355	0.000
Food	0.421	0.000	0.426	0.000	0.425	0.000	0.416	0.000	0.405	0.000	0.420	0.000	0.420	0.000
Water (Trade)	0.352	0.000	0.364	0.000	0.393	0.000	0.377	0.000	0.365	0.000	0.356	0.000	0.350	0.000
Food (Trade)	0.543	0.000	0.540	0.000	0.564	0.000	0.515	0.000	0.565	0.000	0.561	0.000	0.570	0.000
Access	0.384	0.000	0.387	0.000	0.401	0.000	0.402	0.000	0.393	0.000	0.393	0.000	0.399	0.000
Surplus-Demand gap	0.159	0.000	0.186	0.000	0.193	0.000	0.173	0.000	0.196	0.000	0.283	0.000	0.277	0.000
Drought Impact	0.531	0.000	0.535	0.000	0.555	0.000	0.506	0.000	0.553	0.000	0.545	0.000	0.563	0.000

Variable	2010		2011		2012		2013		2014		2015		2016	
	Moran's I	p-value	Moran's I	p-value	Moran's I	p-value	Moran's I	p-value	Moran's I	p-value	Moran's I	p-value	Moran's I	p-value
Conflicts	-0.004	0.603	-0.007	0.636	0.085	0.000	0.002	0.389	-0.008	0.671	0.031	0.012	0.012	0.209
HDI	0.347	0.000	0.328	0.000	0.345	0.000	0.345	0.000	0.427	0.000	0.432	0.000	0.401	0.000
Population	0.812	0.000	0.812	0.000	0.795	0.000	0.801	0.000	0.784	0.000	0.798	0.000	0.805	0.000
Water	0.358	0.000	0.357	0.000	0.356	0.000	0.357	0.000	0.358	0.000	0.356	0.000	0.363	0.000
Food	0.403	0.000	0.415	0.000	0.418	0.000	0.405	0.000	0.397	0.000	0.390	0.000	0.388	0.000
Water (Trade)	0.346	0.000	0.356	0.000	0.355	0.000	0.361	0.000	0.401	0.000	0.367	0.000	0.364	0.000
Food (Trade)	0.576	0.000	0.570	0.000	0.580	0.000	0.575	0.000	0.512	0.000	0.515	0.000	0.564	0.000
Access	0.382	0.000	0.389	0.000	0.382	0.000	0.387	0.000	0.399	0.000	0.364	0.000	0.474	0.000
Surplus-Demand gap	0.264	0.000	0.306	0.000	0.295	0.000	0.323	0.000	0.206	0.000	0.280	0.000	0.326	0.000
Drought Impact	0.552	0.000	0.558	0.000	0.565	0.000	0.560	0.000	0.511	0.000	0.514	0.000	0.560	0.000

S2. The hydrological balance and indices computation

Droughts in Central America are cyclical and closely related to the El Niño period of the Southern Oscillation (ENSO); with respect those occurring in other parts of the World they are more associated to anomaly in precipitation distribution within the rainy period[8]. Vulnerability to drought depends on how communities and productive activities cope with consequences of the rain deficit. Droughts might be classified accordingly to the effects they produce on local precipitation patterns, hydrological cycle, local crop production and water supply for human activities, for industrial, domestic and agricultural purposes[8]. We developed indices representative of these drought's aspects. Water and food indicators were developed from the output of a spatially distributed hydrological balance model WATNEEDS[7], reported in (Eq. S1). The model simulates the vertical soil water balance and introduces a spatially distributed crop specific monthly analysis of crop water requirement for available climatic data. The crop water requirement (mm yr^{-1}) is the volume of water required to compensate for a crop's evapotranspiration losses, without experiencing crop water stress. The crop water requirement has two components: namely, the green crop water requirement (met by available precipitation) and the blue crop water requirement (met by irrigation). The blue water requirement has not been used in the analysis as water used for irrigation accounts for only 1% of the total agricultural water footprint for the considered countries[9]. We calculate yearly green crop water requirement for the main cultivated crops – i.e., maize, pulses, sorghum, sugarcane, oil palm and coffee - covering around 80% of the overall harvested area in the region. Crop planting and harvesting dates, harvested areas and yields are provided by the MIRCA dataset[10]. Tropical fruits and vegetables are also included as they are largely produced in the area (avocado, banana, cauliflower, fresh fruit, lemons, lettuce, mangos, onions, oranges, papaya, pineapple, tomatoes, fresh vegetables, watermelons). Harvested areas for these crops are taken from the EarthStat[28] dataset, as they are not included in the MIRCA dataset.

The WATNEEDS model simulates the time variation of water storage $\frac{\Delta W_i}{\Delta t}$ within a specific cell *i* as the difference between water inputs (precipitation P_{it}) and outputs (deep percolation D_{it}, runoff R_{it} and actual evapotranspiration $ET_{act,it}$), at a daily time scale and a 5 arc-minutes resolution.

(S1) $$\frac{\Delta \mathrm{W_i}}{\Delta \mathrm{t}} = \mathrm{P_{it}} - \mathrm{ET_{act,it}} - \mathrm{D_{it}} - \mathrm{R_{it}}$$

In particular, $\mathrm{W_{it}}$ is the soil moisture at time step t, P_{it} is the daily effective precipitation, retrieved by the CHIRPSv2.0 dataset[11]. D_{it} is the deep percolation, calculated following Chiarelli *et al.*[7], using the maximum deep percolation flux D_{max}, depending on the soil type[12] (Eq. S2) .

(S2) $$\mathrm{D_{it}} = \begin{cases} \mathrm{D_{max}} \frac{\mathrm{W_{it}} - (1-\mathrm{p})\mathrm{S_{max}}}{\mathrm{S_{max}}} & \text{if } (1-\mathrm{p})\,\mathrm{S_{max}} < \mathrm{W_{it}} < \mathrm{S_{max}} \\ 0 & \text{if } \mathrm{W_{it}} < (1-\mathrm{p})\mathrm{S_{max}} \end{cases}$$

The actual evapotranspiration $ET_{act,j}$ of a specific crop *j* is calculated (Eq. S3) as the product between the reference evapotranspiration, referred to the Penman-Monteith equation, ET_0[13], the crop coefficient $k_{c,j}$ related to the growing phase, taken from Allen *et al*. [14] and a crop stress coefficient k_s.

(S3) $$\mathrm{ET_{act,j}} = \mathrm{k_{c,j}} \cdot \mathrm{k_s} \cdot \mathrm{ET_0}$$

The water stress coefficient $k_{s,i,t}$ is calculated at a daily time scale (*t*), for crop *j* following Allen *et al*.[14] (Eq. S4) as a function of the soil water content $W_{i,t}$ and the maximum and the readily available water $\mathrm{RAW_i}$. The soil moisture $\mathrm{W_{i,t}}$ is calculated solving the daily soil water balance at time step t, as function of the soil moisture of the previous time step ($\mathrm{W}_{i,t-1}$) and the water inputs and outputs (Eq. S1). The $\mathrm{RAW_i}$ is calculated as the total available water multiplied $\mathrm{TAW_i}$ by the critical depletion factor p_i (i.e., the actual fraction of water that a crop can uptake from the rooting zone without experiencing crop water stress). For conditions of no water stress the crop stress coefficient is equal to 1.

(S4)
$$\mathbf{k_{s,i,t}} = \begin{cases} \frac{\mathbf{W_{i,t}}}{\mathbf{RAW_i}} & \mathbf{if\ W_{i,t} < RAW_i} \\ \mathbf{1} & \mathbf{if\ W_{\mathit{i},t} \geq RAW_i} \end{cases}$$

$$\mathrm{RAW}_i = \mathrm{TAW}_i * \mathrm{p}_i = \mathrm{z_{ri}} * (\theta_{\mathrm{fc}} - \theta_{\mathrm{wp}}) * \mathrm{p_i}$$

Where θ_{fc} is the water content at field capacity (mm/m) and the and θ_{wp} the water content at wilting point[15] (mm/m), thus, the difference $(\theta_{\mathrm{fc}} - \theta_{\mathrm{wp}})$ represents the maximum soil moisture storage capacity. $\mathrm{z_r}$ (m) is the crop rooting depth[16]. Soil information (e.g., maximum soil moisture storage capacity and maximum infiltration rate) were from Bajties *et al.*[17].In time steps where the sum of the balance (i.e., $\mathrm{W_{it-1}} + \mathrm{P_{it}} - \mathrm{ET_{act,it}} - \mathrm{D_{it}}$) exceeds the TAW_i, $\mathrm{R_{it}}$ – the sub-surface runoff – is calculated as the difference between the sum of the balance and TAW_i.

For each day, each crop, and each grid cell we calculate $ET_{act,j}$ – equal to the green crop water requirement, then we sum the daily green crop water requirements across each month of a crop's growing season to determine monthly green consumptive crop water requirement (mm). We finally assess the monthly green water volume per each grid cell, as the weighted mean of the crop-specific actual evapotranspiration (mm) over the harvested areas retrieved from the MIRCA dataset[10].

We, first, use the outputs of the WATNEEDS model to develop food security and green water availability indicators, at 5 arc-min resolution - as described in the following sections. Second, we rescale each indicator to match the spatial resolution of the grid cell (20 km x 20 km) required by the Econometric model design.

Food availability and access. A strong nexus exists between water availability and food production[18]. We focused on assessing the effects of water stress on the first two pillars of food security, i.e. food availability, intended as the availability of necessary calories at the individual level, and food access, intended as the economic possibility for people to have access to the necessary calories[19]. We calculated the yearly production (in tons) of the six main cultivated crops covering around 80% of the overall harvested area. For this purpose, we adopted the Doorenbos and Kassam formula[20], reported in Eq. S5, for crop yield evaluation in function of the actual crop evapotranspiration and their water demand. This method is commonly used by FAO[20–22]:

(S5)
$$\left(1 - \frac{\mathrm{Y_{a,j}}}{\mathrm{Y_{max,j}}}\right) = \mathrm{k_{y,j}}\left(1 - \frac{\mathrm{ET_{act,j}}}{\mathrm{ET_{p,j}}}\right)$$

where Y_{max} and Y_a are the maximum and actual yields referred to the crop *j*, and $k_{y,j}$ is a yield response factor representing the effect of a reduction in evapotranspiration on yield losses. As maximum yields, those under irrigated conditions provided Monfreda *et al.*[23] were considered, while the actual yields were estimated from Eq. S4. Seasonal value of k_y for the crops involved in the analysis were retrieved from FAO Irrigation and Drainage Paper No. 33[20]. The yearly production of staple crops was then converted into the corresponding kcal supplied per person, using the caloric content conversion (in kcal/100 g)[24], in order to compute the spatially-distributed indicator of food availability. Instead, the yearly cash crop production was involved to define an economic indicator of food access (USD/year) representing the potential income deriving from the market sale of coffee, sugar cane and oil palm (producer prices provided by FAOSTAT[25] have been used).

Different levels of food (in)security can be assessed referring to the Human Energy Requirements (HER)[26]. The reference HER was defined as "*the amount of food energy needed to balance energy expenditure in order to maintain body size, body composition and a level of necessary and desirable physical activity consistent with long term good health*". Following FAO[26], a value of 3000 kcal/cap/day was selected as mean Human Energy Requirement threshold (HER_{mean}), and a value of 1800 kcal/cap/day as the minimum threshold (HER_{min}). The reference values involved in our analysis account also for the fraction of animal calories accordingly to the methodology of Davis *et al.*[27].

Green Water Availability. As the blue water footprint of domestic agricultural production accounts for only 1% of the total agricultural water footprint[9], only green water was included in this analysis. Green water (GW) was computed at 5 arc-min resolution per year as the total amount of water (m^3) needed by the crops to compensate losses from evapotranspiration. The green water demand of each crop was calculated with the WATNEEDS model[7] (mm) and multiplied by the harvested area (ha). The selected crops are 20; harvested areas of the main cultivated cash and staple crops (i.e. sugarcane, sorghum, oil palm, maize, pulses and coffee) were retrieved from the MIRCA dataset[10]. Tropical fruits and vegetables were also included as they are largely produced in the area (avocado, banana, cauliflower, fresh fruit, lemons, lettuce, mangos, onions, oranges, papaya, pineapple, tomatoes, fresh vegetables, watermelons), and harvested areas were taken from the EarthStat[28] dataset, as they are not included in the MIRCA dataset[10]. The total amount of GW was calculated summing green water volumes of each crop and then divided by the density of population, to obtain the water available per capita (m^3/cap/year).

Sensitivity Analysis

We also performed sensitivity analyses on the actual evapotranspiration ET_{act} referred to the growing season of the crops, considering a variation of ±15%. The committed error on actual yields (and thus on the computed crop production) depends on the magnitude of the crop yield response to water deficit, thus, on the Ky value. In our analysis we use Ky values from FAO Irrigation and Drainage Paper No. 33[20]. They have been largely validated and used in several studies to predict crop yield at different locations[29–31]. Some uncertainties related to Ky might depend on the location and the experimental methods used, as other factors (e.g. nutrients, different cultivars, etc.) might affect locally the response to water. For analysis conducted at the regional scale, as in this case, the application of FAO yield response can be considered a robust approach[31]. Ky is crop specific and depend on the growth stage the water stress occurs (higher for flowering and yield formation, lower for vegetative and ripening phases). In our analysis, we used water deficit and Ky values referred to the total growing period of the crop. As high-yielding crops (e.g. sugarcane and maize) are more sensitive to water stress (Ky>1) than low-yielding crops (e.g. sorghum) (ky<1)[30], in our sensitivity analysis we obtained different yield variation, accordingly to the considered crop.

(S6) $$Error\%_{j,i,t} = \frac{|Y_{a,j,i,t} - Y^{\pm}_{a,j,i,t}|}{Y_{a,j,t}}$$

(S7) $$\overline{E\%}_{jt} = \frac{1}{N}\sum_{i=1}^{N} Error\%_{j,i,t}$$

Where $Error\%_{j,i,t}$ is the computed percentage error on the actual yield per crop j, cell i and year t. $Y^{\pm}_{a,j,i,t}$ is the computed actual yield considering a variation of ET_{act} of ±15%, and $\overline{\boldsymbol{E\%}}_{\boldsymbol{jt}}$ is the average percentage error per each crop and year. In Figure S2(A) and Table S4 we summarize per each crop and for all the years, the average percentage error (Eq. S6-S7) committed computing the actual yield (Y_a), using the FAO approach[20], with a 15% variation of ET_{act}. Figure S3(A) reports the computed percentage error $Error\%_{j,i,t=1996}$ per crop, for a fixed year (t=1996) with respect to the actual yield (Y_a). While Figure S2(B) and Table S5 report the average percentage error committed on the production (P), and Figure S3(B) reports the percentage error on the production, for a fixed year (t=1996). The percentage error on Y_a and P is of the same magnitude of ET_{act} variation (15%) for crops with Ky=1 (coffee and oil palm fruit). For crops with Ky>1 (sugarcane, maize and pulses), the error is amplified proportionally to Ky value, with values of $\overline{\boldsymbol{E\%}}_{\boldsymbol{jt}}$ ranging from 18% to 28%, for sorghum (ky<1) the $\overline{\boldsymbol{E\%}}_{\boldsymbol{jt}}$ decreases varying from 11% to 13% (Fig. S2, Tables S4-S5).

Figure S2: Average percentage error $\overline{E\%}$, on the actual yield Ya (A) and on the production P (B) obtained varying ET_{act} of ±15%.

(A) Average percentage error on Ya

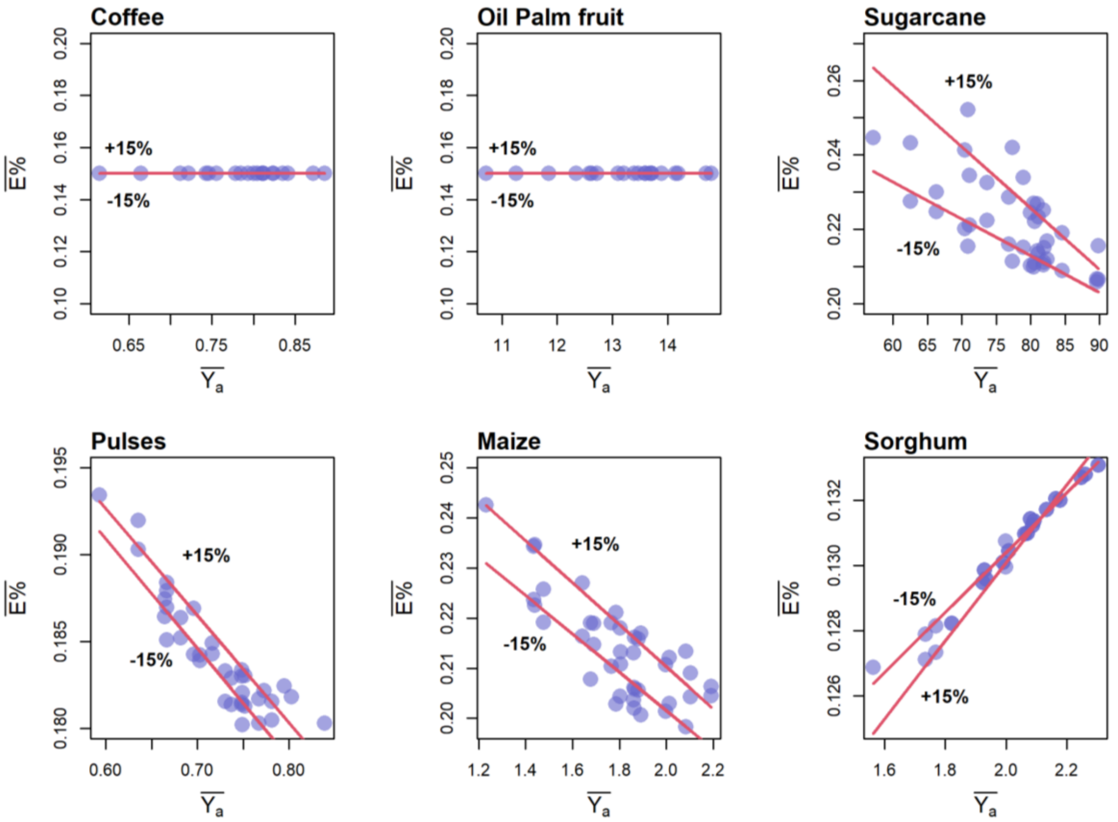

(B) Average percentage error on P

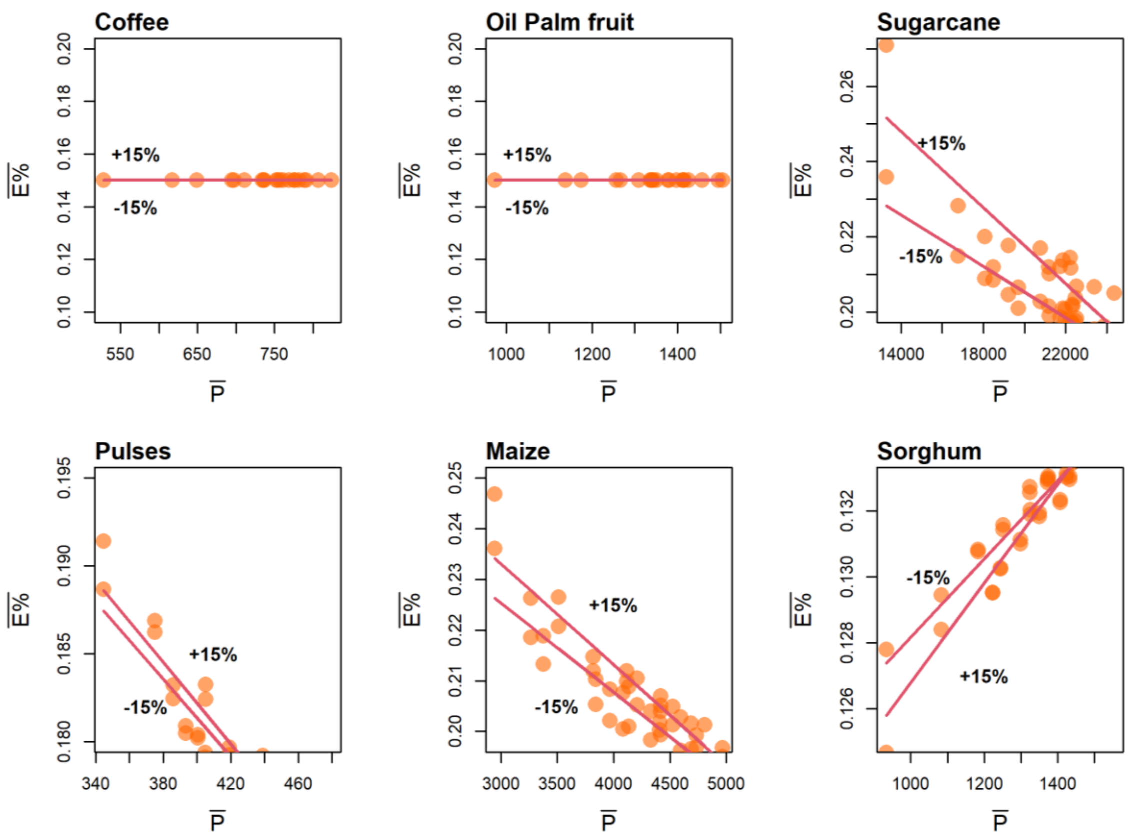

Figure S3: Computed percentage error $Error\%$ on the actual yield Ya (A) and on the production P (B), for a fixed year (1996), obtained varying ET_{act} of ±15%.

(A) Percentage error on Ya

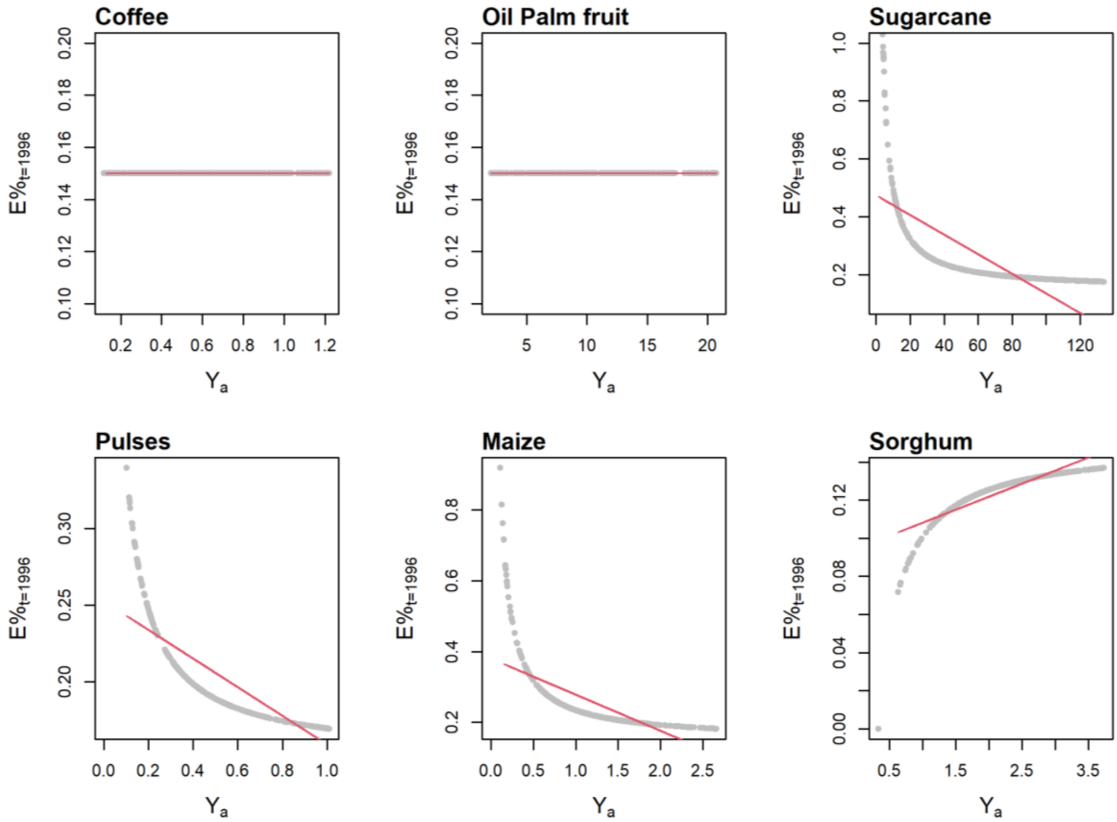

(B) Percentage error on P

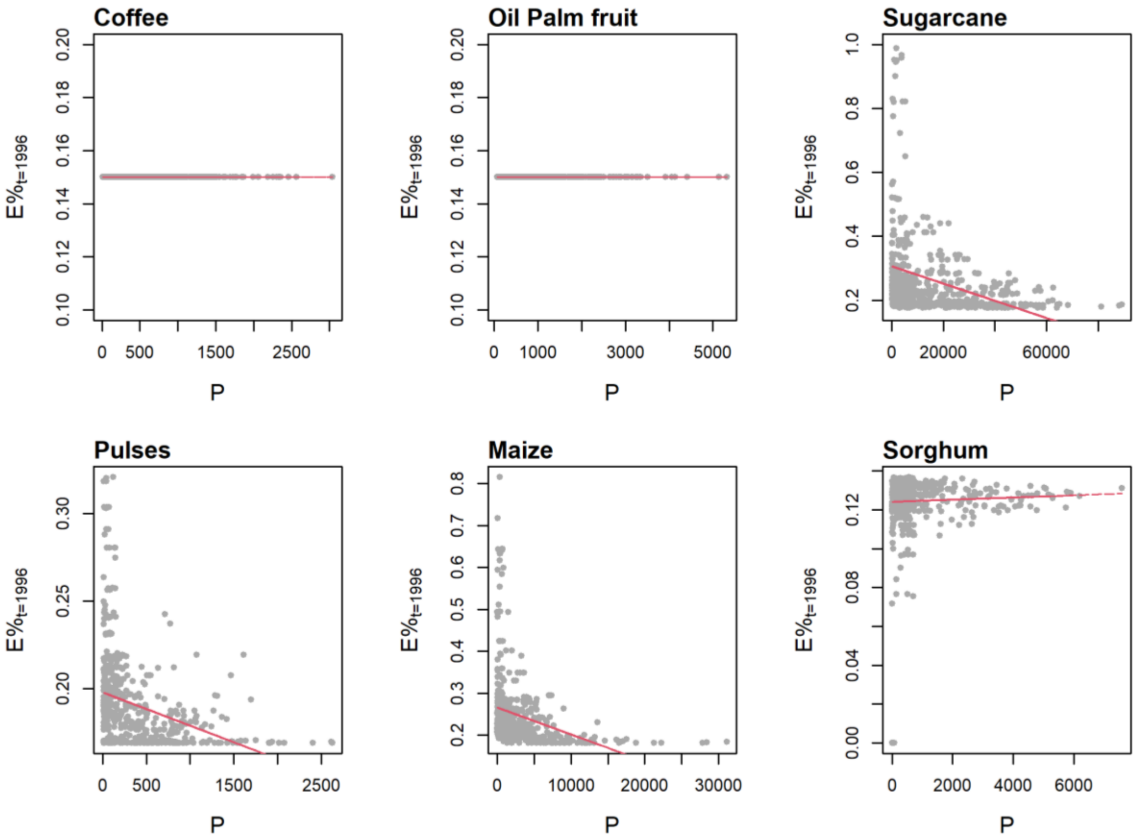

Table S4: Computed percentage error $\overline{E\%}$ on the actual yield per crop and year t.

Crop/Year		1996	1997	1998	1999	2000	2001	2002	2003	2004	2005
Coffee	Ya^-	0.15	0.15	0.15	0.15	0.15	0.15	0.15	0.15	0.15	0.15
	Ya^+	0.15	0.15	0.15	0.15	0.15	0.15	0.15	0.15	0.15	0.15
Oil palm fruit	Ya^-	0.15	0.15	0.15	0.15	0.15	0.15	0.15	0.15	0.15	0.15
	Ya^+	0.15	0.15	0.15	0.15	0.15	0.15	0.15	0.15	0.15	0.15
Sugarcane	Ya^-	0.28	0.24	0.23	0.22	0.23	0.24	0.23	0.23	0.23	0.25
	Ya^+	0.24	0.23	0.22	0.21	0.21	0.22	0.22	0.22	0.21	0.22
Pulses	Ya^-	0.20	0.19	0.19	0.19	0.18	0.19	0.18	0.18	0.18	0.18
	Ya^+	0.19	0.19	0.19	0.18	0.18	0.19	0.18	0.18	0.18	0.18
Maize	Ya^-	0.25	0.23	0.23	0.22	0.21	0.23	0.22	0.22	0.22	0.21
	Ya^+	0.24	0.22	0.22	0.21	0.20	0.22	0.21	0.21	0.21	0.20
Sorghum	Ya^-	0.12	0.13	0.13	0.13	0.13	0.13	0.13	0.13	0.13	0.13
	Ya^+	0.13	0.13	0.13	0.13	0.13	0.13	0.13	0.13	0.13	0.13

Crop/Year		2006	2007	2008	2009	2010	2011	2012	2013	2014	2015	2016
Coffee	Ya^-	0.15	0.15	0.15	0.15	0.15	0.15	0.15	0.15	0.15	0.15	0.15
	Ya^+	0.15	0.15	0.15	0.15	0.15	0.15	0.15	0.15	0.15	0.15	0.15
Oil palm fruit	Ya^-	0.15	0.15	0.15	0.15	0.15	0.15	0.15	0.15	0.15	0.15	0.15
	Ya^+	0.15	0.15	0.15	0.15	0.15	0.15	0.15	0.15	0.15	0.15	0.15
Sugarcane	Ya^-	0.24	0.23	0.23	0.22	0.22	0.23	0.21	0.22	0.22	0.22	0.22
	Ya^+	0.21	0.22	0.21	0.21	0.21	0.22	0.21	0.21	0.21	0.21	0.21
Pulses	Ya^-	0.18	0.18	0.18	0.18	0.18	0.18	0.18	0.18	0.19	0.19	0.18
	Ya^+	0.18	0.18	0.18	0.18	0.18	0.18	0.18	0.18	0.19	0.19	0.18
Maize	Ya^-	0.21	0.21	0.21	0.22	0.21	0.22	0.21	0.21	0.22	0.23	0.22
	Ya^+	0.21	0.20	0.20	0.20	0.20	0.20	0.20	0.20	0.21	0.22	0.20
Sorghum	Ya^-	0.13	0.13	0.13	0.13	0.13	0.13	0.13	0.13	0.13	0.13	0.13
	Ya^+	0.13	0.13	0.13	0.13	0.13	0.13	0.13	0.13	0.13	0.13	0.13

Table S5: Computed percentage error $\overline{E\%}$ on the production per crop and year t.

Crop/Year		**1996**	**1997**	**1998**	**1999**	**2000**	**2001**	**2002**	**2003**	**2004**	**2005**
Coffee	**P^-**	0.15	0.15	0.15	0.15	0.15	0.15	0.15	0.15	0.15	0.15
	P^+	0.15	0.15	0.15	0.15	0.15	0.15	0.15	0.15	0.15	0.15
Oil palm fruit	**P^-**	0.15	0.15	0.15	0.15	0.15	0.15	0.15	0.15	0.15	0.15
	P^+	0.15	0.15	0.15	0.15	0.15	0.15	0.15	0.15	0.15	0.15
Sugarcane	**P^-**	0.27	0.23	0.21	0.20	0.21	0.22	0.22	0.21	0.21	0.22
	P^+	0.24	0.21	0.21	0.20	0.20	0.21	0.20	0.20	0.20	0.20
Pulses	**P^-**	0.19	0.18	0.18	0.18	0.17	0.19	0.18	0.18	0.18	0.18
	P^+	0.19	0.18	0.18	0.18	0.17	0.19	0.18	0.18	0.18	0.18
Maize	**P^-**	0.25	0.23	0.22	0.21	0.20	0.23	0.21	0.21	0.20	0.20
	P^+	0.24	0.22	0.21	0.21	0.19	0.22	0.21	0.20	0.20	0.20
Sorghum	**P^-**	0.12	0.13	0.13	0.13	0.13	0.13	0.13	0.13	0.13	0.13
	P^+	0.13	0.13	0.13	0.13	0.13	0.13	0.13	0.13	0.13	0.13

Crop/Year		**2006**	**2007**	**2008**	**2009**	**2010**	**2011**	**2012**	**2013**	**2014**	**2015**	**2016**
Coffee	**P^-**	0.15	0.15	0.15	0.15	0.15	0.15	0.15	0.15	0.15	0.15	0.15
	P^+	0.15	0.15	0.15	0.15	0.15	0.15	0.15	0.15	0.15	0.15	0.15
Oil palm fruit	**P^-**	0.15	0.15	0.15	0.15	0.15	0.15	0.15	0.15	0.15	0.15	0.15
	P^+	0.15	0.15	0.15	0.15	0.15	0.15	0.15	0.15	0.15	0.15	0.15
Sugarcane	**P^-**	0.24	0.23	0.23	0.22	0.22	0.23	0.21	0.22	0.22	0.22	0.22
	P^+	0.21	0.22	0.21	0.21	0.21	0.22	0.21	0.21	0.21	0.21	0.21
Pulses	**P^-**	0.18	0.18	0.18	0.18	0.18	0.18	0.18	0.18	0.19	0.19	0.18
	P^+	0.18	0.18	0.18	0.18	0.18	0.18	0.18	0.18	0.19	0.19	0.18
Maize	**P^-**	0.21	0.21	0.21	0.22	0.21	0.22	0.21	0.21	0.22	0.23	0.22
	P^+	0.21	0.20	0.20	0.20	0.20	0.20	0.20	0.20	0.21	0.22	0.20
Sorghum	**P^-**	0.13	0.13	0.13	0.13	0.13	0.13	0.13	0.13	0.13	0.13	0.13
	P^+	0.13	0.13	0.13	0.13	0.13	0.13	0.13	0.13	0.13	0.13	0.13

Virtual-Water and Food Trade. Trade associated to food and virtual water fluxes was modelled through two variables of green water availability and food availability, developed summing the local availability to the supply provided by domestic trade. In this analysis we considered a fixed value of food imports from international trade, while for national flows the *Production and Trade Flow Maps* and *Livelihoods Zones* by FEWS NET[32–35] were used to select the main agricultural producer departments, that provide food to the cities. The normalized difference (Δ, Eq. S8) between the food (FA) and water availability (GWA) and the demand, given by the HER and GWD_j thresholds respectively, was calculated per cell as indicator of Deficit (Δ<0) or Surplus (Δ≥0).

(S8) $$\Delta = \frac{\Delta_f + \Delta_w}{2} = \frac{1}{2}\left(\frac{\mathbf{FA-HER}}{\mathbf{HER}} + \frac{\mathbf{GWA-GWD_j}}{\mathbf{GWD_j}}\right)$$

Cells in the domain have then been categorized into three macro groups (importers, exporters or none) according to the value of Δ. A value of $\Delta \geq 1$ corresponded to food-importing cells in the main metropolitan areas; while a value of $\Delta \leq -2$ was used to define exporting cells within the main food-provider departments[32]. Surplus of food (kcal/year) and water (m^3/year) was then calculated for each exporting cell *n*, and then summed to obtain the total domestic surplus per year *t* and country *j* (Eq. S9-S11). Demand of food (kcal/year) and water (m3/year) is calculated for each importing cell m (Eq. S12-S14). Domestic surplus is redistributed per each importing cell proportionally to the demand in the cell, through a spatial weight matrix $\widetilde{W}$ (Eq. S15-S16). To keep into account trade, the imported surplus per each cell *m* was then summed to the food and water available in the same cell. The population density[3] in exporting ($\mathrm{P_{nt}}$) or importing ($\mathrm{P_{mt}}$) cells is accounted, as it affects the redistribution of food and water, influencing both the demand and the surplus of food.

(S9) $$\mathbf{Food\ Surplus_{nt}} = (\mathbf{HER} - \mathbf{FA_{nt}}) * \mathbf{P_{nt}}$$
(S10) $$\mathbf{GW\ Surplus_{nt}} = (\mathbf{GWD_j} - \mathbf{GWA_{nt}}) * \mathbf{P_{nt}}$$
(S11) $$\mathbf{Domestic\ Surplus_{jt}} = \sum_{\mathbf{n \subseteq j}}^{\mathbf{M}} \mathbf{Surplus_{nt}}$$

(S12) $$\mathbf{Food\ Demand_{mt}} = (\mathbf{FA_{mt}} - \mathbf{HER}) * \mathbf{P_{mt}}$$
(S13) $$\mathbf{GW\ Demand_{mt}} = (\mathbf{GWA_{mt}} - \mathbf{GWD_j}) * \mathbf{P_{mt}}$$
(S14) $$\mathbf{Domestic\ Demand_{jt}} = \sum_{\mathbf{m \subseteq j}}^{\mathbf{M}} \mathbf{Demand_{mt}}$$

(S15) $$\mathbf{Imported\ Surplus_{mt}} = \mathbf{Domestic\ Surplus_{jt}} * \widetilde{\boldsymbol{W}}$$

where weights of $\widetilde{W}$ are given by: $\widetilde{w}_{m,j,t} \mid \sum_m^M \widetilde{w}_{m,j,t} = 1$

(S16) $$\widetilde{\mathbf{w}}_{\mathbf{m,j,t}} = \frac{\mathbf{Demand_{mt}}}{\mathbf{Domestic\ Demand_{jt}}}$$

The gap between demand and imported surplus per each importing cell *m* was then calculated (Eq. S17) as ratio of the food demand and the imported surplus.

(S17) $$\mathbf{Demand - Surplus\ Gap_{mt}} = \frac{\mathbf{Demand_{mt}}}{\mathbf{Imported\ Surplus_{mt}}}$$

S3. The Bayesian Zero-Inflated Poisson econometric model

The econometric implementation

Bayesian inference is selected to avoid overfitting as a result of the presence of several heterogeneous parameters[36]. An independent and efficient model design[37,38] is adopted selecting a square grid with a spatial resolution of 20 km x 20 km and a temporal dimension of one year. To reduce heterogeneity and enable comparability, all the variables are normalized within their annual distribution. We selected a Zero-Inflated Poisson[39] (ZIP) regression (Eq. S18) to model conflict count data characterized by excess of zeros. The ZIP model draws only-zero observations with probability θ, and observations from a *Poisson (*λ) distribution, with probability (1 – θ). Hence:

(S18)
$$\begin{cases} \mathbf{P(y=0)} \;=\; \boldsymbol{\theta} + (\mathbf{1}-\boldsymbol{\theta})\mathbf{e}^{-\boldsymbol{\lambda}} \\ \mathbf{P(y=k)} \;=\; (\mathbf{1}-\boldsymbol{\theta})\boldsymbol{Poisson}(\mathbf{k};\boldsymbol{\lambda}),\;\; \mathbf{k}=\mathbf{1},\mathbf{2},.. \end{cases}$$

The empirical hierarchical structure of θ and λ is reported in Eq.s S19-S20. The logarithm of the Poisson intensity parameter λ is a linear function of the covariates. The spatial autocorrelation was modelled via the Spatially Lagged Explanatory Variables X (SLX)[40] specification in the intensity λ, through exogenous spatial interaction effects among covariates, involving neighboring spatial units, namely spatial spillovers[36].

(S19)
$$\log \lambda_{it} = \beta_{0t} + X_t\beta_t + \mathbf{W}X_t\xi_t$$

where $\beta_{k,t} \sim N\left(0, \sigma_{\beta_{k,t}}\right)$ is the regression coefficient, accounting for direct spatial effects, related to the *k*[th] exogenous explanatory variable, for all *k*. Coefficient $\xi_{k,t} \sim N\left(0, \sigma_{\xi_{k,t}}\right)$ is the spatial spillovers, associated with the spatially lagged explanatory variable $\mathbf{W}X_{k,t}$. Matrix $\mathbf{W}$ is the first-order contiguity matrix that has null elements $w_{ij} = 0$ on the principal diagonal and $w_{ij} = 1$ if cell *i* and cell *j* are neighbors. An informative uniform priori distribution for the hyperparameters σ_β and $\sigma_{\boldsymbol{\xi}}$ is selected: $\sigma_{\beta_{k,t}} \sim \mathrm{U}(0,10), \sigma_{\boldsymbol{\xi}_{k,t}} \sim \mathrm{U}\,(0,10)$.

The logistic probability distribution is defined through θ (probability mass in zero):

(S20)
$$\mathrm{logit}\,(\theta_{it}) = \gamma_{0t} + \gamma_t X_t$$

where $\gamma_{k,t} \sim N\left(0, \sigma_{\gamma_{k,t}}\right)$ is the regression coefficient, accounting for direct effects, related to the *k*[th] exogenous explanatory variable $X_{k,t}$, being $\sigma_{\gamma_{k,t}} \sim \mathrm{U}(0,10)$.

The statistical computations and graphics were performed with the R package[41], and the models were coded in Stan[42] . Stan uses Markov chain Monte Carlo (MCMC) techniques and the Gibbs sampling algorithm[43] to generate samples from the posterior distribution for full Bayesian inference. For each model a simulation of one MCMC chain with 100,000 iterations, a burn-in of 50,000 iterations, and a thinning of 10 was performed. Therefore, the final sample is made up of 5,000 simulated values. The convergence diagnostics (Geweke test, traceplot, autocorrelation function), computed for all parameters of each model, indicated that convergence was achieved. A check of robustness was made varying the hyperparameters given by the variances; homogeneous results in terms of posteriori means and medians and Bayesian 90% credible intervals were obtained for each coefficient.

Bayesian goodness-of-fit methods

A Bayesian comparison of the models was performed by computing the logarithm of the pseudo-marginal likelihood (LPML), and the Bayesian percentage outliers with level 90% for every model. A good fit for the SLX implementation of the ZIP models was obtained, with a percentage of total Bayesian outliers per year <2% (Table S6). Results show that the SLX model specification generally led to good model fitting performance, confirming that SLX is the simplest econometric implementation to model flexibly spatial spillover[36,44]. LPML is defined in Eq. S19 as the sum of the logarithms of the Conditional Predictive Ordinates (CPO), and each CPO_{it} is given by the value of the posterior-predictive density evaluated at the actual Y_{it}, conditionally to the sample Y_{it} not containing any data from cell *i* at year *t*. The larger the value of the CPO's (and hence the larger the value of the LPML), the better the fit of the model. Last, Bayesian outliers with level 90% occur when the real density Y_{it} falls into one of the two 5% tails of the marginal posterior-predictive density.

(S21) $$\mathbf{LPML_i} = \sum_{i=1}^{n} \log \mathbf{CPO_{it}}$$

The CD model resulted with an average LPML over years of -1264.27, that is of two orders of magnitude lower than the other models, confirming that the CD model cannot be selected as best performing and explanatory model. Once the best models were determined, following Gelman *et al.* (1996)[45], the fit to the data was evaluated through the chi-squared discrepancy measure. The analysis of discrepancy is a method of posterior predictive checks, in which the observed data are compared to data replicated. The discrepancy referred to the observed data D(y, θ) can be modelled through chi-square X^2 statistic (Eq. S20) and compared to the discrepancy of the replicated data $D(y^{rep}, \theta)$ to check if the model fits the observed data. The Bayesian p-value (P_B) indicates the probability that the discrepancy referred to predictive sample $D(y^{rep}, \theta)$, is more extreme than the observed measure D (y, θ). A p-value close to 0.50 represents adequate model fit.

(S22) $$\mathbf{X^2}(\mathbf{y};\boldsymbol{\theta}) = \sum_{i=1}^{n} \frac{\left(\mathbf{y_i} - \mathbf{E}(\mathbf{y_i}|\boldsymbol{\theta})\right)^2}{\mathbf{Var}\,(\mathbf{y_i}|\boldsymbol{\theta})}$$

Table S6. Bayesian 90% outliers for the computed CWF, CWFs and CWFt models. Bayesian outliers have been reported in per year and calculated as the percentage of observations that don't fall in the 10% credibility interval of the posterior distribution.

Model	1997	1998	1999	2000	2001	2002	2003	2004	2005	2006
CWF	0.7%	1.2%	0.7%	2.1%	1.9%	1.9%	1.7%	2.3%	1.9%	1.2%
CWFs	0.5%	0.9%	0.7%	1.6%	1.4%	1.9%	1.9%	1.6%	1.2%	0.9%
CWFt	0.7%	1.2%	0.7%	2.1%	2.1%	1.9%	2.1%	1.9%	1.6%	1.0%

Model	2007	2008	2009	2010	2011	2012	2013	2014	2015	2016
CWF	2.1%	0.5%	1.9%	0.5%	0.7%	1.2%	1.0%	1.0%	1.2%	1.9%
CWFs	1.7%	0.5%	1.2%	0.3%	0.3%	1.4%	0.7%	1.0%	1.6%	1.9%
CWFt	2.3%	0.5%	1.7%	0.5%	0.7%	1.2%	1.0%	1.2%	1.6%	2.3%

Supplementary Notes

S4. Urban conflicts characterization

High levels of violence and criminality in Central American cities are generated by youth street gangs who create territories within the settlements and engage in drug-taking and homicides[46]. Other types of violence are mainly transnational organized crime, domestic violence, drug trafficking and corruption[47]. Poverty and inequality have consistently been recognized as key variables behind high rates of crime[47–49]. Moreover, the economic globalization and the 1990s transition from authoritarian rule to democratic institution, accompanied by civil war, produced a social disruptive process of unemployment and migration, dynamics of translocation and segregation of urban spaces[49,50]. The rise of criminal economies around the transnational drug business, the state weakness, and the existence of a predominantly young population have also been pointed to as driving factors behind Central American violence[46,47,49,51].

From the literature we know that armed conflicts tend to cluster spatially in certain geographic areas[52–55]. On the other hand, cities, with their high population densities, behave as ‘pools’ of recruits[56]. Indeed, geographical proximity tends to enhance collective action of groups intended to exploit the state incapacity as reaction to alienation and segregation[54]. Moreover, a similar tendence to spatial aggregation of conflicts in urban contexts can be observed in all Central America countries. As suggested by some studies[52,55,56] this might be the result of a process of violence diffusion occurring among confining countries with transnational ethnic linkages and similar characteristics that increase the risk of conflict, as country poverty and an autocratic regime. In our analysis, to study local trends of food security and conflicts (Fig.s S4-S7), we selected the peri-urban area[4] (approximately 900 km^2) surrounding the main urban centers that resembles the geographical extent of conflict clusters. Indeed, the urban dimension might include also peri-urban areas, as they contribute in shaping food security of the rural-urban food system[4,57]. It is plausible that urban conflicts associated to a phase of food insecurity develop with a certain delay - that is difficult to estimate due to the different seasonality of agricultural calendars and the endemic presence of violence in these countries - with respect to the emergence of food shortage conditions. We reasonably assume a time lag ranging from few months to one year. For consistency, we have also tested other lags. The Social Conflict Analysis Database (SCAD)[2] collects information on protests, riots, strikes, and other social disturbances, in Africa, Latin American and the Caribbean, from 1990 to 2017. The dataset provides detailed information for each event, such as, the location, the date, the issues, duration, escalation, etc., for each event also a brief description of the incident is provided. In our analysis we classified conflict events accondirngly to the first *issue* mentioned as source of the tension/disorder. We considered seven typologies of conflict event, summarizing the information provided in the dataset: discrimination (that includes ethnic and religious discrimination), economy (economy, job and subsistence, economic resources), violence (domestic war, violence, terrorism), internal policy (elections, pro-government), foreign affairs, human rights, environment (environmental degradation). In Fig S8 the urban conflicts occurred from 1996 to 2016 in the main cities are reported for each typology as percentage of the total number of events occurred. The majority depend on issues related to violence (39%), economy (20%) and internal policy (20%). Environmental degradation (1%) and discrimination (3%) causes are less relevant, even if they can be hidden by other more prominent issues (such as economy and politics).

Figure S4: Food security trends and conflict occurrences. The reference area is the urban, peri-urban zone surrounding the capital city of San Salvador, in El Salvador. The temporal scale refers to conflict occurrence (year t), while food availability oscillations have been reported with a temporal delay of six months. Most intense food security falls have been related to the evidence of the '*canicula*'. It becomes visible when comparing the precipitation pattern of a specific drought year to the average precipitation rates of the historical series. Rain trends have been reported both for the same area of conflicts occurrence (a) and the related food-suppliers (b), (c).

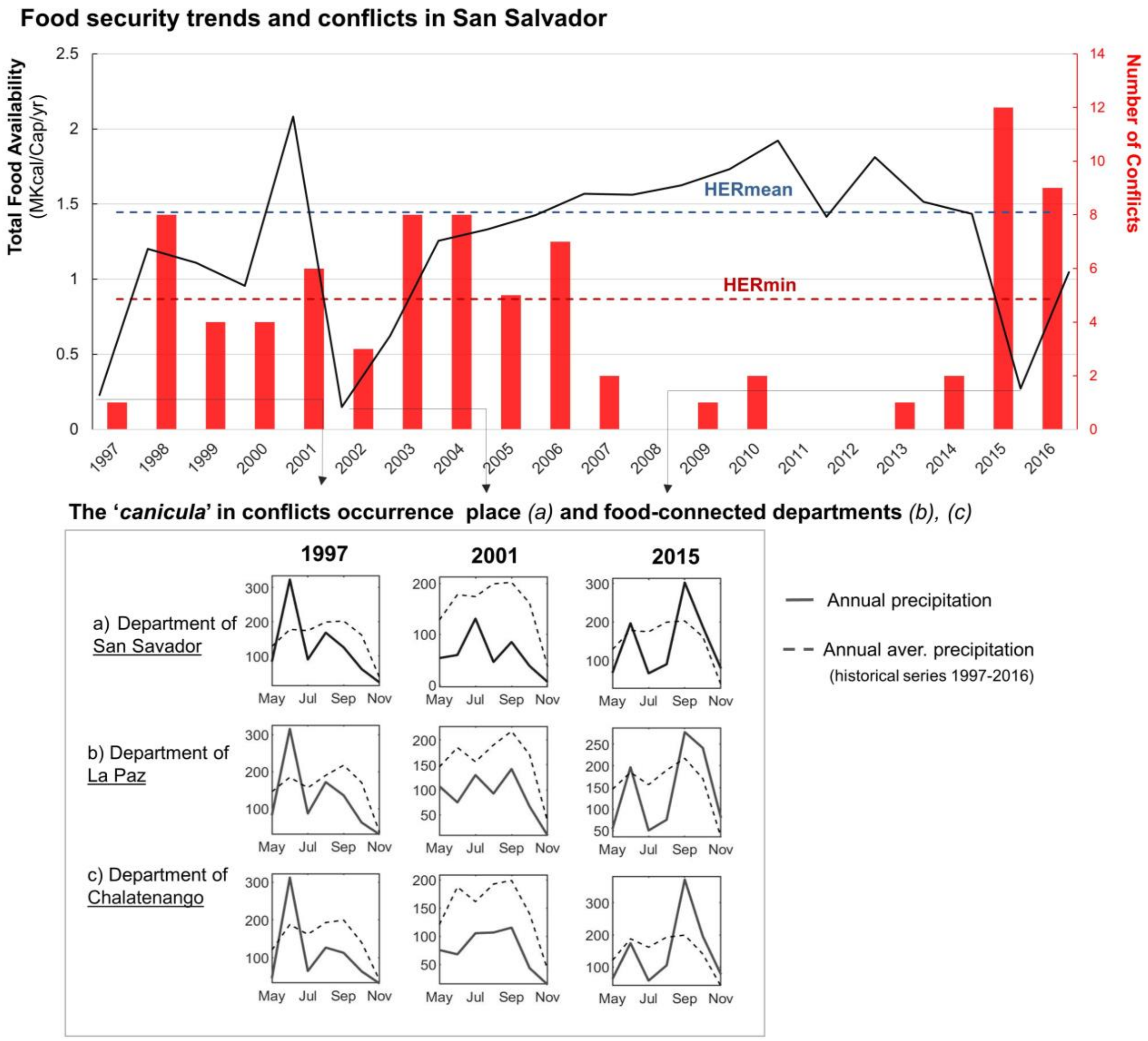

Figure S5: Food security trends and conflict occurrences. They refer to the urban and peri-urban area surrounding Guatemala City. Food security drops can be related to the evidence of the '*canicula*', which have been assessed by comparing the precipitation pattern of the specific year to the average precipitation rates of the historical series for the reference areas of conflict occurrence *(a)* and food-supplier departments *(b), (c).*

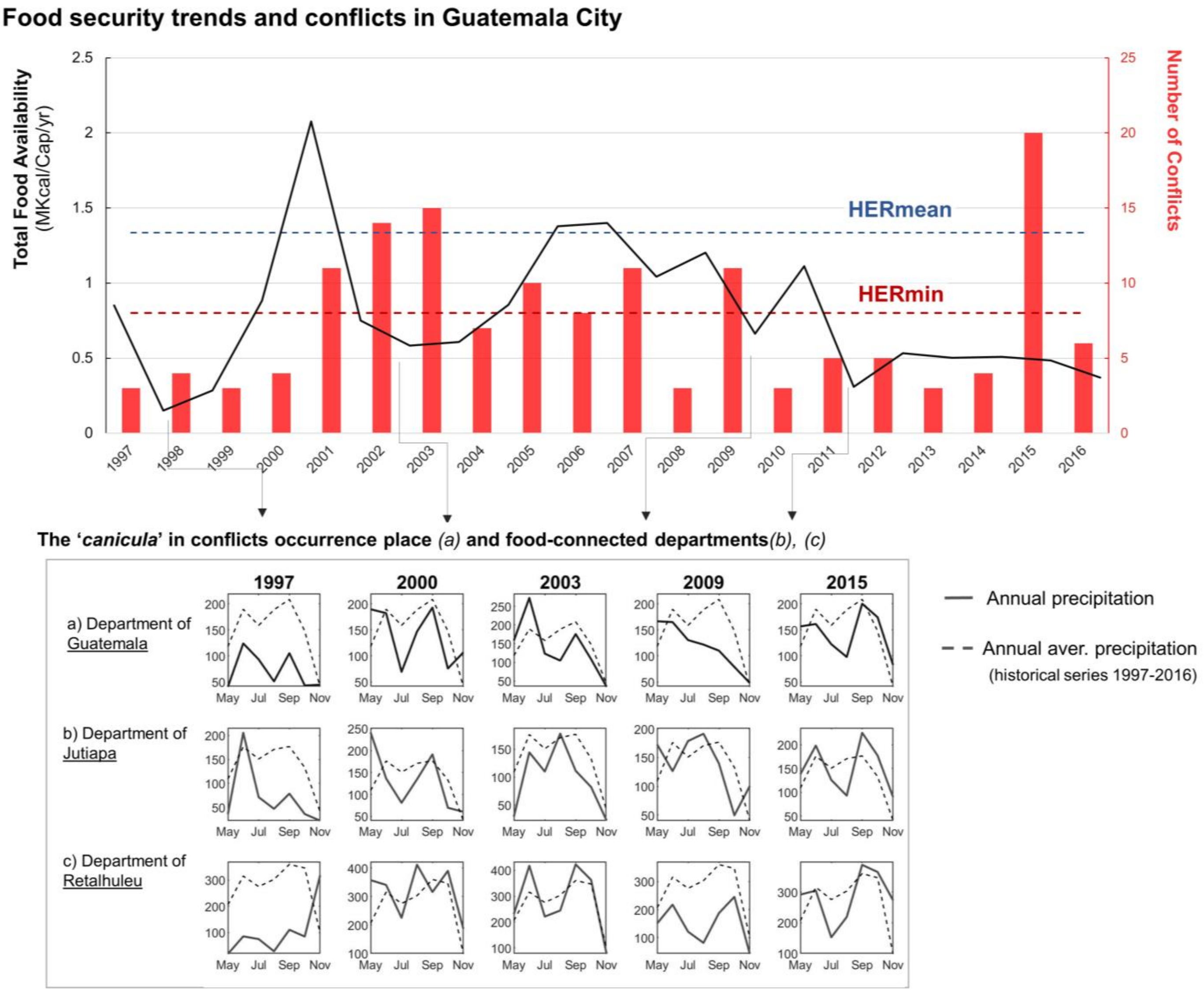

Figure S6: Food security trends and conflict occurrences. They refer to the urban and peri-urban area surrounding the capital city of Honduras, Tegucigalpa. Food security drops can be related to the evidence of the '*canicula*', which have been assessed by comparing the precipitation pattern of the specific year to the average precipitation rates of the historical series for the reference areas of conflict occurrence *(a)* and food-supplier department *(b).*

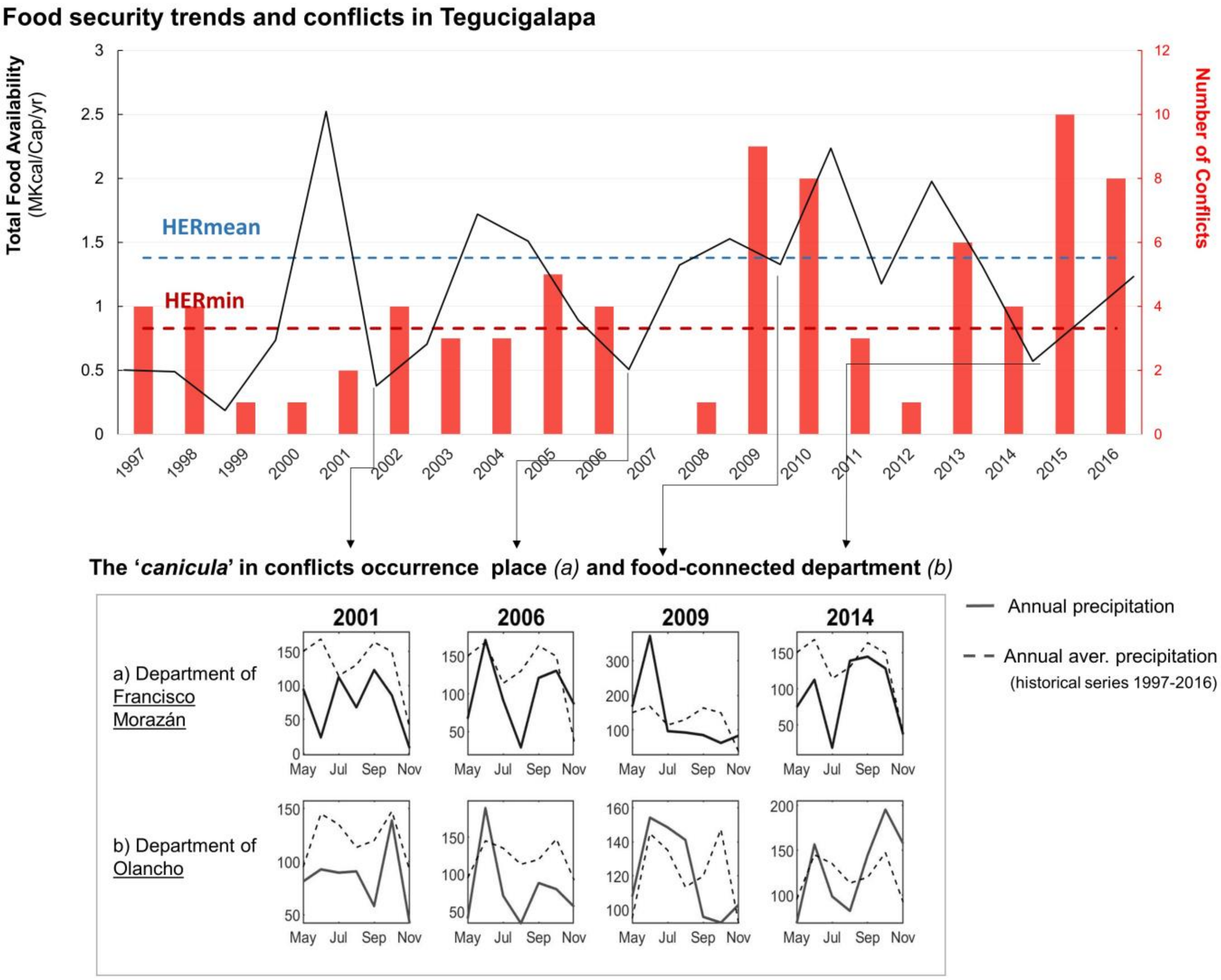

Figure S7: Food security trends and nature of conflicts. They refer to the urban and peri-urban area surrounding the three capital cities of Honduras (a), Guatemala (b) and El Salvador (c). Seven types of conflict issue have been identified basing on the classification and the event description provided by SCAD (2).

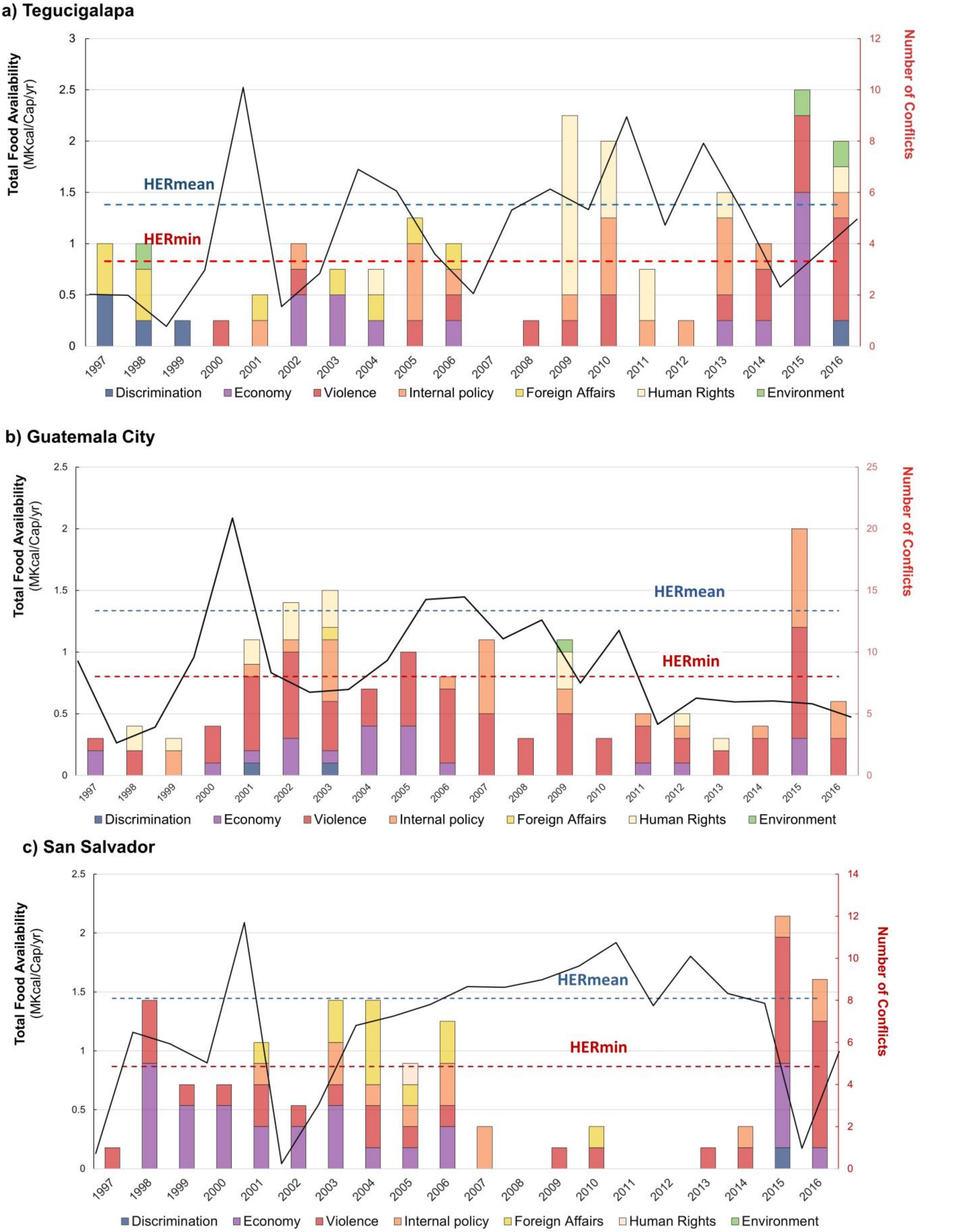

Figure S8: The seven typologies of conflicts. The total number of conflicts has been represented with a subdivision into seven classes related the issue/nature of the events. The conflicts occurrences are reported in the pie chart as percentage of the total conflicts observed in the three cities between 1996 and 2016. Those classes have been identified thanks to dataset information and description provided by SCAD[2].

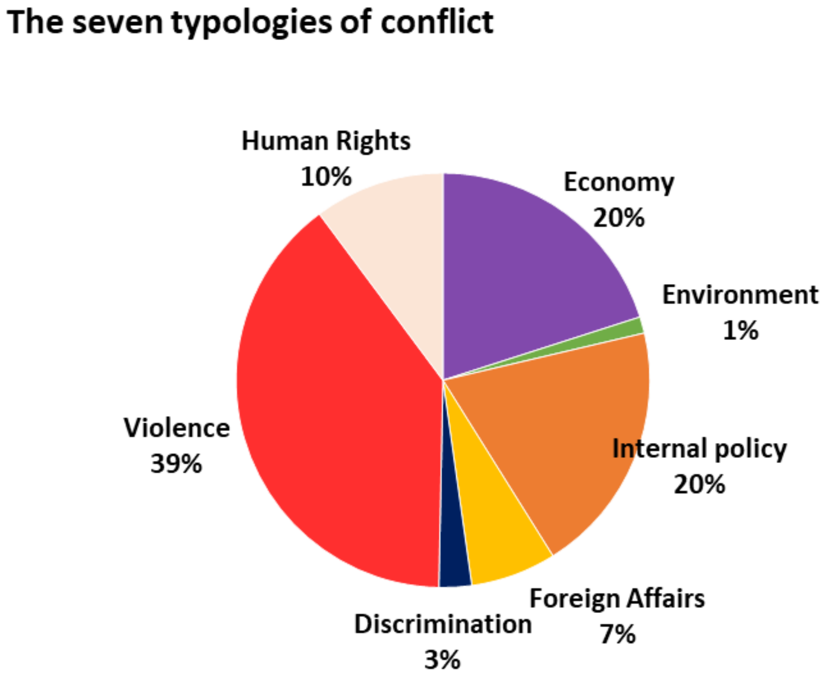

S5. The major drought events and the Conflict-Drought (CD) model

In Fig.s S9-S11, results in terms of Bayesian credibility intervals for the CD model are reported. In Fig. S9, it is evident that, in most of cases, the effects of a drought are perceived with a certain delay, that may vary according to the event characteristics (severity, impact and duration) and geographic localization. The temporal influence of the impacts of each event was defined as the double of the real duration of the event. Immediate influence has resulted for the events occurred in 1997 and 1998. Especially the drought occurred in 1998 is related to one of the most intense El-Niño events globally registered; in Central America it was associated with severe wildfire spreading through Mexico, Guatemala, Nicaragua, Honduras, El Salvador and Costa Rica and it is responsible of burning around 2 million of hectares of land. In the beginning of 1998, the livestock subsector suffered major damage due to the reduced availability of pasture areas[8]. Delayed effects can be observed for droughts in 2000 and 2001 for the subsequent few years. Drought events in 2000-2001, even if not related to the El Niño phenomenon, represents the most important recent drought in terms of the severity of its impacts. This event caused food insecurity and hunger for between 600 thousand and 1.5 million people affected by hunger and food insecurity[58]. Particularly severe were the consequences perceived in Honduras, where huge losses interested the industrial sector, behind the agricultural: 542 million US dollars, equivalent to 36% of regional losses. Moreover 1.8 million people suffered from lack of potable water. In 2009 and 2014 relevantly intense events were registered in all the region. Nutrition, basic agriculture and employment sectors resulted affected in the three countries. Bean, sorghum, corn, and cassava production decreased by more than 50% and 25.6% of households reported job losses due to drought[8]. Effects were perceived both immediately and delayed (the temporal influence of 2014 event was limited by the data availability). Drought events occurred in the years 2002, 2004, 2012 interested mainly Honduras, their impact resulted to influence conflicts uniformly throughout their entire duration of perception.

Figure S9: 90% Bayesian credible intervals of direct effects of the Poisson intensity λ, under Droughts-Conflict Nexus (DC) Model. Credible intervals are shown for time-lagged drought's intensity covariate and are drowned from a sample of 5,000 posterior simulated values. Solid blue circles denote the posterior medians, red cross points denote posterior means.

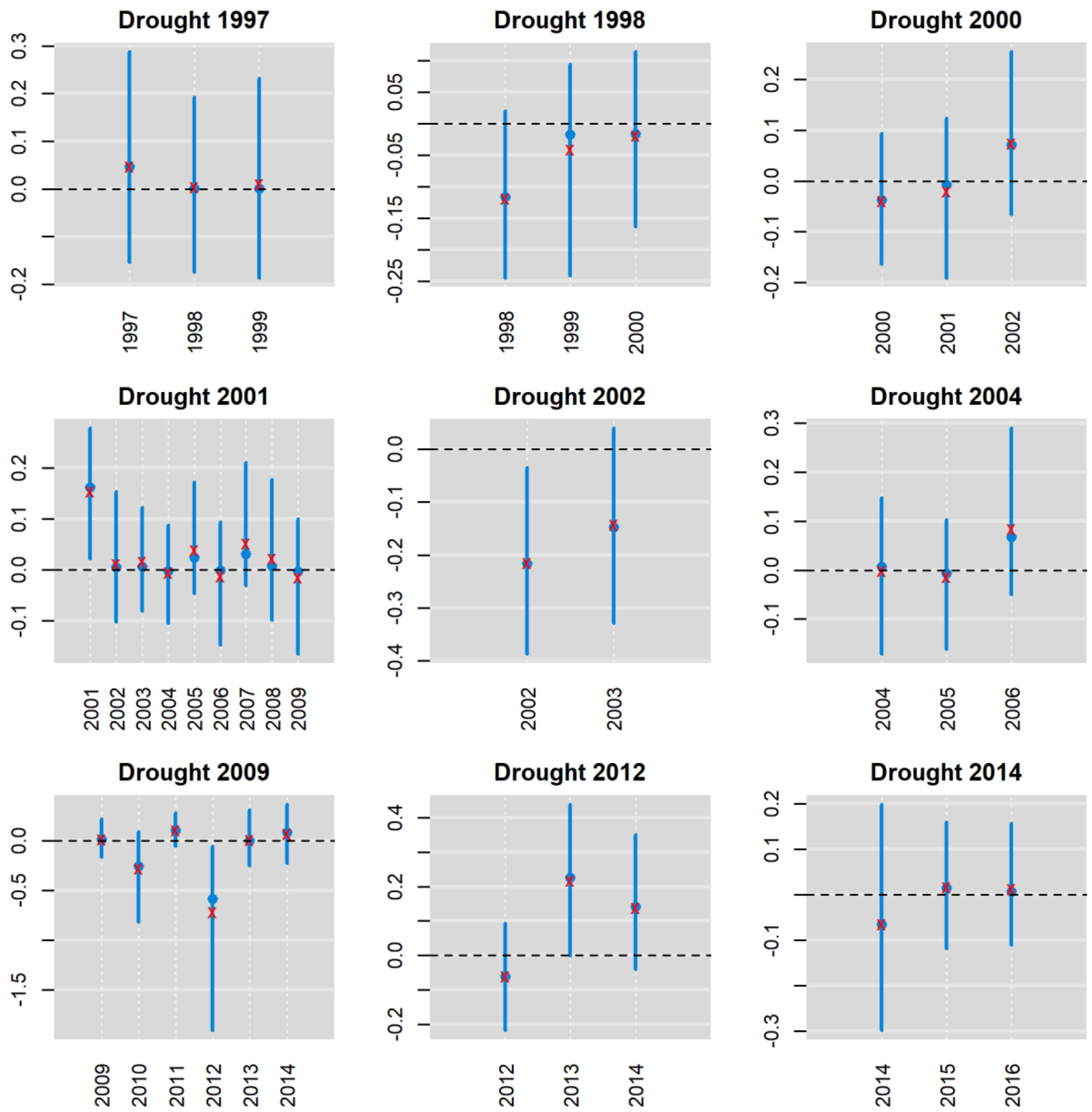

Figure S10: 90% Bayesian credible interval of the direct effect of population density on the Poisson intensity λ, under Droughts-Conflict Nexus (DC) Model. Solid blue circles denote the posterior medians, red cross points denote posterior means. Bayesian credible intervals are drowned from a sample of 5,000 posterior simulated values.

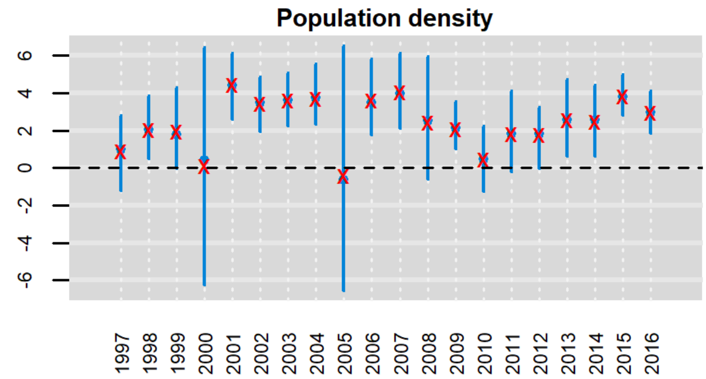

Figure S11: 90% Bayesian credible intervals of the direct effects of population density and Human Development Index on the point mass zero θ, under Droughts-Conflict Nexus (DC) Model. Solid blue circles denote the posterior medians, red cross points denote posterior means. Bayesian credible intervals are drowned from a sample of 5,000 posterior simulated values.

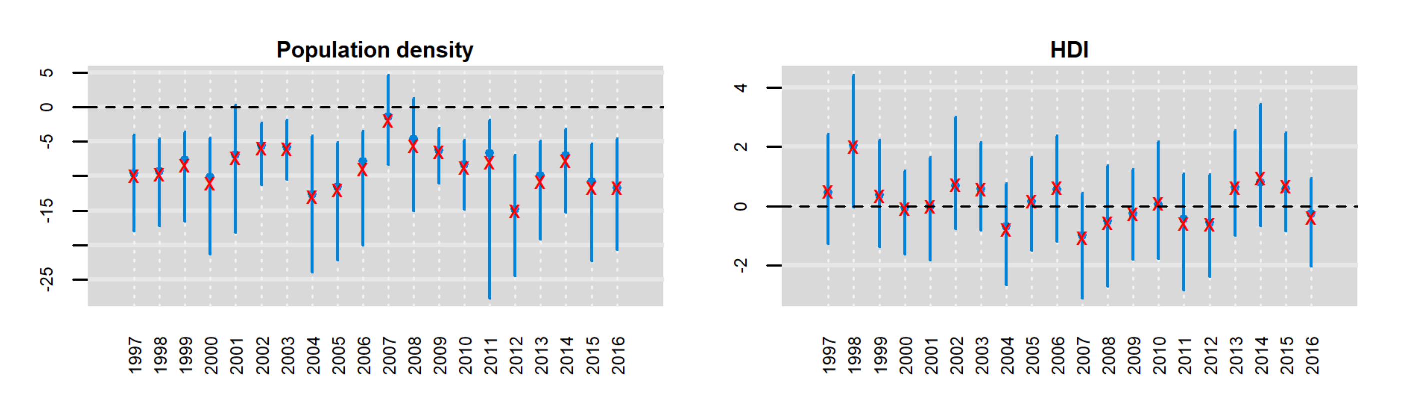

Additional Supplementary Figures and Tables

Figure S12: Country average diet pattern in Central America. Source: FAO food balance sheets[54].

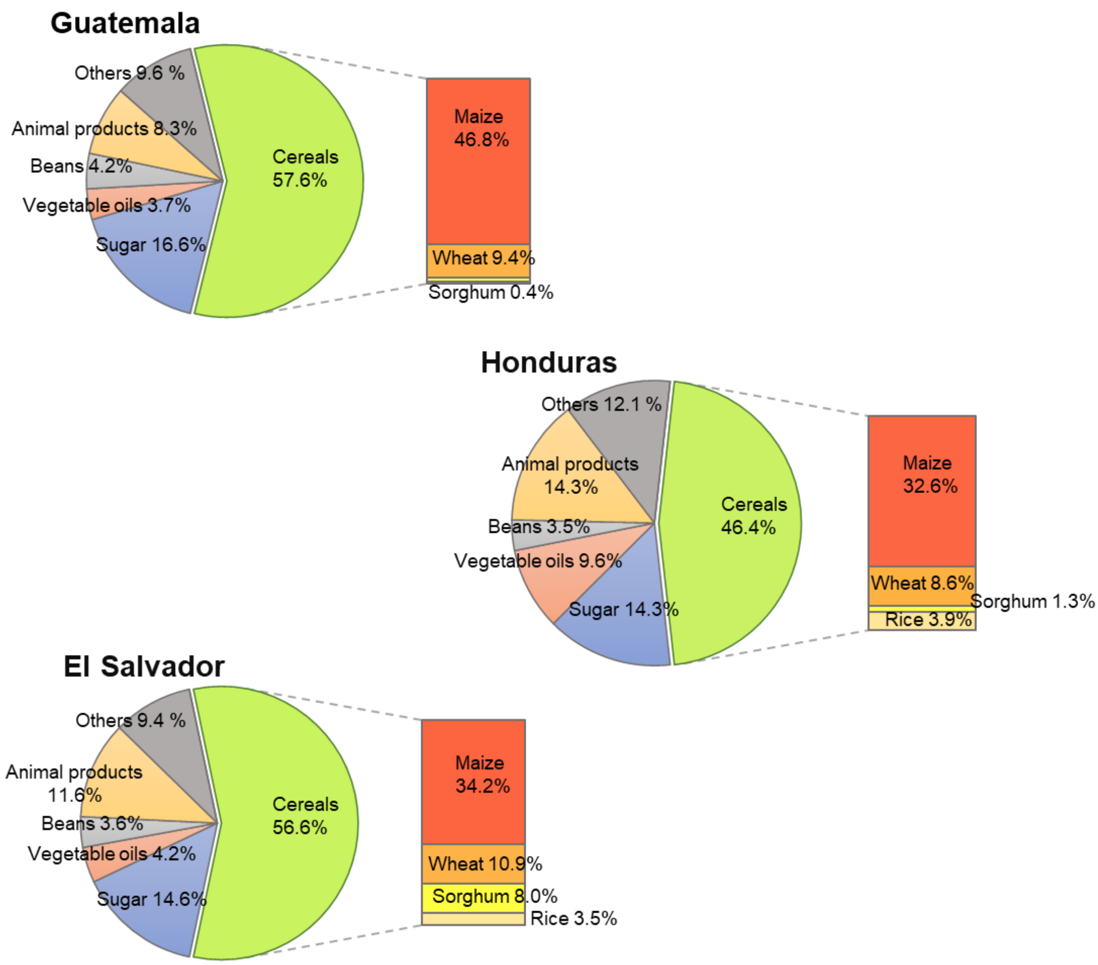

Annual Precipitation patterns per department

Figure S13: Annual precipitation patterns in Guatemala. The rain rates referred to a certain department have been plotted per year and compared to the average annual rate of the historical series (1996-2016). The plots refer to the same area of conflicts occurrence (red) and to the food trade-connected areas (blue).

(a) Guatemala department

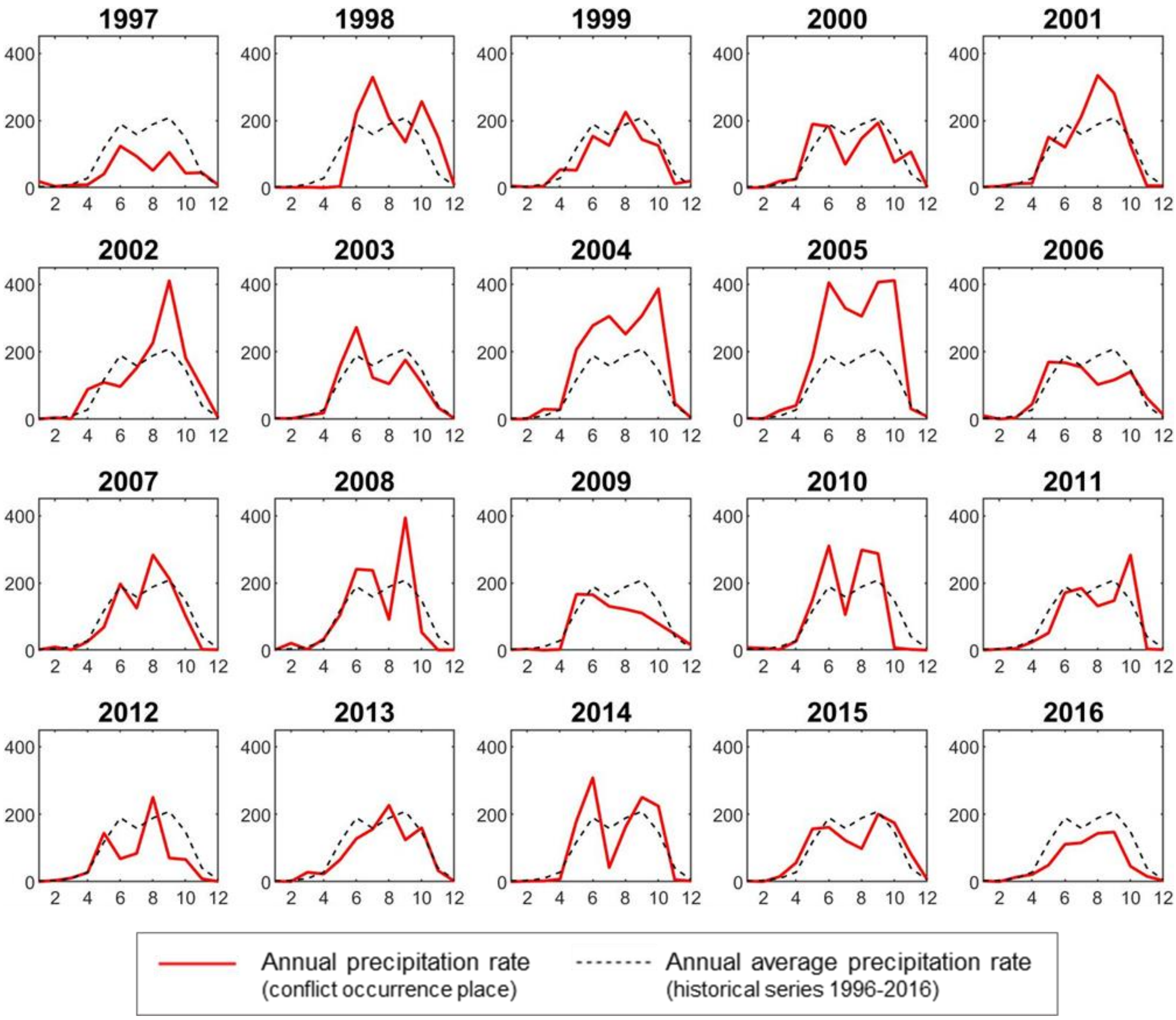

(b) Jutiapa department

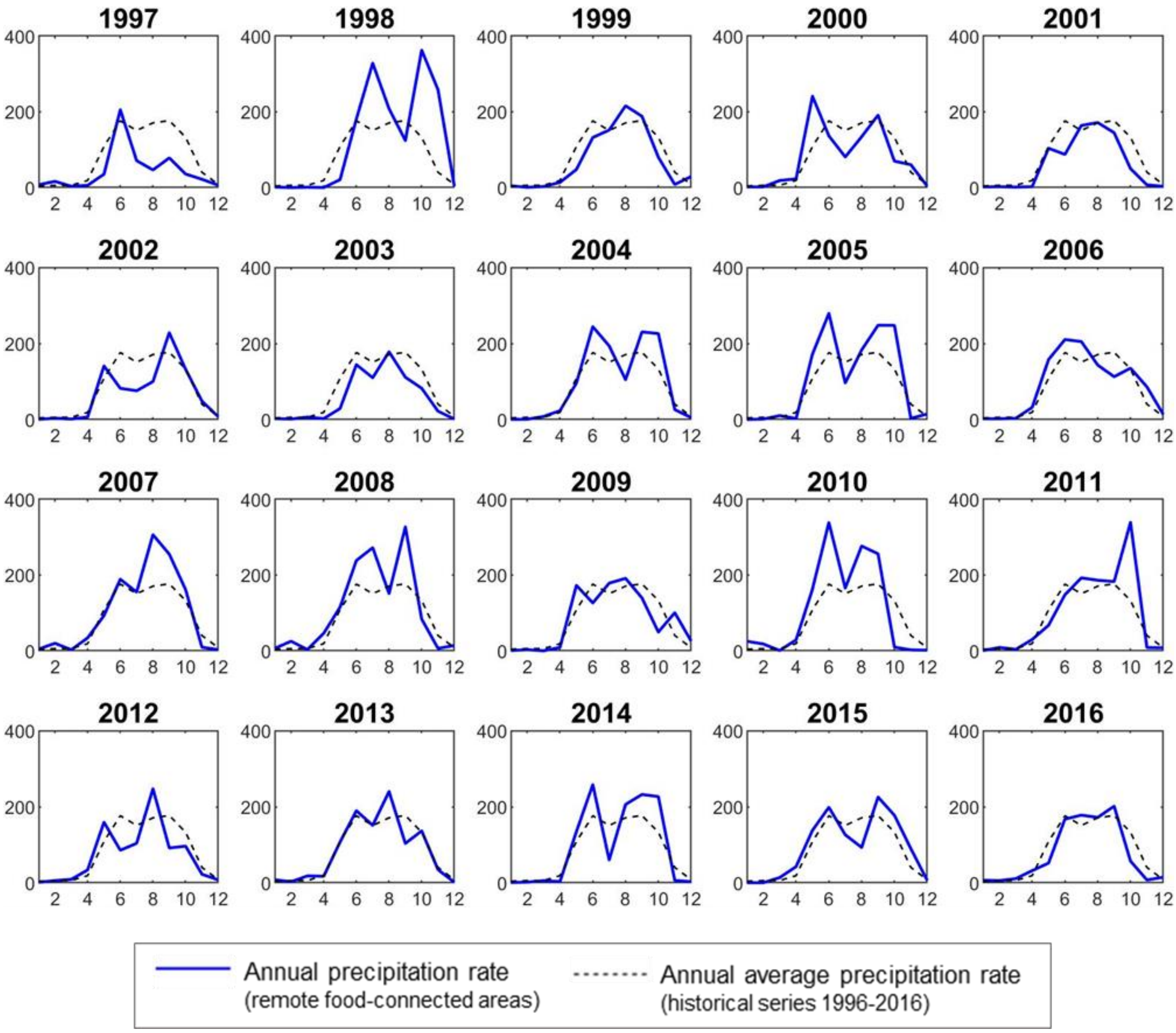

(c) Retalhuleu department

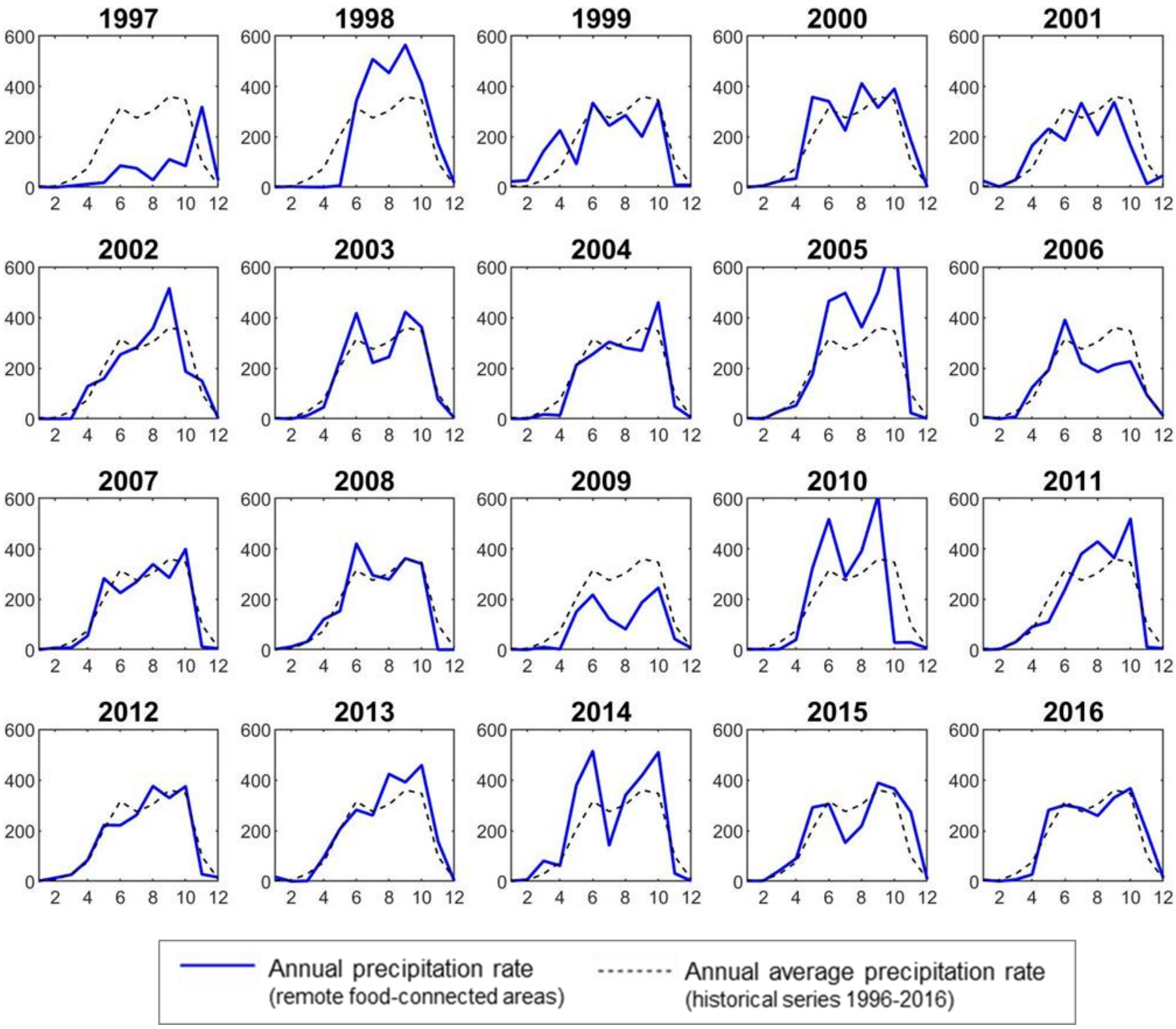

Figure S14: Annual precipitation patterns in Honduras.

(a) Francisco Morazán department

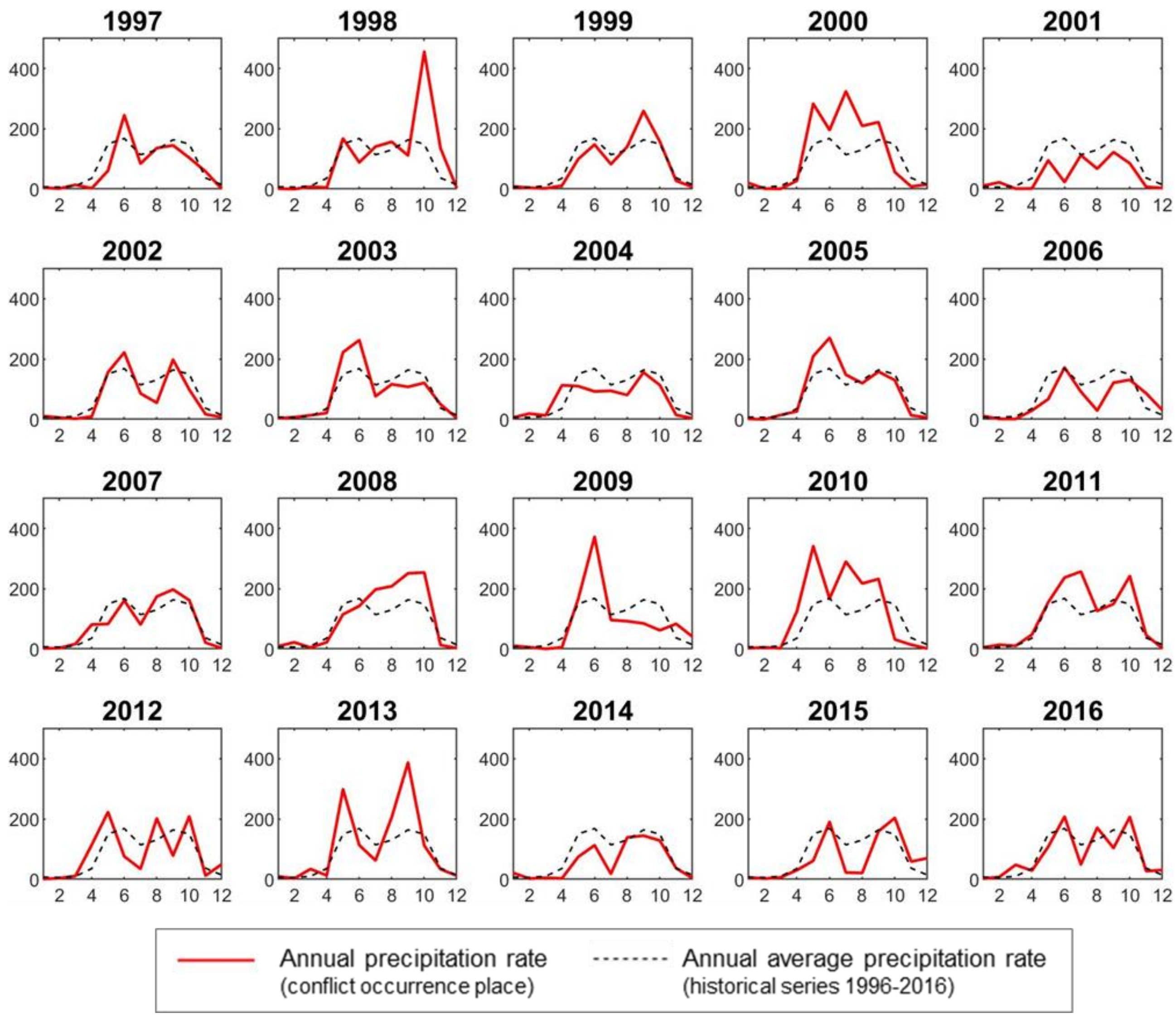

(b) Olancho department

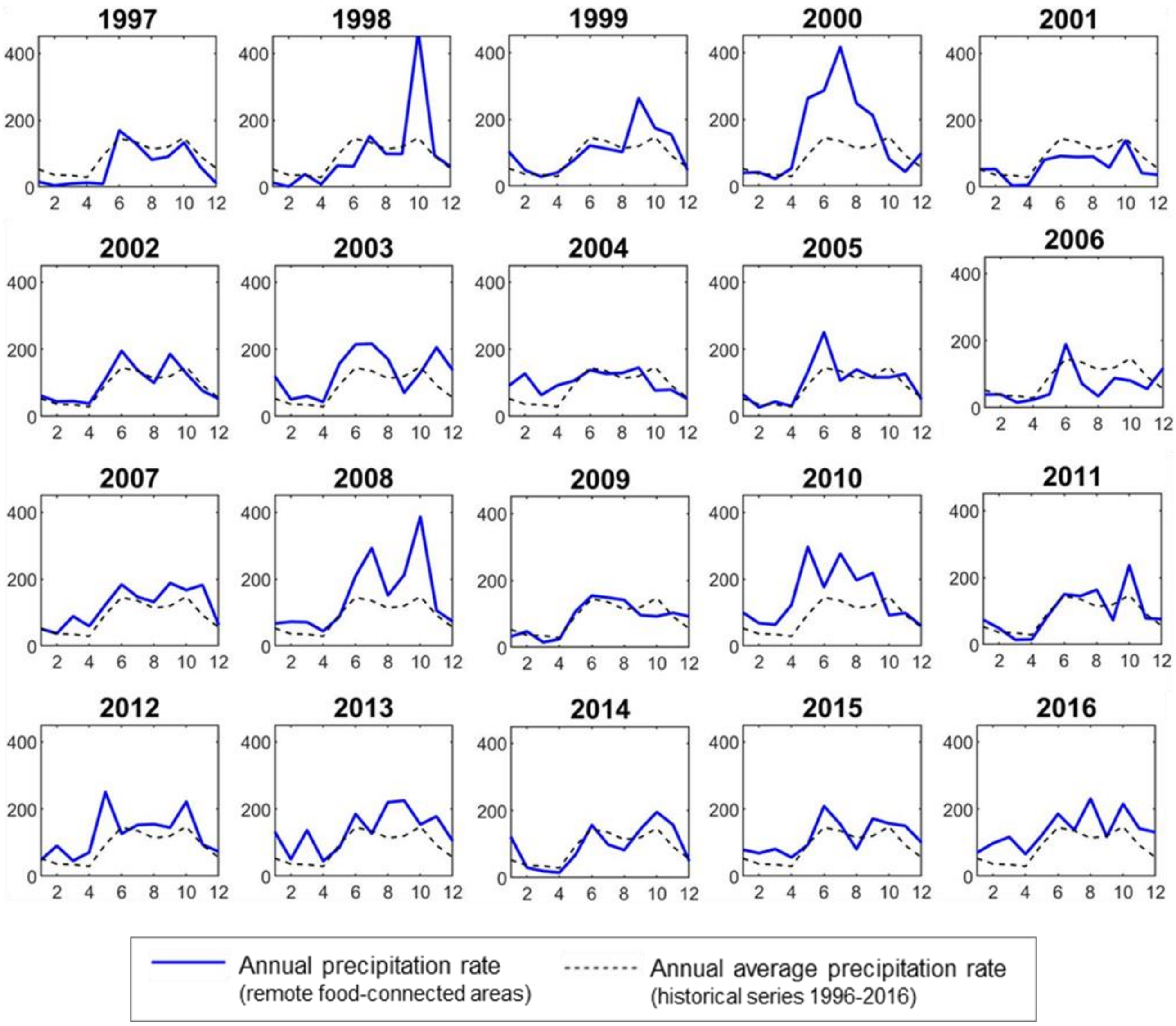

Figure S15: Annual precipitation patterns in El Salvador.

(a) San Salvador department

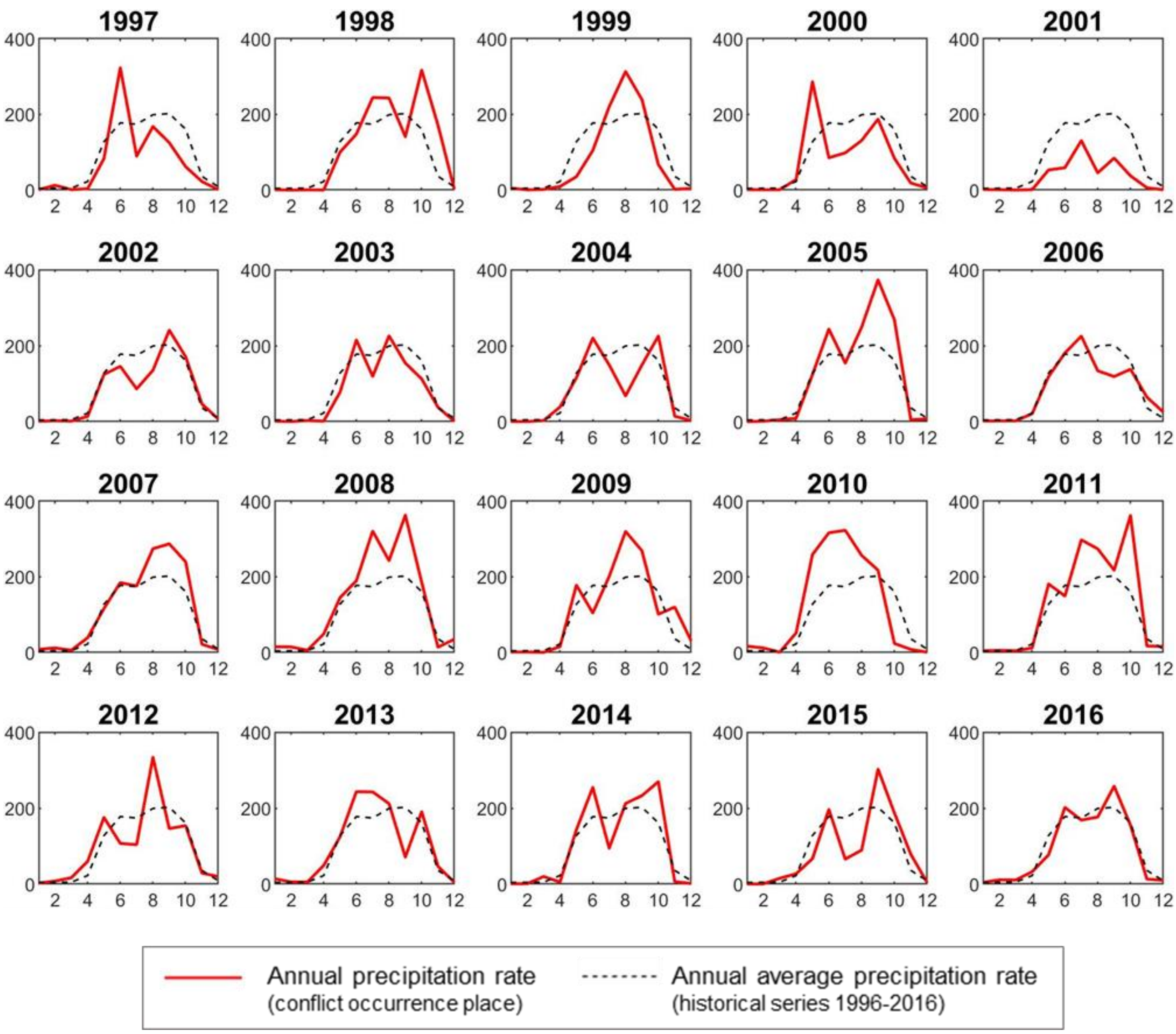

(b) La Paz department

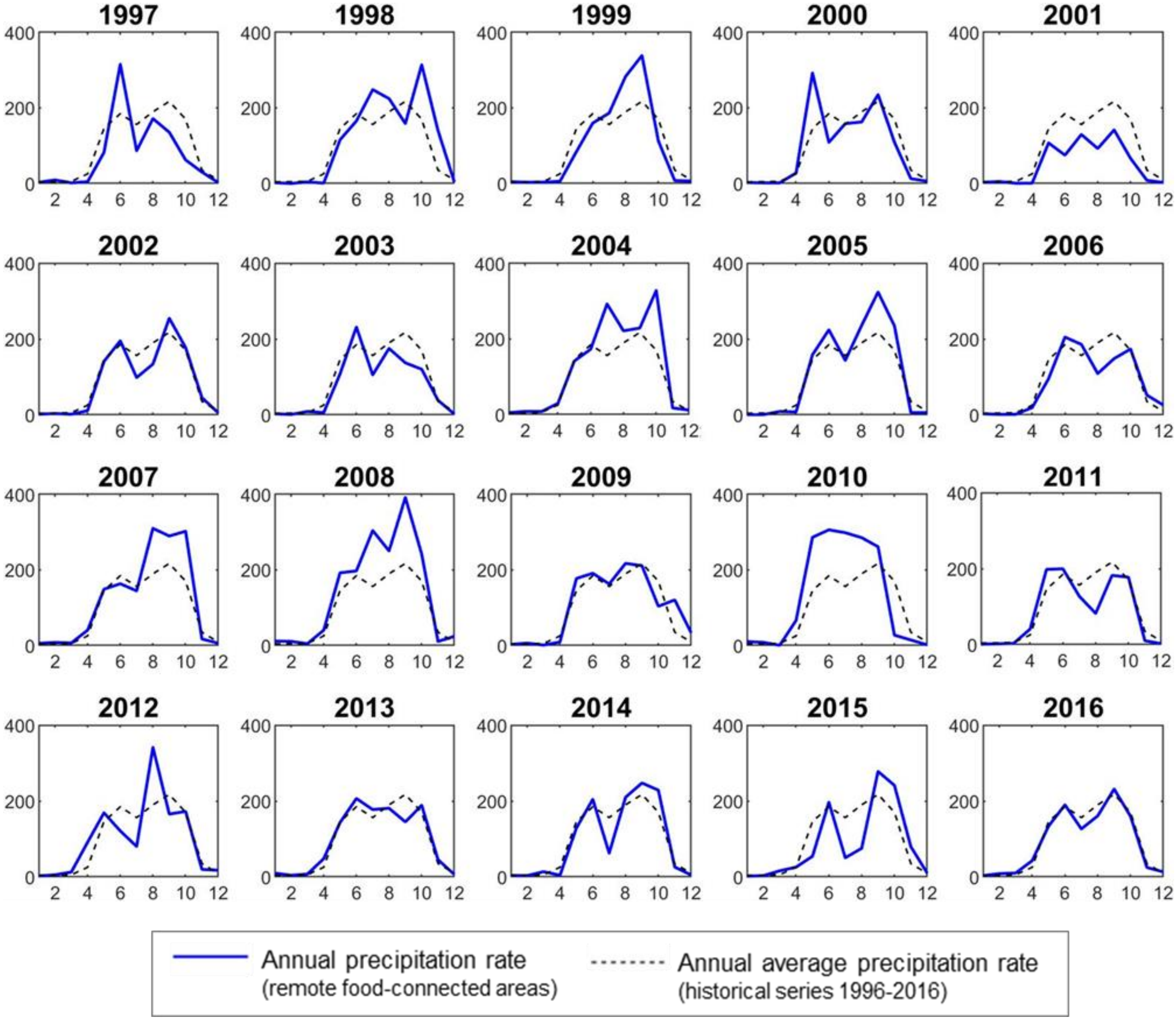

(c) Chalatenango department

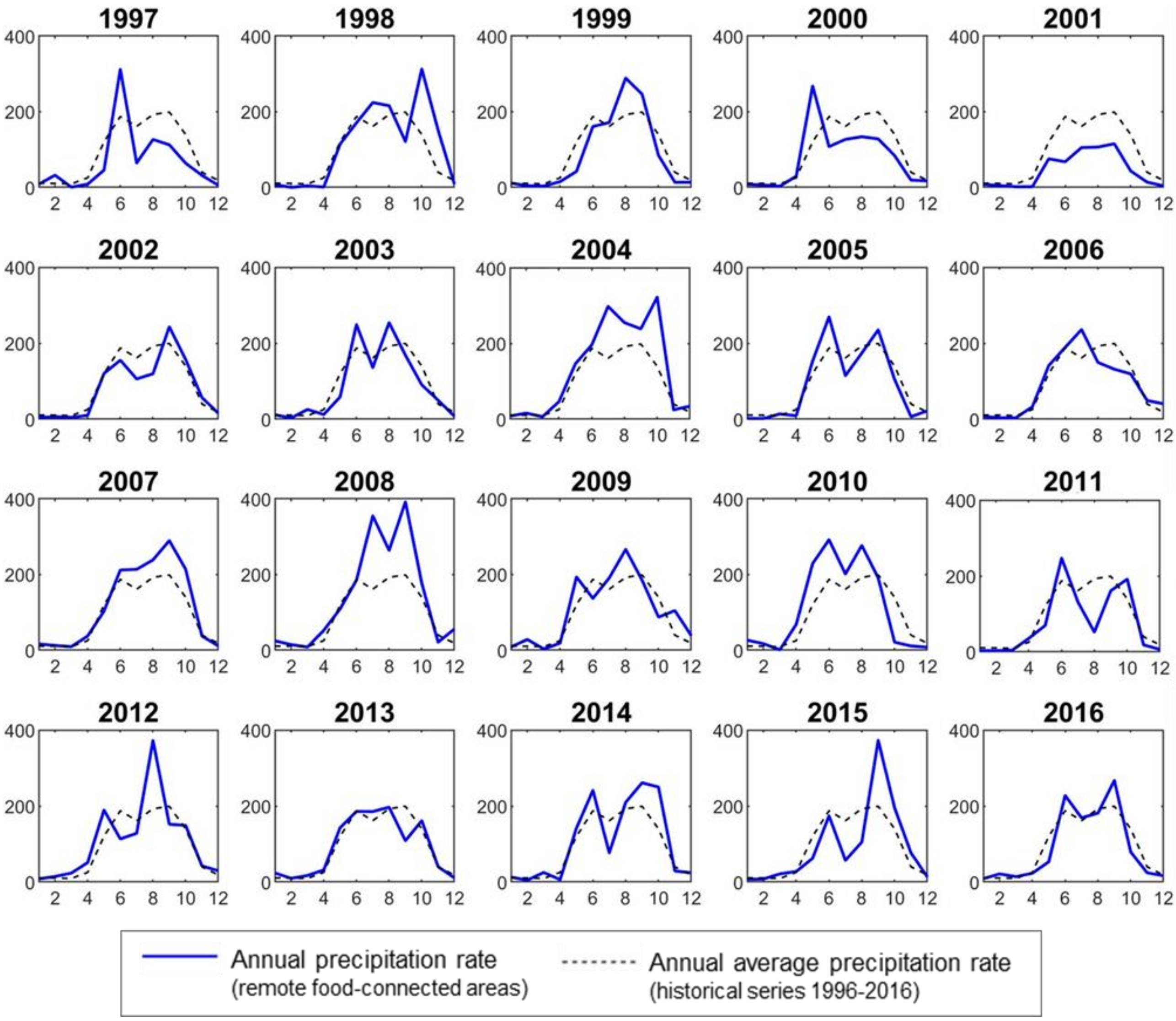

Bayesian credible intervals for the CWF, CWFt models

Figure S16. 90% Bayesian credible intervals of the direct effects of population density, green water availability, food availability, and food access on λ, under the CWF Model. Solid blue circles denote the posterior medians, red cross points denote posterior means. Bayesian credible intervals are drowned from a sample of 5,000 posterior simulated values.

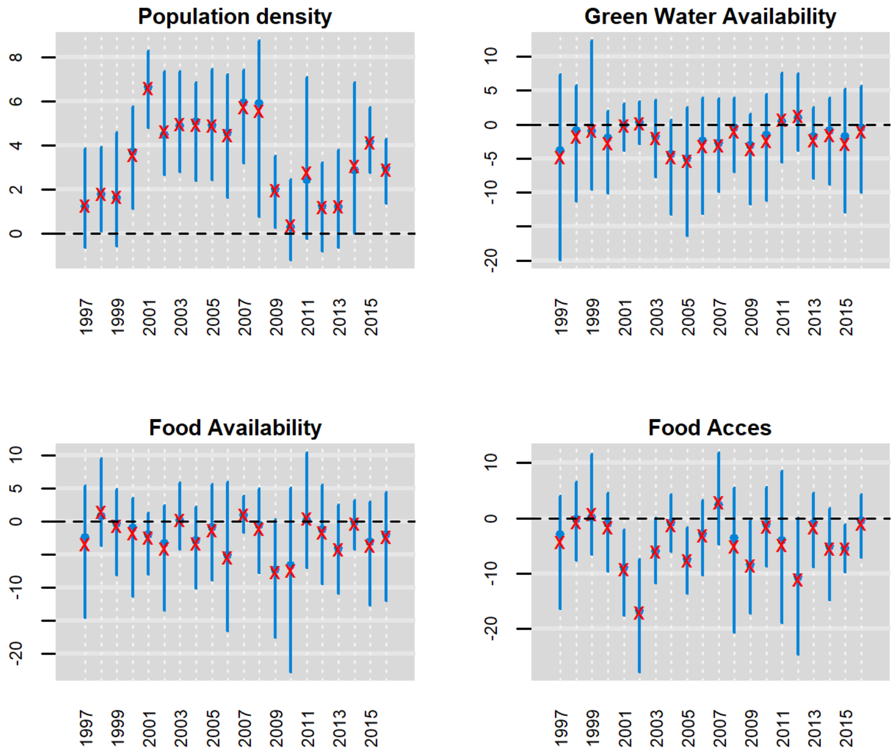

Figure S17. 90% Bayesian credible intervals of spatial spillover effects of spatial-lagged population density, green water availability, food availability and food access on the Poisson intensity λ, under the CWF Model. Solid blue circles denote the posterior medians, red cross points denote posterior means. Bayesian credible intervals are drowned from a sample of 5,000 posterior simulated values.

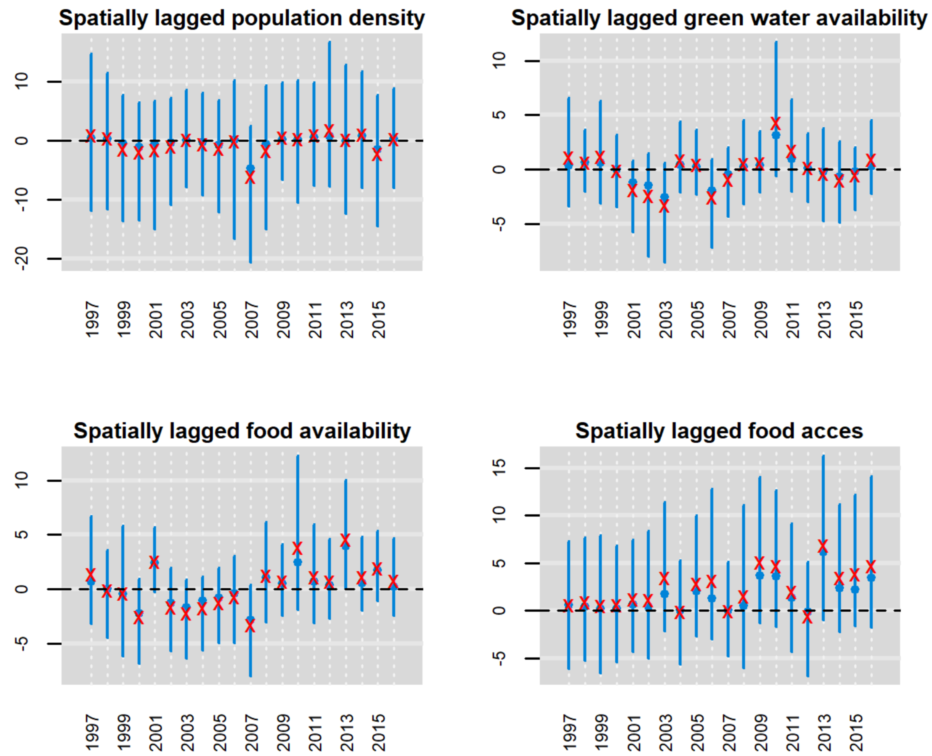

Figure S18. 90% Bayesian credible intervals for the direct effects of population density, Human Development Index, green water availability, food availability and food access on the point mass zero θ under the CWF Model. Solid blue circles denote the posterior medians, red cross points denote posterior means. Bayesian credible intervals are drowned from a sample of 5,000 posterior simulated values.

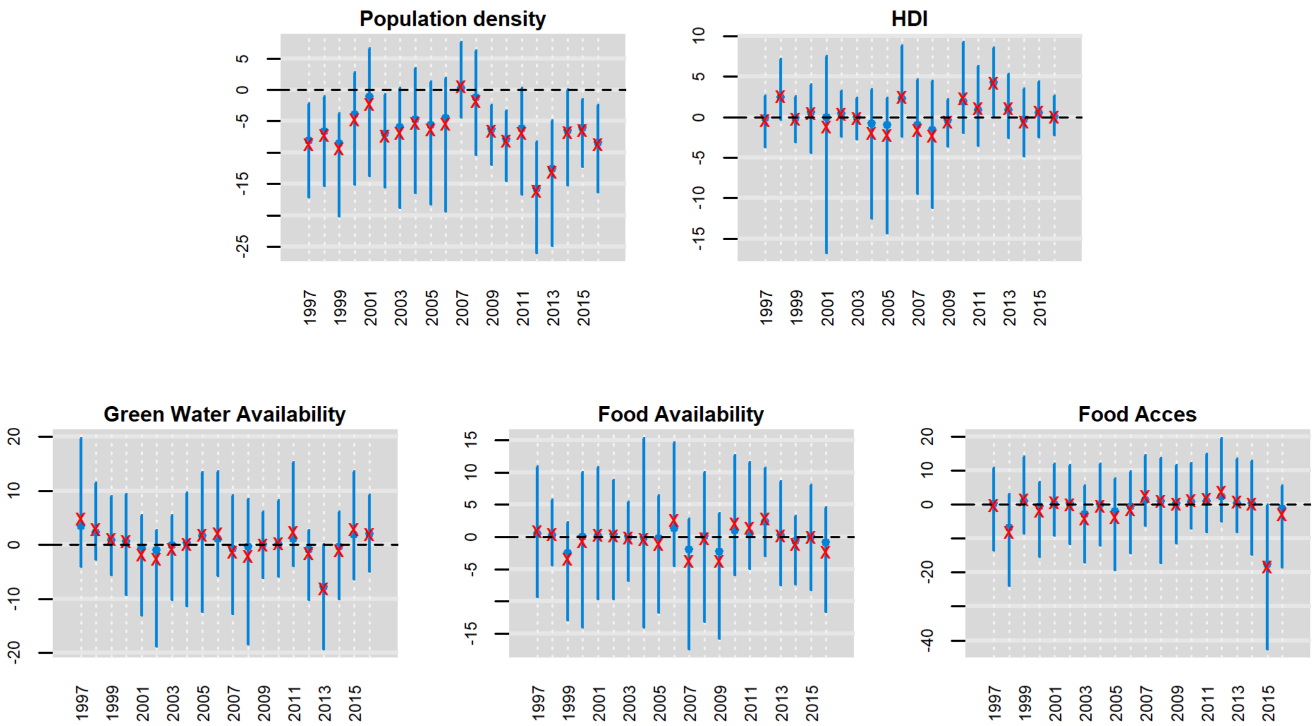

Figure S19. 90% Bayesian credible intervals of direct effects of population density, green water availability (+virtual water trade), food availability (+trade) and food access on λ, under the baseline CWFt Model. Solid blue circles denote the posterior medians, red cross points denote posterior means. Bayesian credible intervals are drowned from a sample of 5,000 posterior simulated values.

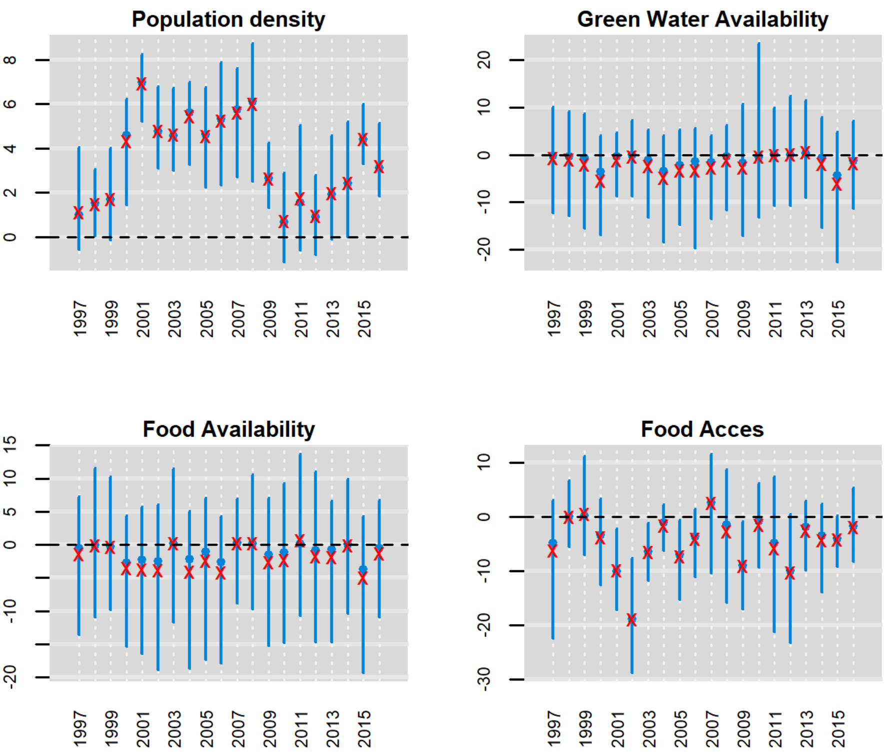

Figure S20. 90% Bayesian credible intervals of spatial spillover effects of spatially lagged population density, green water availability (+virtual water trade), food availability (+trade) and food access on λ, under the baseline CWFt Model. Solid blue circles denote the posterior medians, red cross points denote posterior means. Bayesian credible intervals are drowned from a sample of 5,000 posterior simulated values.

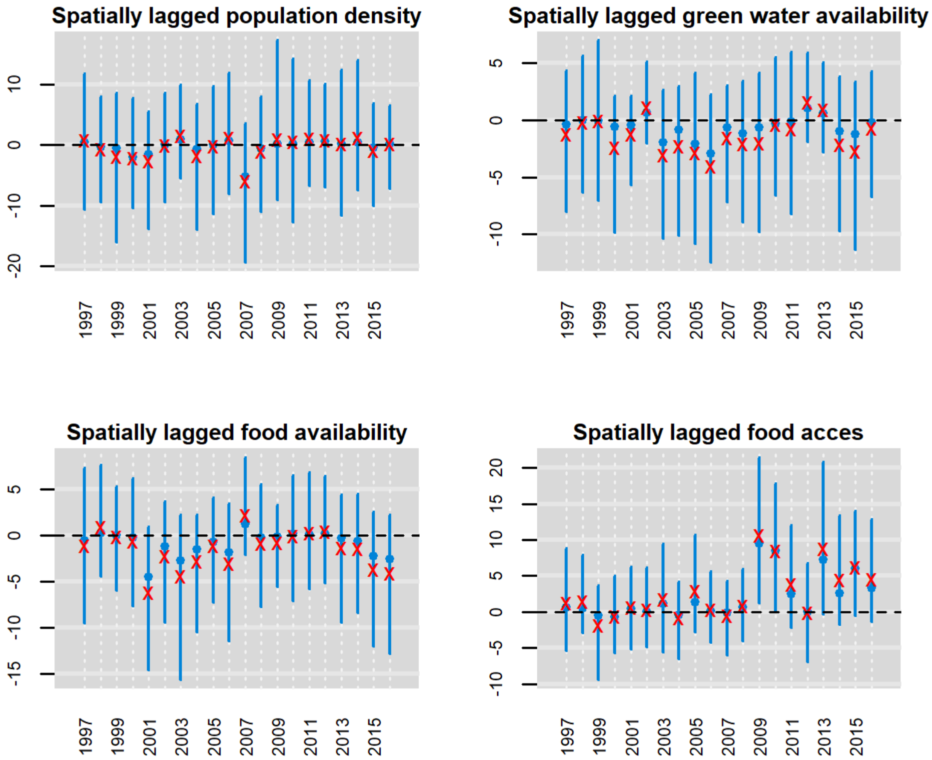

Figure S21. 90% Bayesian credible intervals of the direct effects of population density, Human Development Index green water availability (+virtual water trade), food availability (+trade) and food access on the point mass zero θ under the CWFt Model. Solid blue circles denote the posterior medians, red cross points denote posterior means. Bayesian credible intervals are drowned considering a sample of 5,000 posterior simulated values.

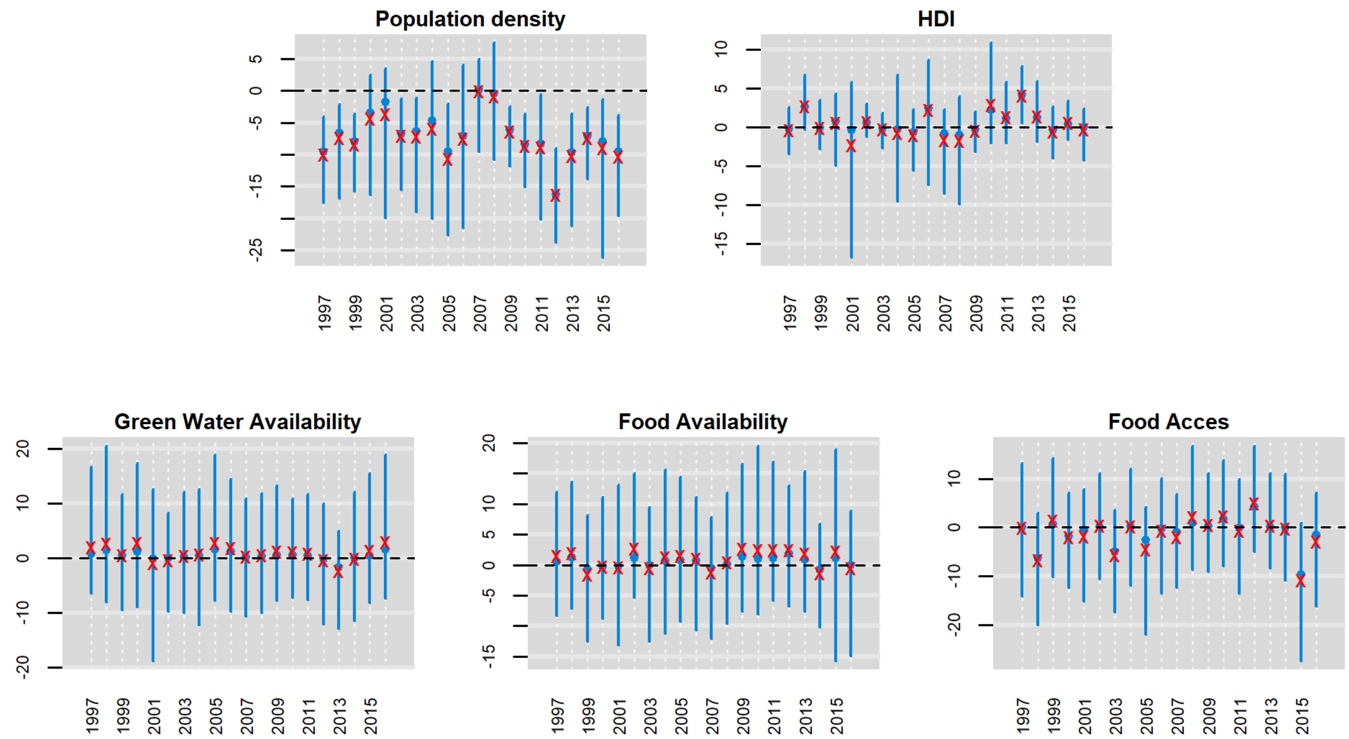

Figure S22. 90% Bayesian credible intervals of the direct effects of population density, Human Development Index green water availability, food availability and demand-surplus gap on the point mass zero θ under the CWFs Model. Solid blue circles denote the posterior medians, red cross points denote posterior means. Bayesian credible intervals are drowned from a sample of 5,000 posterior simulated values.

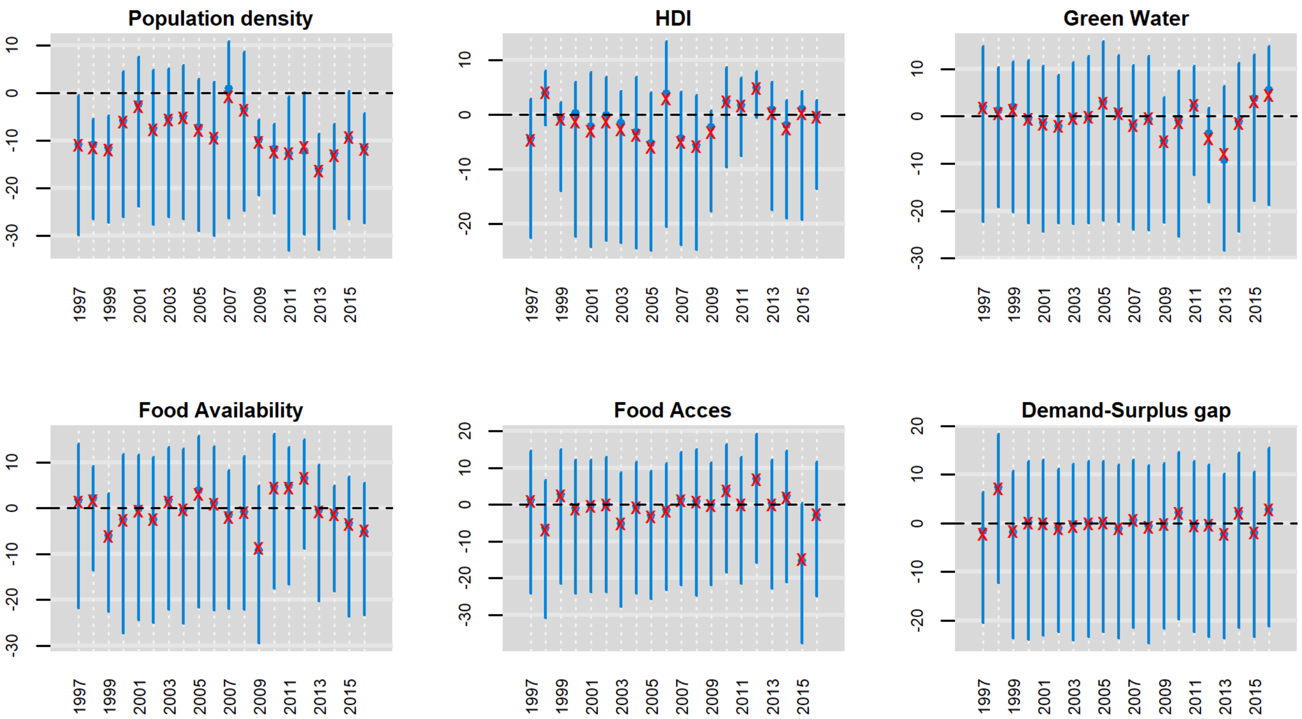

The model goodness-of-fit

Table S7. Bayesian p-value (P_B) for the computed CWF, CWFs and CWFt models. P_B indicates the probability that the predictive distribution takes a more extreme value than the observed distribution.

Model	1997	1998	1999	2000	2001	2002	2003	2004	2005	2006
CWF	0.280	0.476	0.287	0.240	0.157	0.190	0.393	0.113	0.185	0.128
CWFs	0.256	0.533	0.233	0.219	0.249	0.316	0.247	0.276	0.307	0.404
CWFt	0.630	0.682	0.338	0.441	0.460	0.576	0.571	0.647	0.643	0.734

Model	2007	2008	2009	2010	2011	2012	2013	2014	2015	2016
CWF	0.381	0.235	0.051	0.129	0.235	0.276	0.164	0.334	0.112	0.296
CWFs	0.250	0.218	0.246	0.245	0.242	0.475	0.352	0.200	0.291	0.261
CWFt	0.574	0.449	0.664	0.600	0.436	0.566	0.638	0.478	0.563	0.517

Table S8: Means of the Logarithm of Pseudo-Marginal Likelihood (LPML) for the CWF, CWFs and CWFt models per year from 1996 until 2016. LPML is an indicator of model performance. The higher the LPML values (less negative), the better the model fit.

Model	1997	1998	1999	2000	2001	2002	2003	2004	2005	2006
CWF	-39.499	-59.969	-45.945	-75.599	-76.044	-80.717	-80.501	-78.035	-68.534	-49.756
CWFs	-35.617	-54.295	-43.656	-73.615	-72.233	-79.907	-78.454	-75.150	-64.806	-46.312
CWFt	-40.218	-60.090	-46.437	-76.940	-76.928	-81.587	-81.581	-80.365	-69.544	-51.014

Model	2007	2008	2009	2010	2011	2012	2013	2014	2015	2016
CWF	-82.390	-36.476	-71.022	-34.815	-43.172	-75.539	-55.786	-54.670	-92.857	-102.232
CWFs	-78.226	-33.512	-66.646	-30.914	-38.949	-70.737	-50.848	-50.294	-86.865	-99.227
CWFt	-83.670	-36.116	-73.381	-37.642	-43.075	-75.869	-59.238	-54.299	-95.265	-102.438

Figure S23. Comparison between the observed and simulated values of conflicts, under the CWF model. The histograms refer to the observed number of conflicts per year (grey) and the median posterior densities (red) are reported for the simulated values.

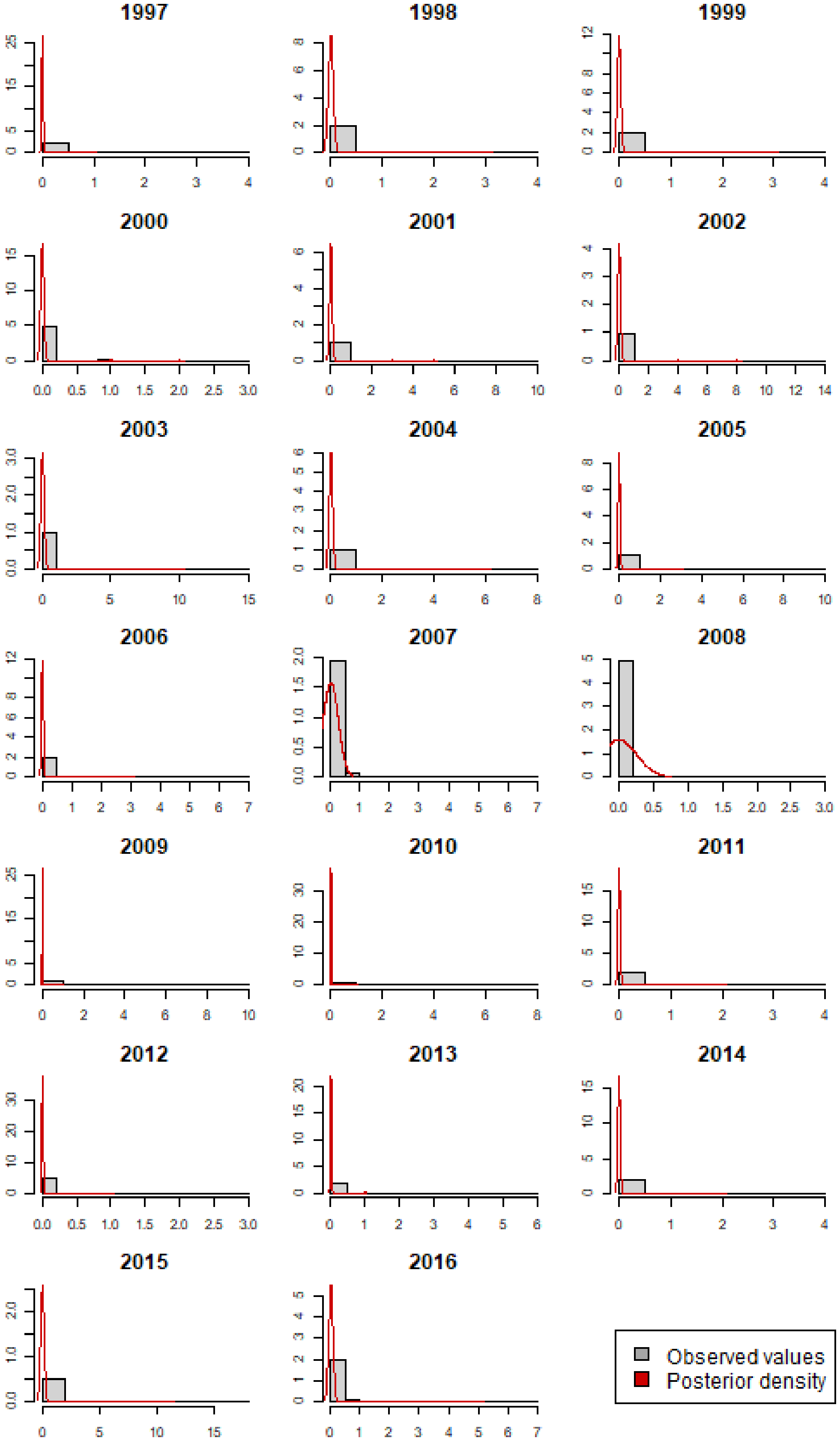

Figure S24. Comparison between the observed and simulated values of conflicts, under the CWFt model. The histograms refer to the observed number of conflicts per year (grey) and the median posterior densities (red) are reported for the simulated values.

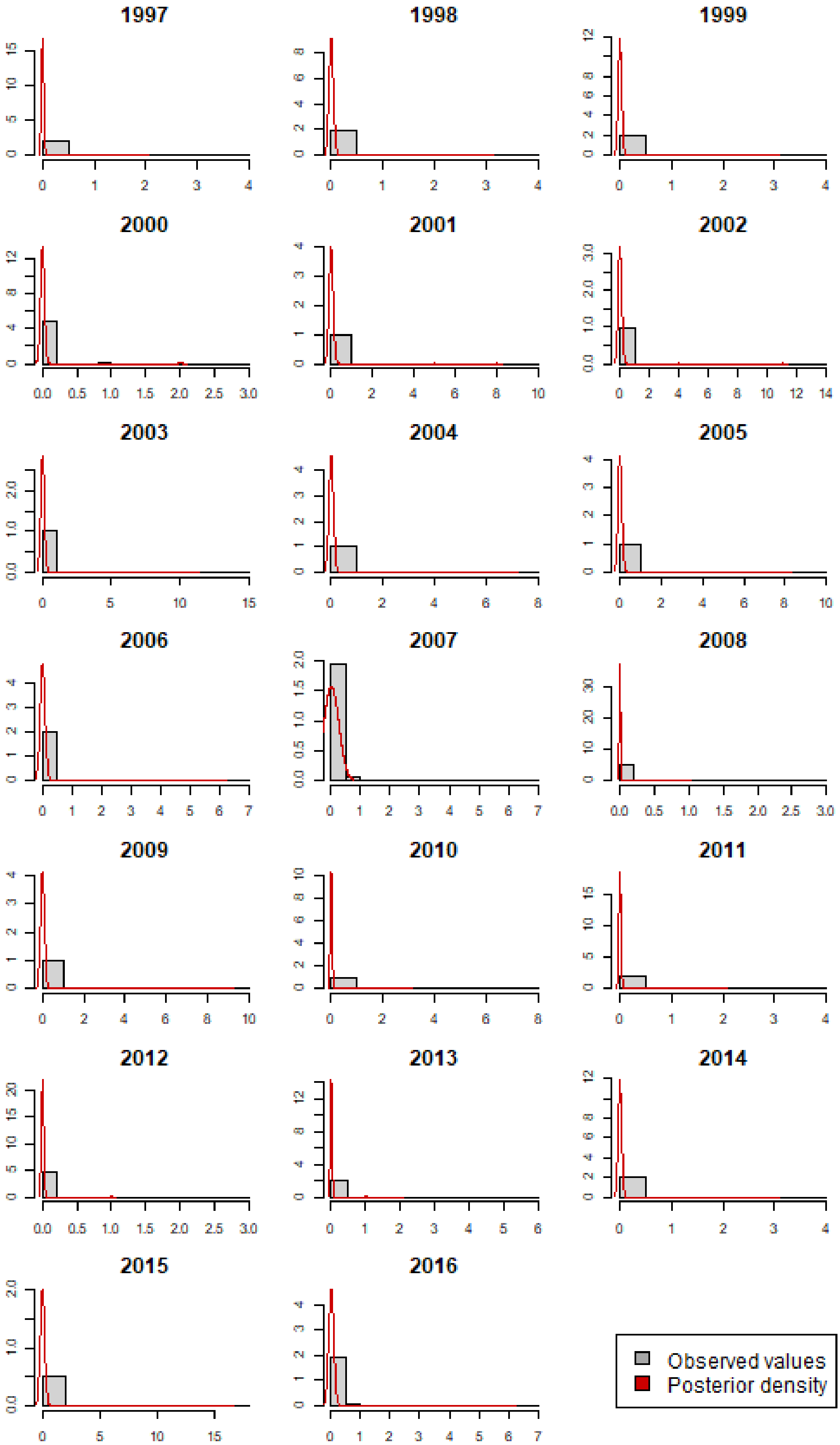

Figure S25. Comparison between the observed and simulated values of conflicts, under the CWFs model. The histograms refer to the observed number of conflicts per year (grey) and the median posterior densities (red) are reported for the simulated values.

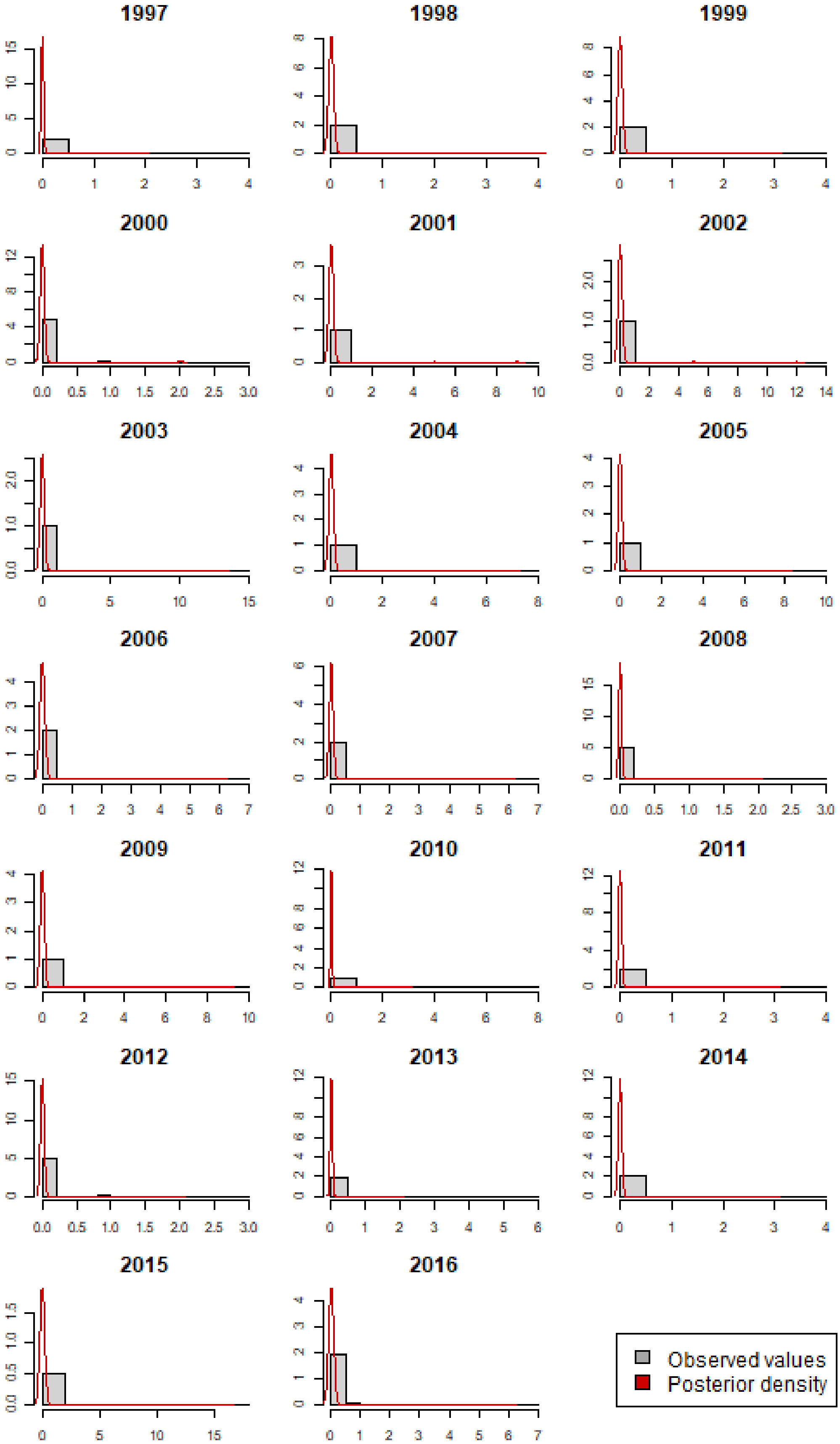

Figure S26: Comparison between observed (Y) and simulated (Y sim) conflicts occurrences per year, in the spatial domain discretized over the square grid of 20 km x 20 km, under the CWFs model.

a) Period: 1997 - 2001

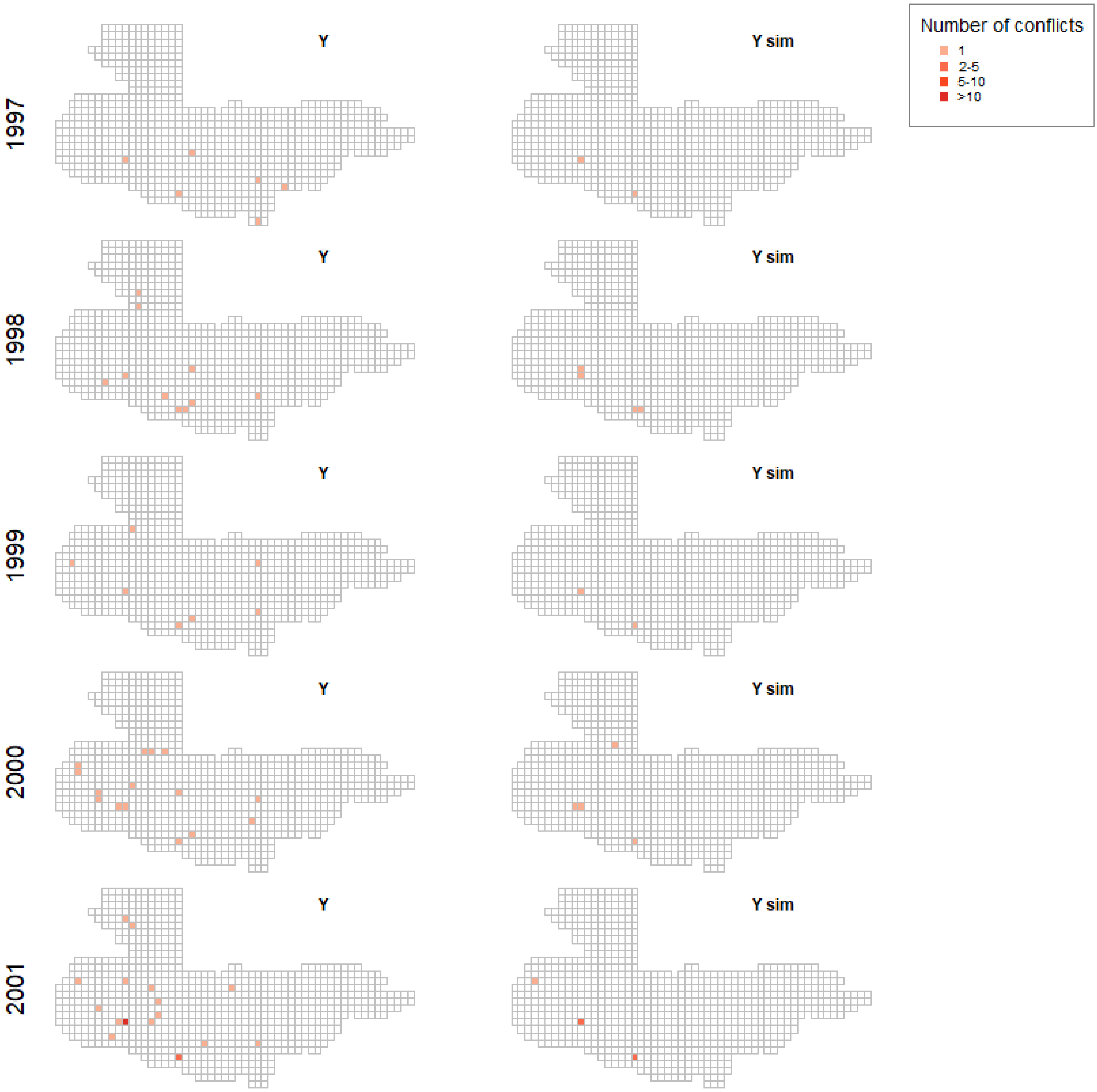

b) Period: 2002 - 2006

c) Period: 2007 - 2011

d) Period: 2012 - 2016

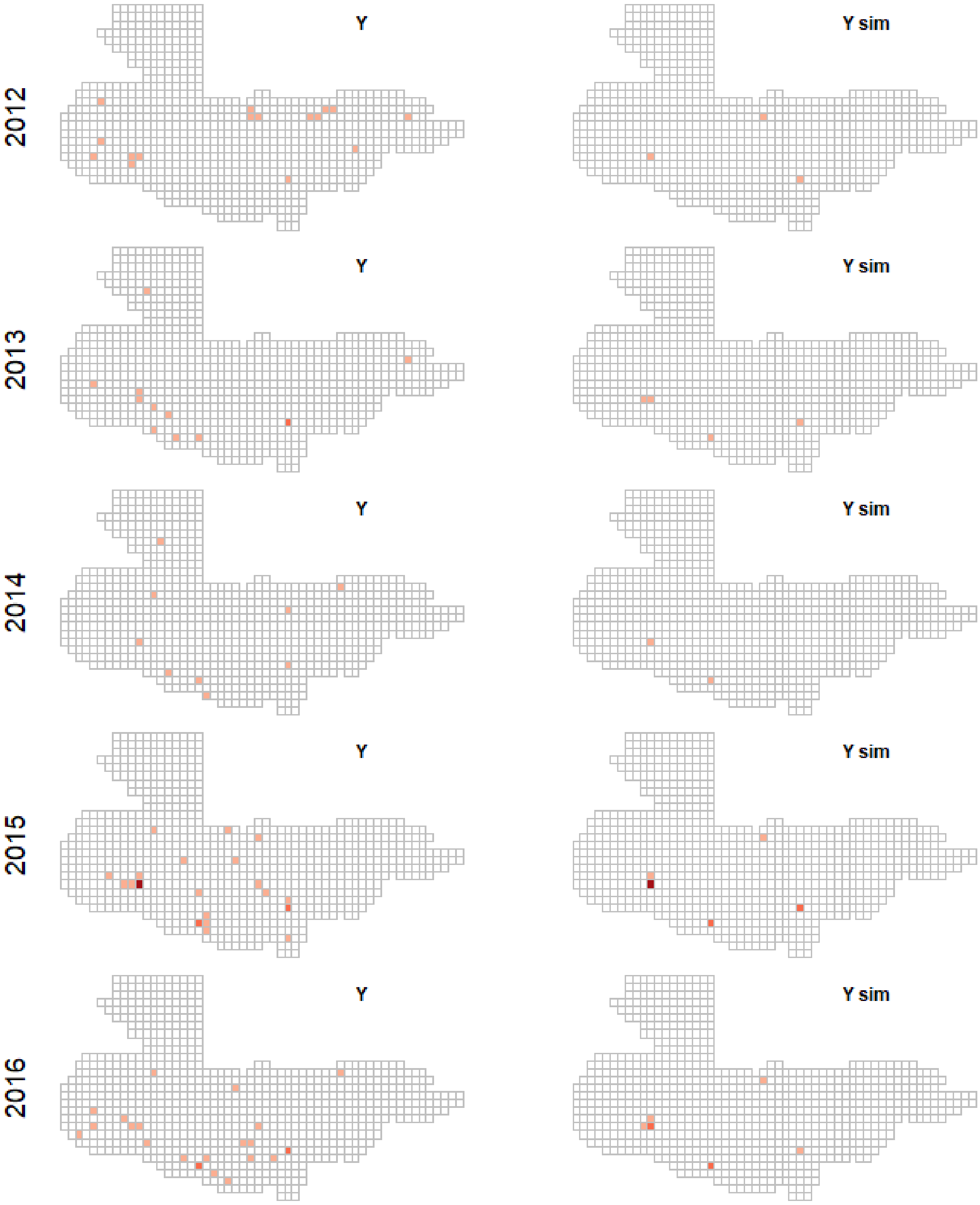

Agricultural production and food security trends per department

Figure S27. Yearly agricultural production and food security trends for the studied period (1996-2016), in Honduras. Trends refer to the urban, peri-urban area surrounding Tegucigalpa city (a) and the food-supplier department of Olancho (b). Yearly agricultural production is reported (in tons) for the main staple (maize, pulses) and cash crops (coffee, sugarcane), and compared to the average annual production. Basing of them, respectively the first and second pillars of food security (i.e., food availability and access) have been calculated (in kcal/cap/year). The total food supply due to the local production is the sum of these two contributions. Internal trade determines incoming food fluxes in the Francisco Morazán department, and corresponding outflows from the food supplier department of Olancho, determining food security oscillation within the HER thresholds in the capital city of Tegucigalpa.

a) Tegucigalpa (Francisco Morazán department)

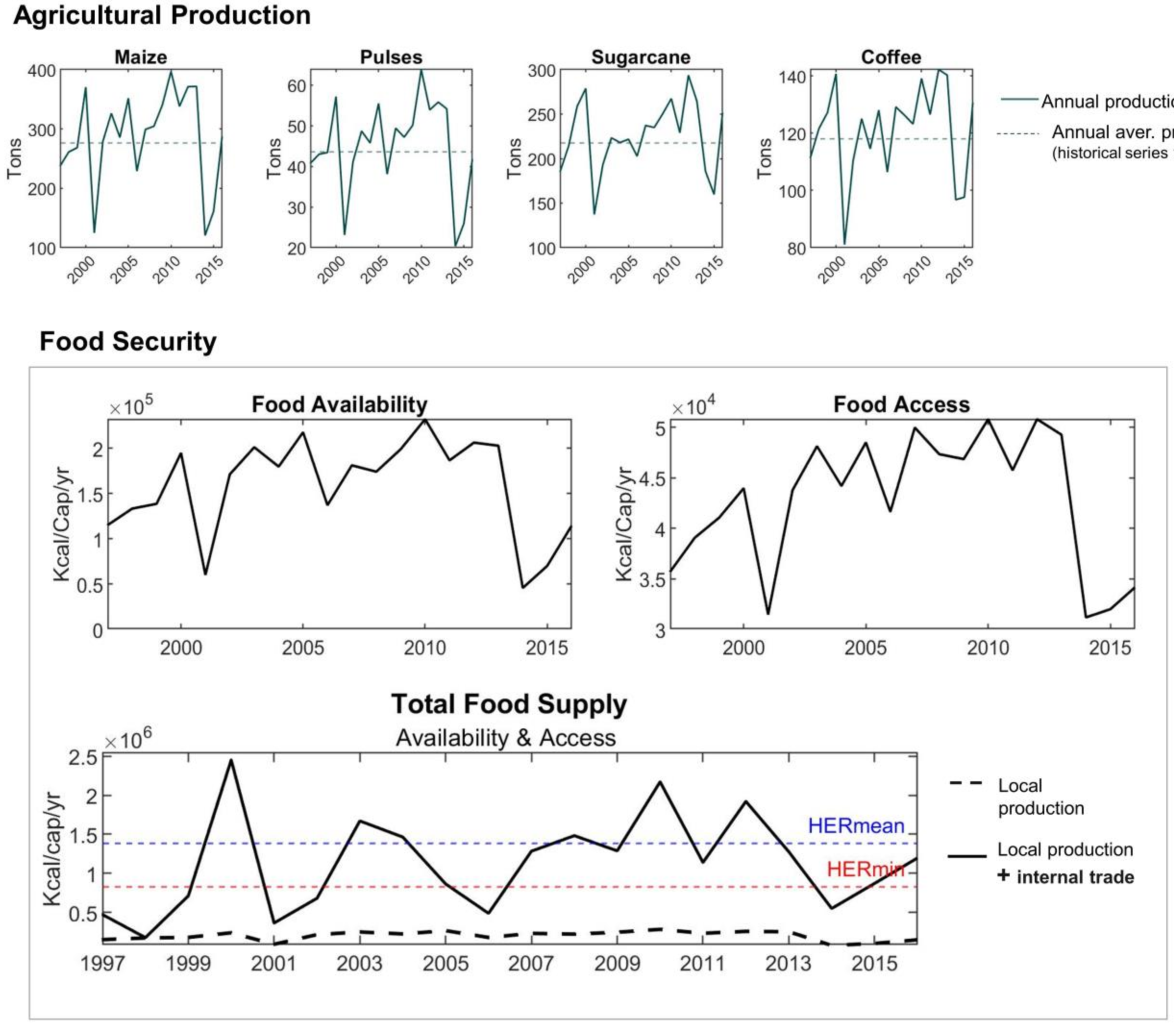

b) Olancho department

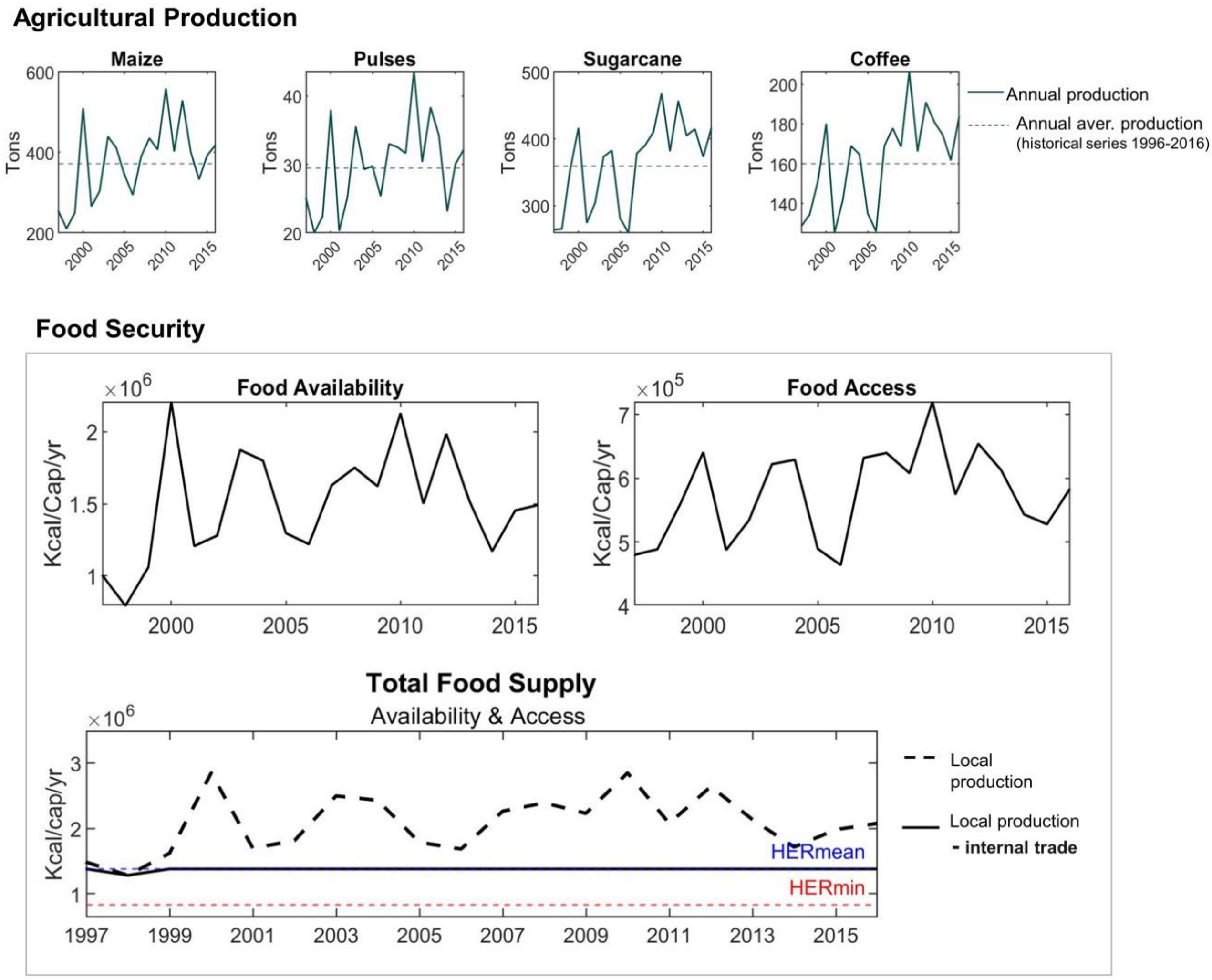

Figure S28. Yearly agricultural production and food security trends, in Guatemala. They refer to Guatemala City urban area *(a)* and the exporter departments of Jutiapa *(b)* and Retalhuleu *(c),* for the time period studied (1996-2016). Yearly agricultural production is reported (in tons) for the main staple (maize, pulses) and cash crops (coffee, sugar cane) cultivated in the region, and compared to the average annual production. They have been used to calculate the first and second pillars of food security, namely food availability and the food access (kcal/cap/year). The total food available locally has been evaluated as the sum of the two contributions deriving from the local production, a comparison has been made with the total food also supplied by internal trade. Food security has been represented in comparison to the HER thresholds.

a) Guatemala City

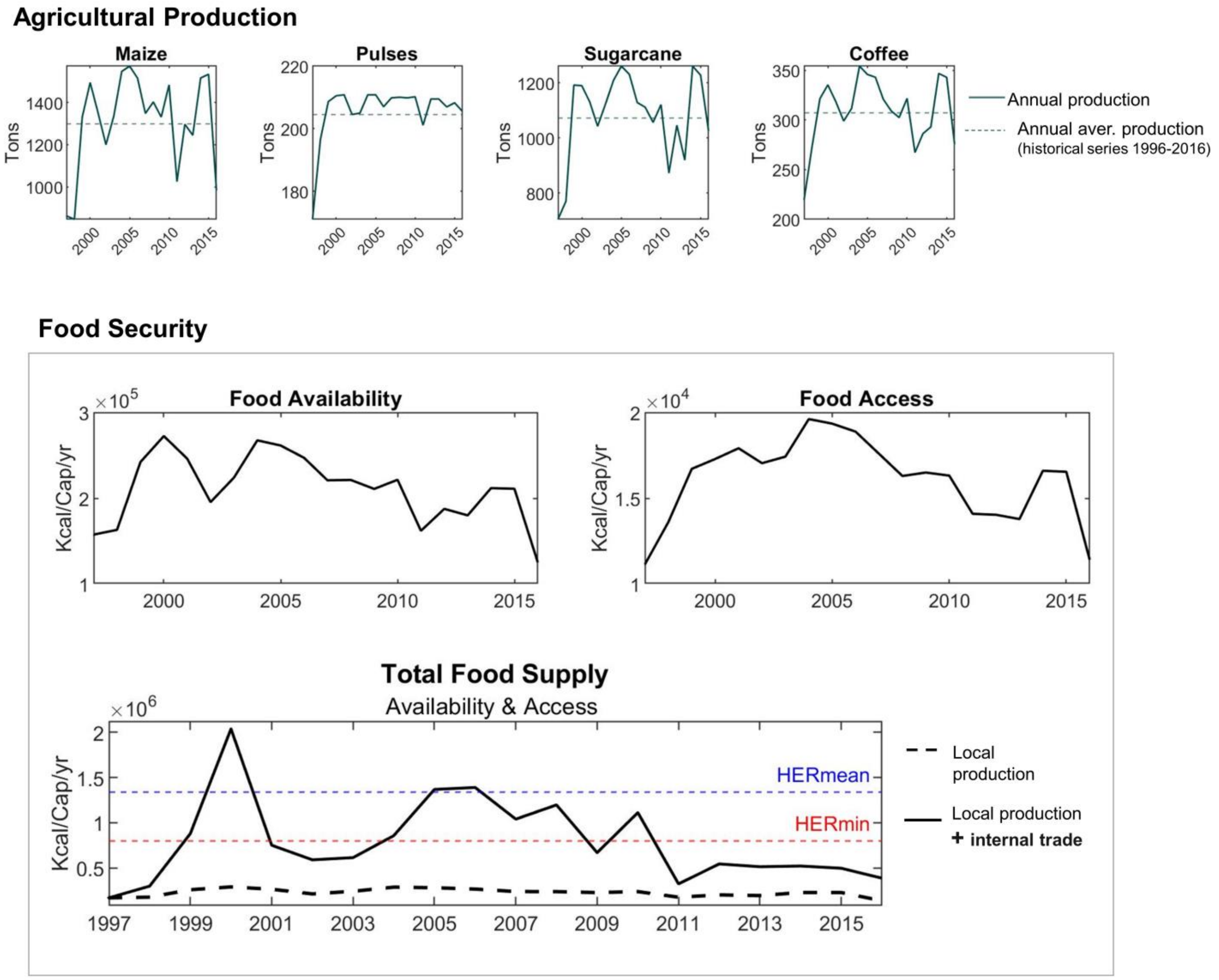

b) Jutiapa department

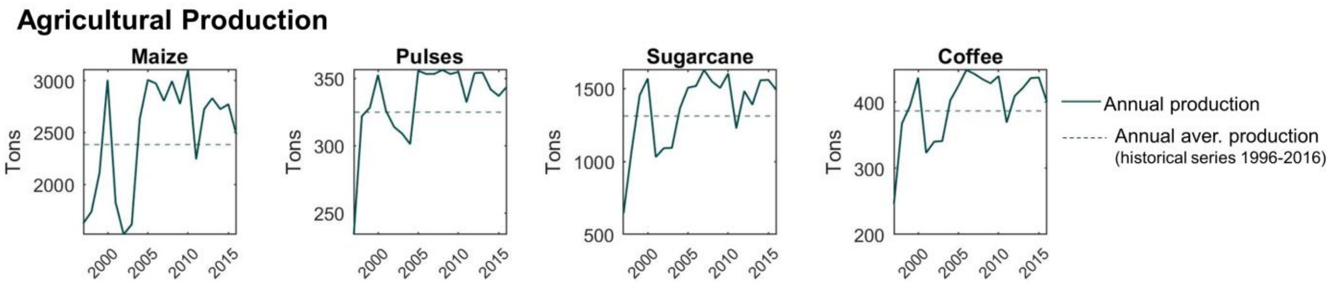

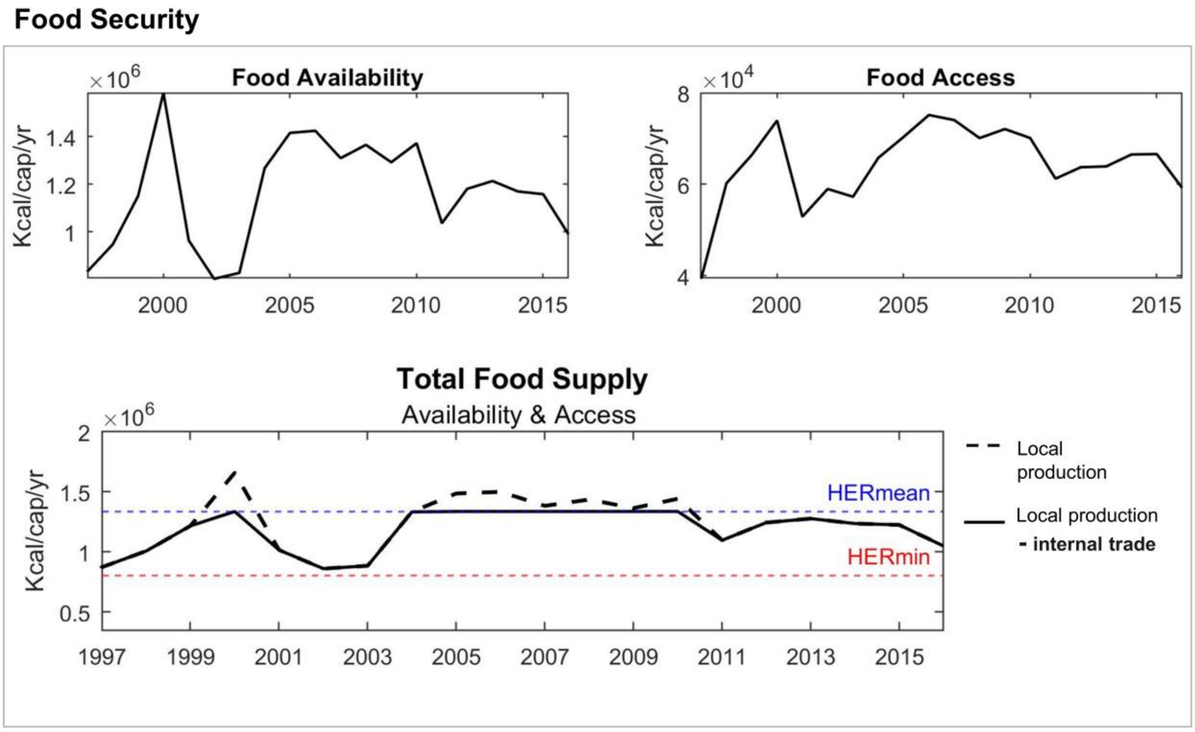

c) Retalhuleu department

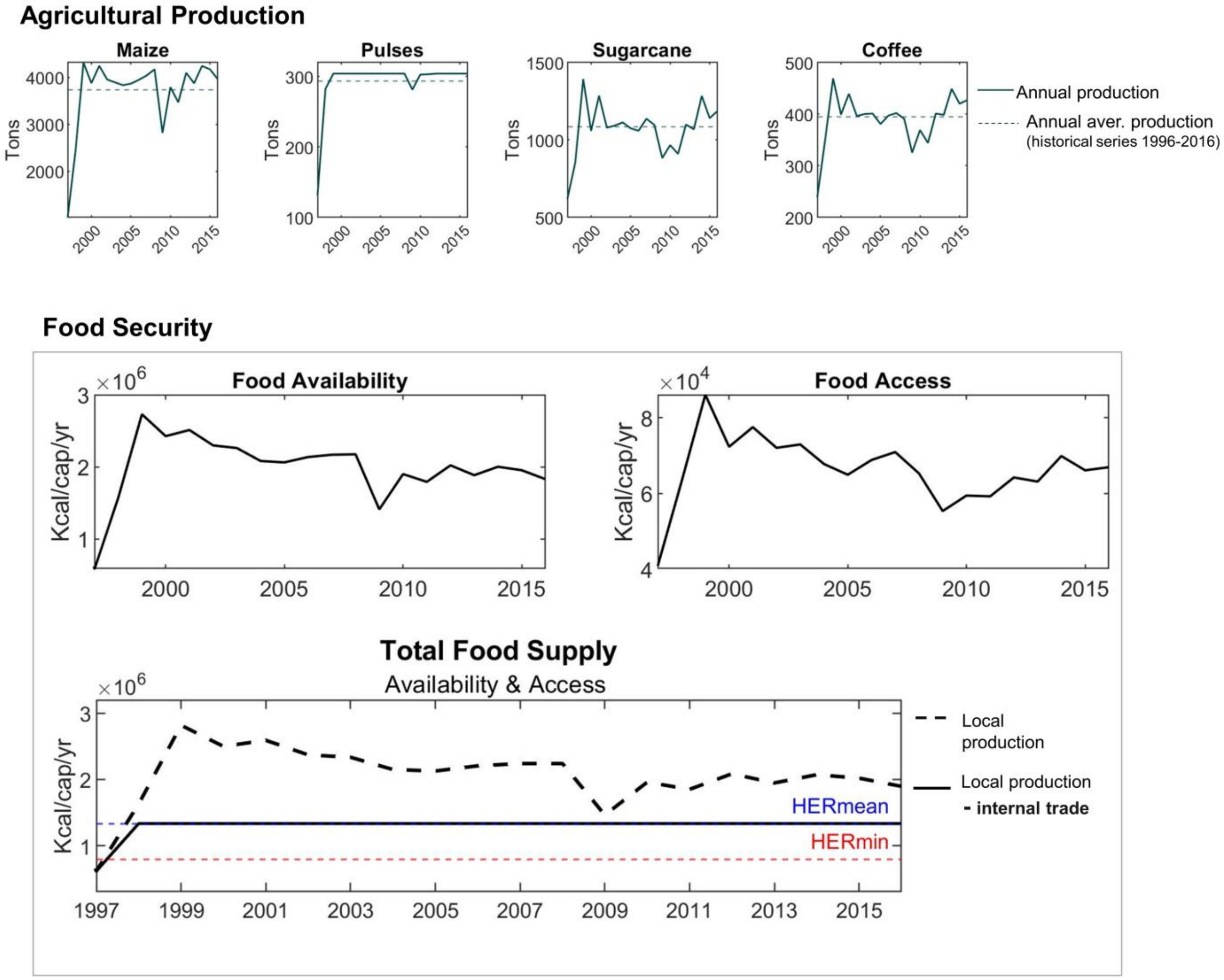

Figure S29. Yearly agricultural production and food security trends, in El Salvador. They refer to San Salvador urban area *(a)* and the exporter departments of Chalatenango *(b)* and La Paz *(c),* for the time period studied (1996-2016). Yearly agricultural production is reported (in tons) for the main staple (maize, pulses) and cash crops (coffee, sugar cane) cultivated in the region, and compared to the average annual production. They have been used to calculate the first and second pillars of food security, namely food availability and the food access (kcal/cap/year). The total food available locally has been evaluated as the sum of the two contributions deriving from the local production, a comparison has been made with the total food also supplied by internal trade. Food security has been represented in comparison to the HER thresholds.

a) San Salvador

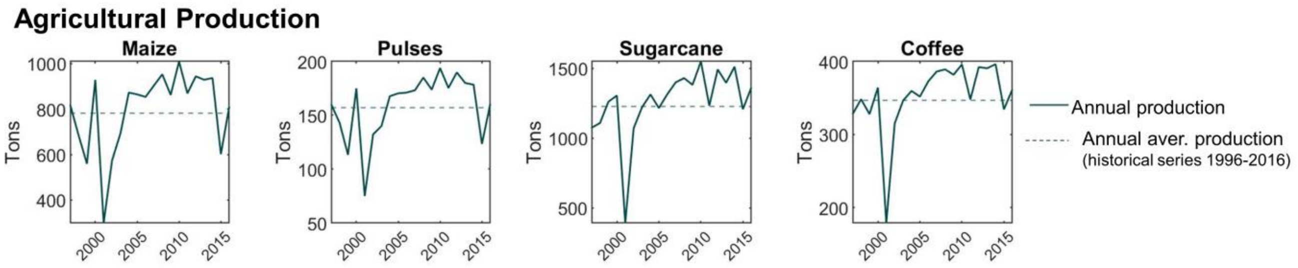

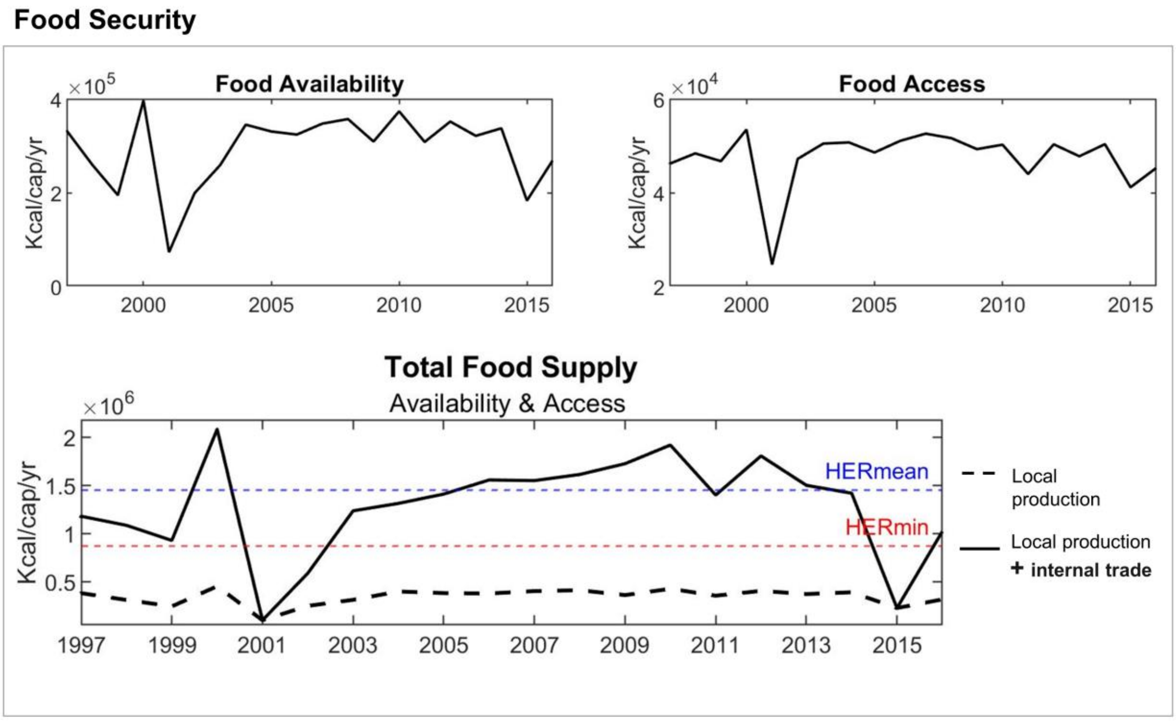

b) Chalatenango department

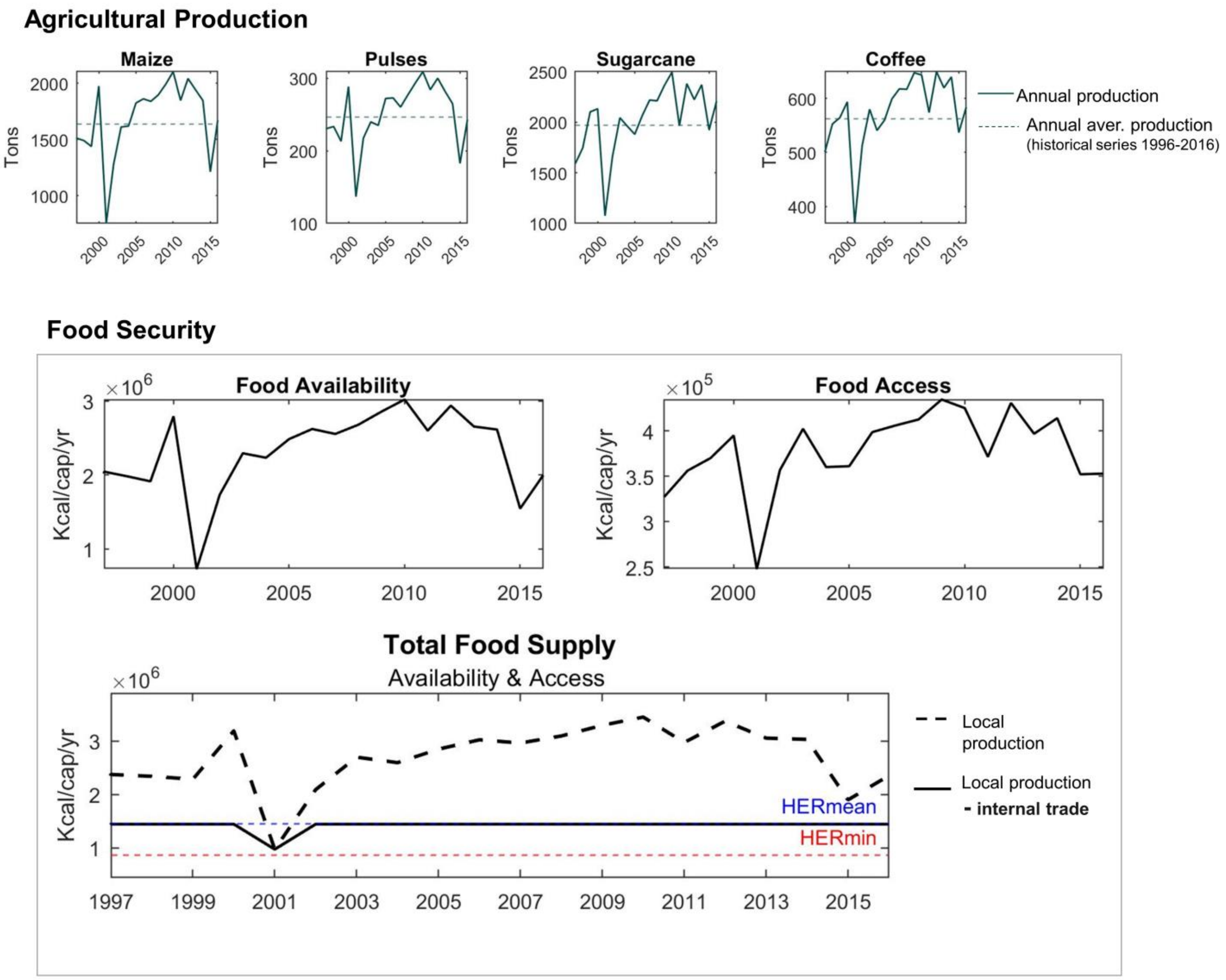

c) La Paz department

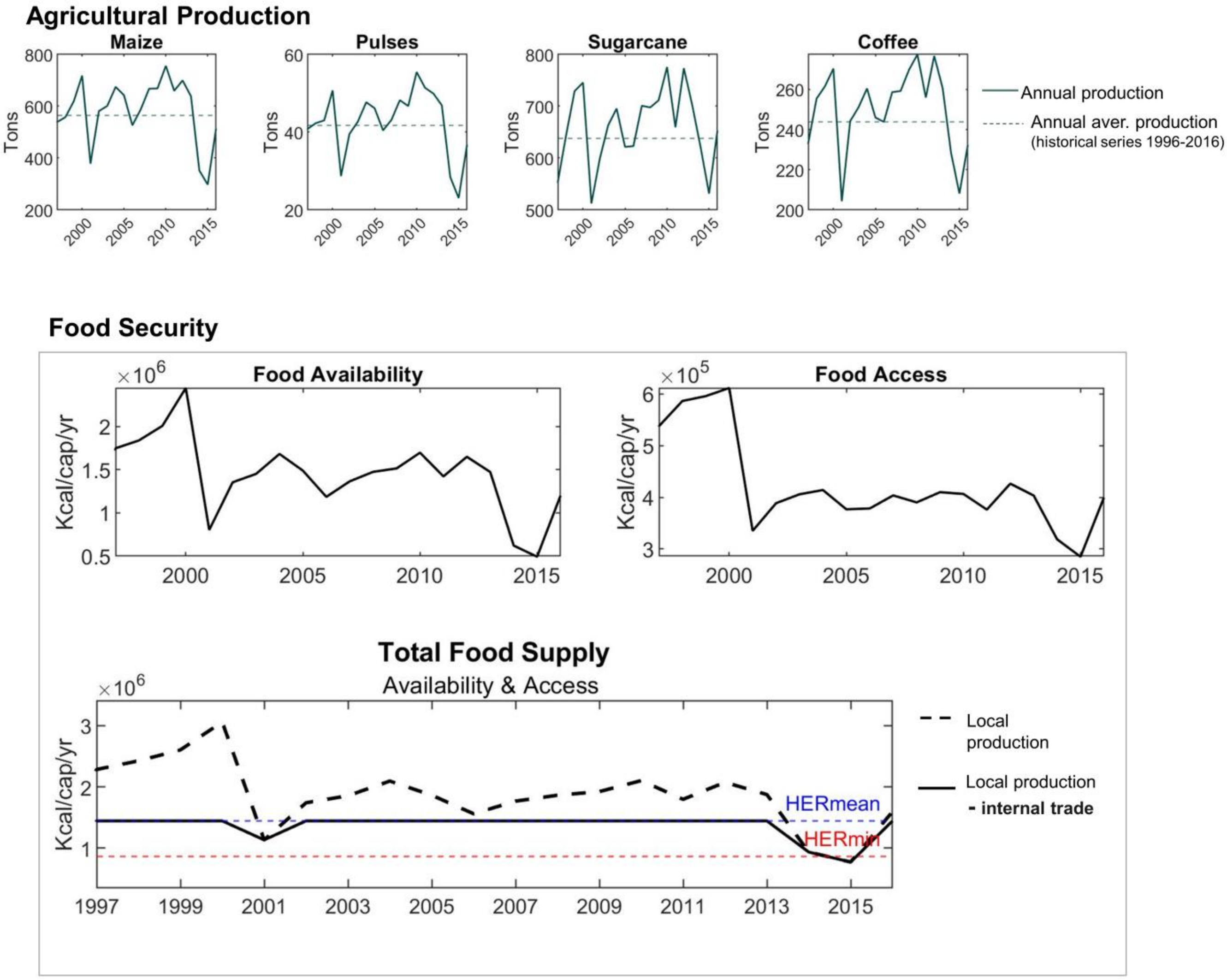

Figure S30: Green Water Availability trends and conflict occurrences in San Salvador. Temporal trends of both Local GWA (light green), and GWA + virtual-water Trade (dark green) have been reported. The reference area is the urban, peri-urban zone surrounding the capital city of San Salvador, in El Salvador. The temporal scale refers to conflict occurrence (year t), while GWA oscillations have been reported with a temporal delay of six months.

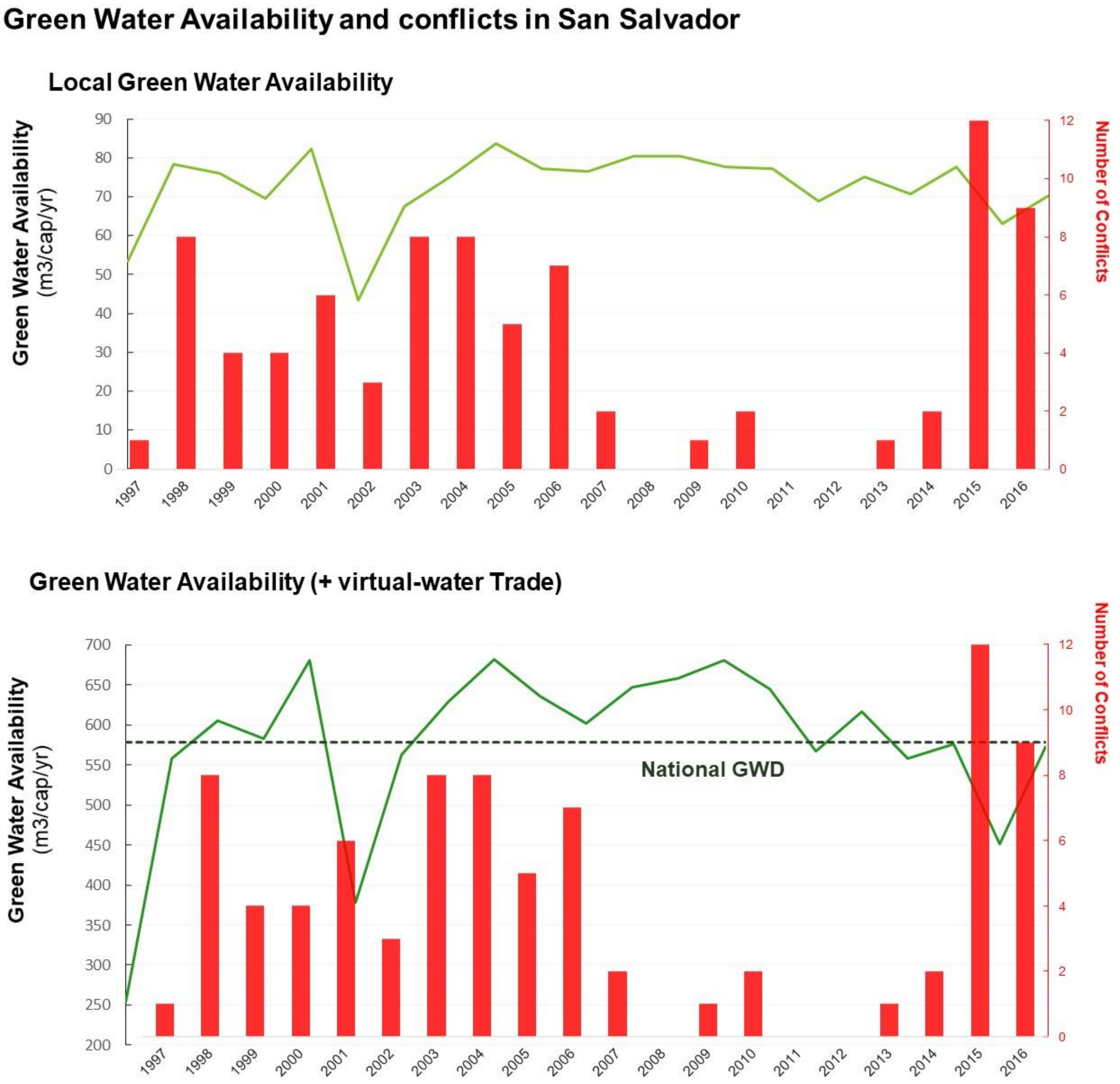

Figure S31: Green Water Availability trends and conflict occurrences in Guatemala City. Temporal trends of both Local GWA (light green), and GWA + virtual-water Trade (dark green) have been reported. The reference area is the urban, peri-urban zone surrounding the capital city of Guatemala City, in Guatemala. The temporal scale refers to conflict occurrence (year t), while GWA oscillations have been reported with a temporal delay of six months.

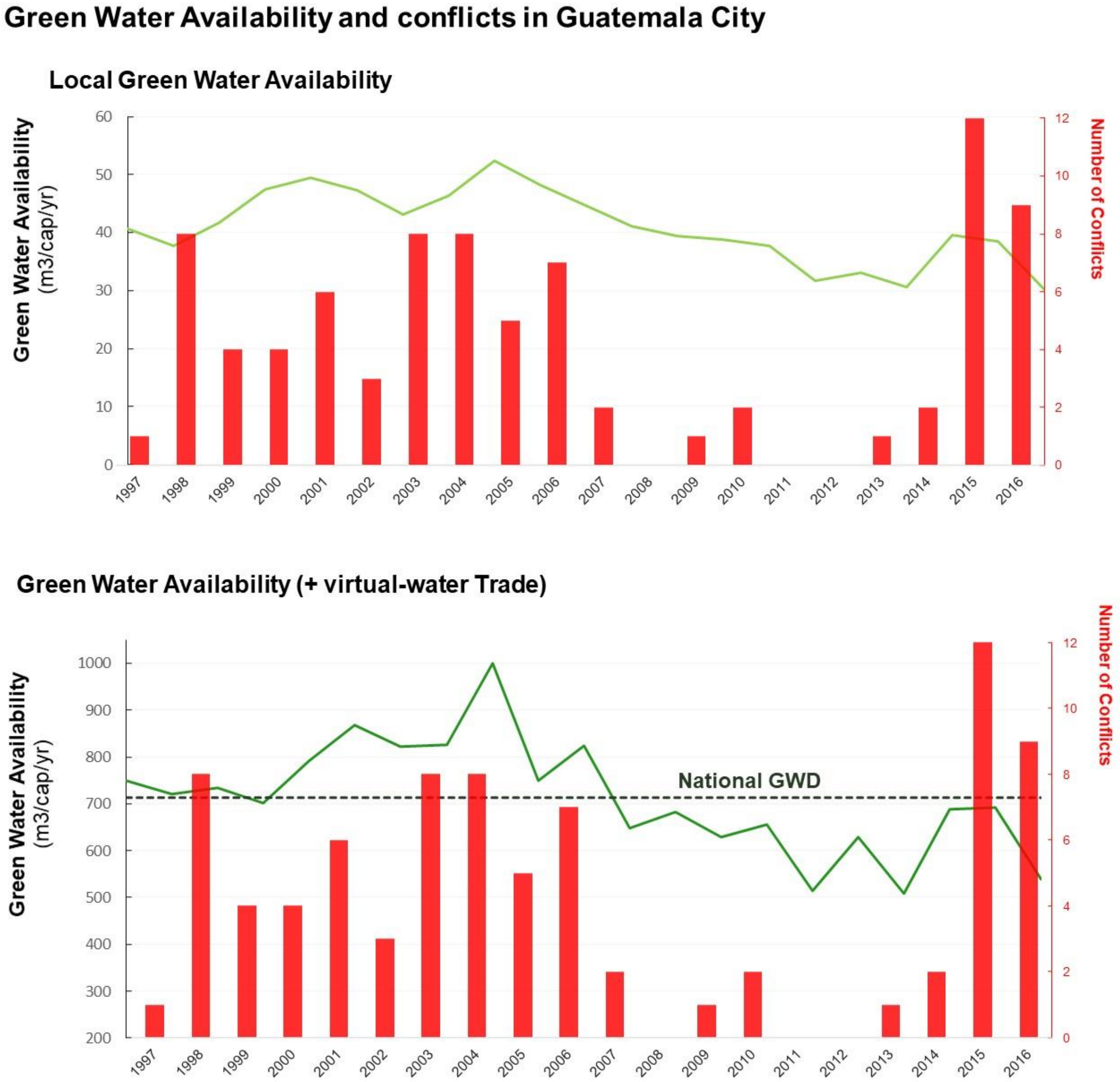

Figure S32: Green Water Availability trends and conflict occurrences in Tegucigalpa. Temporal trends of both Local GWA (light green), and GWA + virtual-water Trade (dark green) have been reported. The reference area is the urban, peri-urban zone surrounding the capital city of Tegucigalpa, in Honduras. The temporal scale refers to conflict occurrence (year t), while GWA oscillations have been reported with a temporal delay of six months.

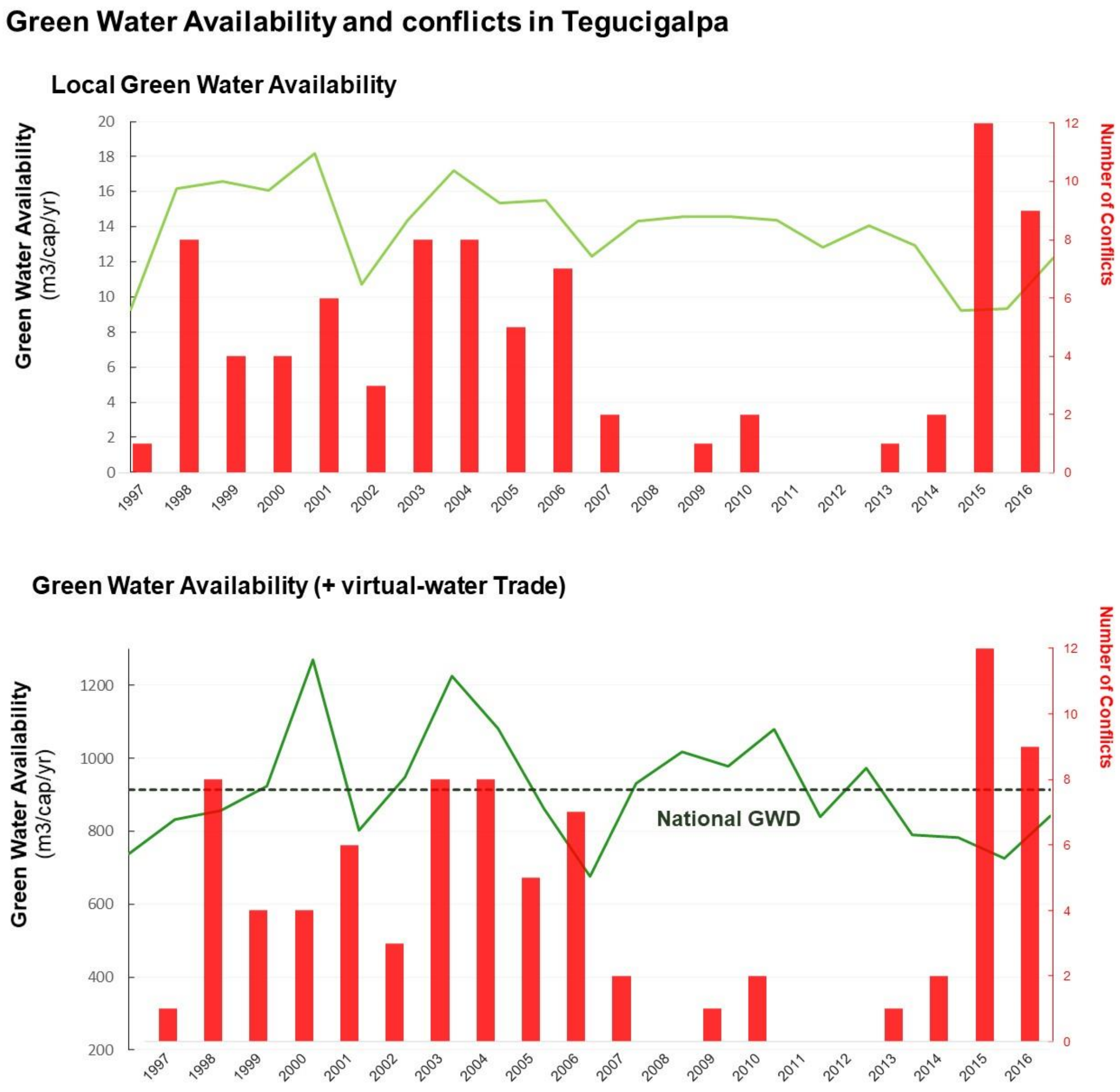

SI References

1. D. Guha-Sapir, R. Below, P. H. EM-DAT: The CRED/OFDA International Disaster Database – Université Catholique de Louvain – Brussels – Belgium. (2019).
2. Salehyan, Idean, Cullen S. Hendrix, Jesse Hamner, Christina Case, Christopher Linebarger, Emily Stull, and J. W. Social conflict in Africa (SCAD): A new database. *Int. Interact.* **38**, 503–511 (2012).
3. Tatem, A. J. WorldPop, open data for spatial demography. *Sci. Data* **4**, (2017).
4. Cattaneo, A., Nelson, A. & McMenomy, T. Global mapping of urban-rural catchment areas reveals unequal access to services. *Proc. Natl. Acad. Sci. U. S. A.* **118**, (2021).
5. Institute for Management Research - Radboud University. Global Data Lab. *Subnational Human Development Index* https://globaldatalab.org/shdi/shdi/?levels=1%2B4&interpolation=0&extrapolation=0&nearest_real=0 (2018).
6. United Nations Development Reports. Human Development Index (HDI) | Human Development Reports. *United Nations* http://hdr.undp.org/en/content/human-development-index-hdi (2020).
7. Chiarelli, D. D. *et al.* The green and blue crop water requirement WATNEEDS model and its global gridded outputs. *Sci. Data* **7**, 1–9 (2020).
8. Bonilla Vargas, A. Patrones de sequía en Centroamérica. Su impacto en la producción de maíz y frijol y uso del Índice Normalizado de Precipitación para los Sistemas de Alerta Temprana. 52 (2014).
9. Mekonnen, M. M. & Hoekstra, A. Y. Value of Water Research Report Series No. 50 National water footprint accounts: The green, blue and grey water footprint of production and consumption Volume 2: Appendices Value of Water. (2011).
10. Portmann, F. T., Siebert, S. & Döll, P. MIRCA2000-Global monthly irrigated and rainfed crop areas around the year 2000: A new high-resolution data set for agricultural and hydrological modeling. *Global Biogeochem. Cycles* **24**, n/a-n/a (2010).
11. CHIRPSv2.0. *Climate Hazards Group*. (2015) doi:https://doi.org/10.15780/G2RP4Q.
12. Richts, A., Struckmeier, W. F. & Zaepke, M. WHYMAP and the Groundwater Resources Map of the World 1:25,000,000. in *Sustaining Groundwater Resources* 159–173 (Springer Netherlands, 2011). doi:10.1007/978-90-481-3426-7_10.
13. Harris, I., Jones, P. D., Osborn, T. J. & Lister, D. H. Updated high-resolution grids of monthly climatic observations - the CRU TS3.10 Dataset. *Int. J. Climatol.* **34**, 623–642 (2014).
14. Allen, R. G., Pereira, L. S., Raes, D., & Smith, M. *Crop evapotranspiration-Guidelines for computing crop water requirements. FAO Irrigation and Drainage paper 56*. http://www.kimberly.uidaho.edu/water/fao56/fao56.pdf%5Cnhttp://linkinghub.elsevier.com/retrieve/pii/S1161030110001103 (1998).
15. Hoogeveen, J., Faurès, J. M., Peiser, L., Burke, J. & Van De Giesen, N. GlobWat - A global water balance model to assess water use in irrigated agriculture. *Hydrol. Earth Syst. Sci.* **19**, 3829–3844 (2015).
16. Siebert, S. & Döll, P. Quantifying blue and green virtual water contents in global crop production as well as potential production losses without irrigation. *J. Hydrol.* **384**, 198–217 (2010).
17. Batjes Niels H. ISRIC-WISE derived soil properties on a 5 by 5 arc-minutes global grid. http://www.isric.org/sites/default/files/isric_report_2012_01.pdf (2012).
18. Rulli, M. C., Bellomi, D., Cazzoli, A., De Carolis, G. & D'Odorico, P. The water-land-food nexus of first-generation biofuels. *Sci. Rep.* (2016) doi:10.1038/srep22521.
19. Martin-Shields, C. P. & Stojetz, W. Food security and conflict: Empirical challenges and future opportunities for research and policy making on food security and conflict. *World Dev.* **119**, 150–164 (2019).
20. J Doorenbos, A. K. Yield Response to Water. *Irrig. Drain. Pap. N. 33* 257–280 (1979) doi:10.1016/b978-0-08-025675-7.50021-2.
21. Doorenbos, J. & Pruitt, W. O. Guidelines for predicting crop water requirements. *FAO Irrig. Drain. Pap.* **24**, 144 (1977).
22. FAO. Early agrometeorological crop assessment. *Plant Prod. Prot.* **Paper No.**, (1986).
23. Monfreda, C., Ramankutty, N. & Foley, J. A. Farming the planet: 2. Geographic distribution of crop areas, yields, physiological types, and net primary production in the year 2000. *Global Biogeochem. Cycles* **22**, (2008).
24. D'Odorico, P., Carr, J. A., Laio, F., Ridolfi, L. & Vandoni, S. Feeding humanity through global food trade. *Earth's Futur.* **2**, 458–469 (2014).
25. FAOSTAT. Producer Prices. (2015).
26. FAO. Human energy requirements: report of a joint FAO/ WHO/UNU Expert Consultation. *Food Nutr. Bull.* **26**, 166 (2005).
27. Davis, K. F., D'Odorico, P. & Rulli, M. C. Moderating diets to feed the future. *Earth's Futur.* **2**, 559–565 (2014).
28. University of Minnesota & The University of British Columbia. EarthStat - GIS data for agriculture and the environment. *Global Landscapes Initiative* http://www.earthstat.org/ (2021).
29. Ghahraman, B. & Sepaskhah, A. R. Linear and non-linear optimization models for allocation of a limited water supply. *Irrig. Drain.* **53**, 39–54 (2004).
30. Kaboosi, K. & Kaveh, F. Sensitivity analysis of FAO 33 crop water production function. *Irrig. Sci.* **30**, 89–100 (2012).
31. Marsal, J. FAO irrigation and drainage paper 66. *Crop yield response to water. Sweet Cherry* 449–457 (2012).
32. FEWS NET. Famine Early Warning Systems Network. Markets and Trade. (2012).
33. FEWS-NET. El Salvador - livelihood zones. (2010).

34. FEWS NET. Guatemala - livelihood zones. (2016).
35. FEWS NET. Honduras - livelihood zones. (2014).
36. Epifani, I., Ghiringhelli, C. & Nicolini, R. Population distribution over time: modelling local spatial dependence with a CAR process. *Spat. Econ. Anal.* **15**, 120–144 (2020).
37. Gleditsch, N. P. Whither the weather? climate change and conflict. *J. Peace Res.* **49**, 3–9 (2012).
38. Raleigh, C., Witmer, F. D. W. & O'Loughlin, J. *A review and assessment of spatial analysis and conflict: The geography of war*. *The International Studies Encyclopedia* vol. 10 http://www.colorado.edu/ibs/pec/johno/pub/compendium.pdf (2010).
39. Arab, A. Spatial and spatio-temporal models for modeling epidemiological data with excess zeros. *International Journal of Environmental Research and Public Health* vol. 12 10536–10548 (2015).
40. Elhorst, J. P. *Dynamic models in space and time*. *Geographical Analysis* vol. 33 (2001).
41. Agency, E. R Core Team (2020). https://www.eea.europa.eu/data-and-maps/indicators/oxygen-consuming-substances-in-rivers/r-development-core-team-2006.
42. Team, S. D. Stan Development Team. *RStan: the R interface to Stan. R package version 2.19.2* 1–142 http://mc-stan.org/ (2019).
43. Geman, S. & Geman, D. *Stochastic Relaxation, Gibbs Distributions, and the Bayesian Restoration of Images*. *IEEE TRANSACTIONS ON PATTERN ANALYSIS AND MACHINE INTELLIGENCE* (1984).
44. Elhorst, J. P. *et al. Spatial Econometrics From Cross-Sectional Data to Spatial Panels*. vol. 16 http://www.springer.com/series/10096 (2014).
45. Gelman, A., Meng, X. L. & Stern, H. Posterior predictive assessment of model fitness via realized discrepancies. *Stat. Sin.* **6**, 733–807 (1996).
46. Nett, K. & Rüttinger, L. Insurgency, Terrorism and Organised Crime in a Warming Climate. *Climate Diplomacy* 66 www.auswaertiges-amt.de (2016).
47. United Nations Office on Drugs and Crime and Leggett, T. (UNODC) & May, C. *CRIME AND DEVELOPMENT IN CENTRAL AMERICA Caught in the Crossfire*. (2007).
48. Moser, C. & Winton, A. Violence in the Central American Region: Towards an Integrated Framework for Violence Reduction. 1–64 (2002).
49. PNUD. Informe sobre Desarrollo Humano. *Relac. Int.* **0**, (2010).
50. Lungo, M. & Martel, R. Ciudadanía social y violencia en las ciudades centroamericanas. *Real. Rev. Ciencias Soc. y Humanidades* 485–510 (2003) doi:10.5377/realidad.v0i94.3950.
51. Vilalta, C. J., Castillo, J. G. & Torres, J. A. *Violent Crime in Latin American Cities*. http://www.iadb.org (2016).
52. Buhaug, H. & Gleditsch, K. S. *Contagion or confusion? Why conflicts cluster in space*. *International Studies Quarterly* vol. 52 http://dvn.iq.harvard.edu/dvn/dv/isq (2008).
53. O'Loughlin, J. Spatial Models of International Conflicts: Extending Current Theories of War Behavior. *Ann. Assoc. Am. Geogr.* **76**, 63–80 (1986).
54. Raleigh, C. & Hegre, H. Population size, concentration, and civil war. A geographically disaggregated analysis. *Polit. Geogr.* **28**, 224–238 (2009).
55. Ravi Bhavnani, M. R. The Morphology of Urban Conflict | Global Challenges. https://globalchallenges.ch/issue/5/the-morphology-of-urban-conflict/.
56. Weidmann, N. B. Geography as Motivation and Opportunity. *J. Conflict Resolut.* **53**, 526–543 (2009).
57. Cattaneo, A. *et al.* Economic and social development along the urban–rural continuum: New opportunities to inform policy. *World Dev.* **157**, 105941 (2022).
58. Unidas, N. *Climate Change in Central America: Potential Impacts and Public Policy Options*. www.cepal.org/en/suscripciones (2008).